***Front cover illustration:*** *The development of 'activity directed synthesis' by the Nelson and Warriner groups. Its application to the discovery of novel small molecule scaffolds with agonist activity against the androgen receptor was published in Nature Chemistry and is described on pages 57-58.*

**Acknowledgement**
The Astbury Centre for Structural Molecular Biology thanks its many sponsors for support of the work and its members for writing these reports. The report is edited by David Brockwell.

This report is also available electronically via http://www.astbury.leeds.ac.uk

## Mission Statement

***The Astbury Centre for Structural Molecular Biology will promote interdisciplinary research of the highest standard on the structure and function of biological molecules, biomolecular assemblies and complexes using physico-chemical, molecular biological and computational approaches.***

# Introduction

Another year has passed by very quickly and it does not seem long since I was writing the Introduction to last years' Astbury Annual Report! 2014 proved to be another busy and successful year for the Centre, as this letter and the scientific reports that follow portray. In the following pages you will find new and exciting research which spans fundamental research in Structural Molecular Biology, Biophysics, Chemical Biology and Cell Biology, alongside the exploitation of the results obtained in biotechnology, bioengineering and medicine, each made possible by the inter- and multidisciplinary research within the Centre. I would like to thank every member of the Centre for their hard work over the year: our Support staff, Technicians, Facility Managers, Students, Post-docs, Fellows and Academic staff. Our success comes from our strong multidisciplinary science, as well as our collegiality and teamwork.

During 2014 the Centre continued in its quest of "Understanding Life in Molecular Detail" through multiple different activities, including seminars, publications, public lectures and other events. We continued to enjoy an excellent seminar series (organised by one of our recently appointed PIs, Anastasia Zhuravleva), hosting 11 lectures during 2014 with speakers from the UK, Germany, Belgium, Sweden, New Zealand and the USA. The eighth Annual Astbury Lecture was given by Professor Andrew Hamilton, FRS (University of Oxford) on "Targeting protein surfaces using designed proteomimetics". This annual event was its usual success, with a brilliant lecture, much fun and physical exertion at the sports day, and a much enjoyed barbecue hosted by the Astbury Society. The Centre's Biennial Away Day, held this year on September 19$^{th}$ at the Thackray Medical Museum was a sell-out, with 130 members attending the day to share their recent exciting scientific discoveries, through the popular "Flash Poster" presentations, as well as posters and talks. Finally, we were proud and excited to host our first joint research symposium with the Max Planck Institute for Biochemistry (Martinsried, Germany). This involved seminars, discussions, posters, networking events and a grand dinner attended by the Vice Chancellor, Sir Alan Langlands. Superb science was enjoyed by all who participated. We hope this will develop into strong on-going research links into the future.

The Centre welcomed seven new academic staff members in 2014 (Junk-uk Shim (Microfluidics and Single Molecule Science), John Ladbury (Protein Signalling and Cancer Biology), Alex Breeze (NMR and Chemical Biology Approaches for the Study of Cancer and Bacterial Infection), Patricija van Oosten-Hawle (Protein Conformational Disorders studies using C. elegans), Alison Baker (Peroxisomes and Protein Trafficking), Ryan Siepke (Natural Products and Synthetic Biology) and Joe Cockburn (X-ray crystallography, Molecular Motors and Transport)). We were sorry to lose Nigel Hooper from the membership in 2014 as he took up an academic position elsewhere and Arwen Pearson changed her status to "Visiting Member" following her move to the University of Hamburg. Sadly, Steve Baldwin died following a long illness, leaving behind many friends and collaborators, and an active research group who are continuing on the projects he had initiated. We were delighted to welcome many PhD students and postdocs to the Centre this year, bringing our total numbers to >300, including 61 academic staff, 150 PhD students, 89 postdoctoral researchers and 8 research fellows.

Astbury Centre members published their research in a wide range of journals in 2014, with a total of 149 manuscripts being published, including >20 papers in the highest impact journals (including Nature Structural and Molecular Biology, Nature Chemistry, Nature Methods, EMBO J, Angewandte Chemie, JACS, Nucleic Acids Research, Cell, and Molecular Cell). A full list can be found in the Annual Report. In terms of grant income, Astbury members also enjoyed success in 2014. Highlights included a €1.9M ERASynBio grant on "Synthetic Glycobiology" headed by

Bruce Turnbull with partners across Europe, a BBSRC Alert 14 grant to Alison Ashcroft and nine Astbury colleagues for new equipment for biological mass spectrometry (£680k investment); and an ~£880k investment (Wellcome Trust) in new equipment to enhance biological NMR (750MHz) headed by Sheena Radford and ten other Astbury and University colleagues. Finally, the renewal (valued at ~£11M) of the White Rose BBSRC Doctoral Training Partnership (a partnership between the Universities of Leeds, York and Sheffield) which funds 4 year PhDs in "Mechanistic Biology and its Strategic Application" led by Michelle Peckham ensures that future generations of PhD students can enjoy all the Astbury Centre and the partner Universities offer. Together with £8.3M new grant income raised for project and programme grants, this brings the Astbury portfolio to a £44.5M share of £77M of grants in 2014: an impressive figure that is testament to the hard work and success of our members. We are much indebted to the funding agencies that support our science, including BBSRC, EPSRC, MRC, the Wellcome Trust, other charities, ERC, EU and Industry. We also acknowledge, with thanks, the support of the University of Leeds; the Faculties of Biological Sciences and Maths and Physical Sciences and the Schools of Chemistry, Molecular and Cellular Biology and Physics and Astronomy for their support of the Centre and our research.

2014 saw continuing success of the members of the Astbury Centre in terms of peer recognition. Sheena Radford was delighted to be elected as FRS, following in Bill Astbury's footsteps. To celebrate, the Vice Chancellor and university hosted 450 guests to attend her celebratory lecture (a copy can be viewed at https://www.youtube.com/watch?v=r1eK3DLCMcM). Congratulations also to Alison Ashcroft who was awarded the 2014 Harold Edwin Potts Medal from the University of Liverpool for "Outstanding contributions to Chemistry". Our students and post-docs also were awarded many prizes for their contributions at conferences and meetings that span the globe, including Caroline Pritchard (Cogent Life Sciences Postgraduate of the year), Diana Monteiro (best oral presentation PPI-Net Young Researcher Symposium), Daniel Hurdiss (poster and oral presentation Society of General Microbiology) and Sam Hickman, Shaun Rawson, Sophie Schumann and Jo Shaw who all won awards at the Faculty of Biological Sciences Postgraduate Symposium. Well done all.

The Astbury Society, led by the presidents Katherine Horner and Claire Windle in 2014, alongside the current presidents Paul Devine and Matt Balmforth, played a magnificent role in Astbury activities in 2014. Events included a Games night, Easter Bake-off, Wine Ale and Cheese night, the now-famous Christmas quiz night, and a highly successful second May Ball. Through an Astbury Tough-Mudder team and much-enjoyed cake bakes and coffee mornings, the Society has now raised a magnificent £2150 for the "Leeds Children's Charity".

I hope that you enjoy reading this Annual Report whether you are a member of the Centre, a visitor, a member of our Industrial Advisory Board, a member of a funding agency that supports our activities or a passing reader with an interest in Structural Molecular Biology and the activities of our Centre. Thank you to David Brockwell and Lucy Gray for editing this report, everyone who contributed to it, and all who participated in the Astbury Centre's activities in 2014. I look forward to continuing our successes in 2015!

Sheena E. Radford
*Director, Astbury Centre for Structural Molecular Biology,*
*Leeds, April 2015*

Please note that this report (as well as those from previous years) is also available as a PDF document which can be downloaded from our website (www.astbury.leeds.ac.uk).

**CONTENTS**

## Contributions indexed by Astbury Centre Principal Investigator

# Biomolecular mass spectrometry

James Ault, Helen Beeston, Antonio Calabrese, Paul Devine, Henry Fisher, Kate Groves, Patrick Knight, Negar Rajabi, Charlotte Scarff, Tom Watkinson, Leon Willis, Lydia Young and Alison Ashcroft

## Introduction

Our research is focussed on the development and application of mass spectrometry (MS) to investigate the structure and function of biomolecules. We use non-covalent electrospray ionisation (ESI)-MS and tandem mass spectrometry (MS/MS) to determine the mass, conformational properties, stoichiometry, stability, and binding characteristics of biomolecules and their complexes. We are pioneers of the use of ion mobility spectrometry (IMS)-MS for biomolecular applications; IMS-MS is a technique that can separate co-populated biomolecular species on the basis of their shape and measure their mass and cross-sectional area in a single, rapid (≤ 2 mins) experiment. The main focus of our research is to study protein folding, function and self-aggregation, protein-ligand interactions, biomolecular complex assembly, and oligonucleotide structure [1-11].

## Results

We use a variety of chemical labelling methods in conjunction with ESI-MS and ESI-IMS-MS to map protein folding and aggregation pathways, and to characterise non-covalently bound biomolecular complexes and protein-ligand interactions (Figure 1).

Our current projects are aimed at characterising amyloid protein aggregation and modes of inhibition [1,3,6,10], for which we have developed a high-throughput screening method to evaluate potential small molecule amyloid inhibitors [1,10], mapping virus capsid assembly pathways [4,5], and developing new MS methods for the determination of membrane protein structure and function [9,11] (Figure 2).

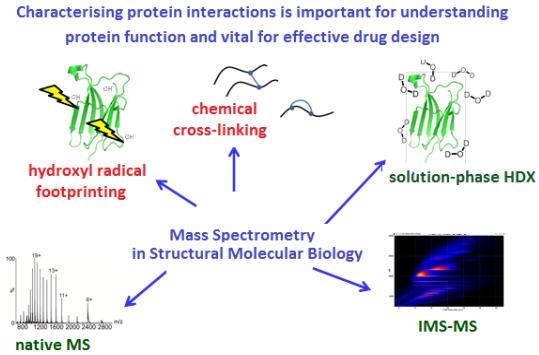


**Figure 1**: Chemical labelling methods used with MS in structural biology.

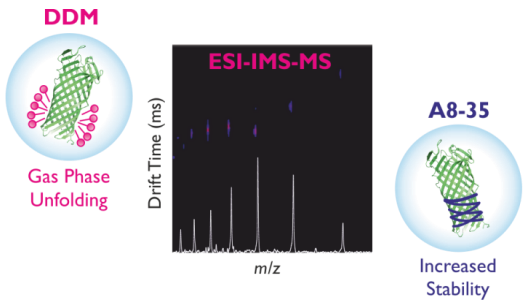


**Figure 2**: Using detergents and amphipols to solubilise outer membrane proteins for ESI-IMS-MS analysis.

## Publications

Young, L., Cao, P., Raleigh, D., Ashcroft, A. & Radford, S. (2014) Ion mobility spectrometry-mass spectrometry defines the oligomeric intermediates in amylin amyloid formation and the mode of action of inhibitors. *J. Am. Chem. Soc.* **136**: 660-670.

Eves-van den Akke, S., Lille, C. J., Ault, J. R., Ashcroft, A. E., Jones, J. T. & Urwin, P. E. (2014) The feeding tube of cyst nematodes: Characterisation of protein exclusion. *Plos One* **9**: e87289.

Leney, A., Pashley, C., Scarff, C., Radford, S. & Ashcroft, A. (2014) Insights into the role of the β2-microglobulin D-strand in amyloid propensity revealed by mass spectrometry. *Mol. Biosyst.* **10**: 412-420.

Voeroes, J., Urbanek, A., Rautureau, G., O'connor, M., Fisher, H., Ashcroft, A. & Ferguson, N. (2014) Large-scale production and structural and biophysical characterizations of the human hepatitis B virus polymerase. *J. Virol.* **88**: 2584-2599.

Shepherd, D. A., Arizal, A., Barr, J. N., Edwards, T., Stonehouse, N. J. & Ashcroft, A. E. (2014) Probing Bunyavirus N protein oligomerisation using mass spectrometry. *Rapid Commun. Mass Spectrom*., **28:** 793-800.

Preston, G. W., Radford, S. E., Ashcroft, A. E. & Wilson, A. J. (2014) Analysis of amyloid nanostructures using photo-cross-linking: *In situ* comparison of three widely used photo-cross-linkers. *ACS Chemical Biology*, **9**: 761-768.

Pritchard, C., Groves, K. J., Biesenbruch, S., O'Connor, G., Ashcroft, A. E., Arsene, C., Henrion, A., Schulze, D. & Quaglia, M. (2014) The quantification of human growth hormone in serum with a labelled protein as an internal standard: critical considerations. *Anal. Chem*., **86**: 6525-6532.

Elsheshiny, A., Ashcroft, A. E. & Harris, S. A. (2014) A comparison of the electromechanical properties of structurally diverse proteins by molecular dynamics simulation. *J. Biomolecular Structure & Dynamics*, **32**: 1734-1741.

Giusti, F., Rieger, J., Catoire, L., Qian, S., Calabrese, A. N., Watkinson, T. G., Pemboung, G., Casiraghi, M., Radford, S. E., Ashcroft, A. E. & Popot, J-L. (2014) Synthesis, characterization and applications of a perdeuterated amphipol. *J. Membr. Biol*., **247**: 909-924.

**Funding**
This work was funded by the BBSRC, the EPSRC, the Wellcome Trust, Waters UK Ltd., LGC, AZ, GSK, UCB, & Medimmune. We thank the BMSS for student travel grants.

**Collaborators**
***University of Leeds:*** J. Barr, T. Edwards, S. Harris, P. Henderson, S. Radford, D. Rowlands, P. Stockley, N. Stonehouse, P. Urwin and A. Wilson.
***External:*** S. Arscott (CNRS, Lille, France), M. Quaglia (LGC, UK), M. Morris & K. Giles (Waters UK Ltd.), N. Ferguson (UCD, Eire), S. Macedo-Ribeiro (IBMC, Portugal), D. Raleigh (Stonybrook, NY, USA) and J-L. Popot (Paris, CNRS, France).

# Peroxisomal ABC transporters

David Carrier, Honglin Rong, Stephen Baldwin and Alison Baker

## Introduction

The beta oxidation pathway is central to peroxisomal metabolism, but the substrates processed are very diverse, reflecting the diversity of peroxisome across species. Substrates for beta oxidation enter peroxisomes via ABC transporters of the ABCD sub family and are activated by specific acyl CoA synthetases for further metabolism. Humans have 3 peroxisomal ABCD family members, which are half transporters that homodimerise and have distinct but partially overlapping substrate specificity; S. cerevisiae has 2 half transporters that heterodimerise and plants have a single peroxisomal ABC transporter that is a fused heterodimer and which appears to be the single entry point into peroxisomes for a very wide variety of beta oxidation substrates. Our previously published work suggests that the Arabidopsis peroxisomal ABC transporter AtABCD1 (COMATOSE/PXA1/PED3) accepts acyl CoA substrates, cleaves them before or during transport followed by reactivation by peroxisomal synthetases.

## Results

Our current work is directed towards optimising purification and reconstitution protocols for AtABCD1. This will allow direct measurement of transport and the interrelationship between ATPase activity, thioesterase activity and transport to be studied. We are also working on various approaches to study substrate binding and interaction between AtABCD1 and peroxisomal acyl CoA synthetases.

## Funding

This work is funded by BBSRC

## Collaborators

***External:*** F. Theodoulou (Rothamsted Research, UK), C. van Roermund (Amsterdam Medical Centre, Netherlands)

# Plant Chemical Genetics

Rupesh Paudyal, Stuart Warriner and Alison Baker

## Introduction

Small molecules are extremely powerful in interrogating and unpicking complex pathways such as protein trafficking where mutations frequently lead to pleoitropic effects (even lethality) that can confound analysis. While small molecules frequently have off target effects that must be taken into account, the ability to control application in terms of concentration and timing and the ability to hit multiple members of redundant gene families makes this an attractive strategy, especially when coupled with the capability to synthesise focussed libraries of the initial hit and refine the selectivity and potency. A screen for small molecules that lead to mislocalisation of a peroxisome targeted reporter in transgenic Arabidopsis seedlings led to identification and characterisation of compounds that inhibited primarily the PTS1 import pathway and also oil body breakdown which have been published by our lab previously. One of the molecules that was identified from the screen turned out not to have a primary mode of action on peroxisomes but instead affected trafficking through the plant endomembrane system.

## Results

We showed that this molecule, that we subsequently named TENin1 for trafficking and endocytosis inhibitor1, affected endocytosis and recycling of the auxin transport protein PIN2. We showed that treatment with TENin1 resulted in accumulation of PIN2 in prevacuolar compartments and upregulated transport to the vacuole. As expected the treatment with the compound resulted in whole seedling phenotypes consistent with deficiency in auxin response such as agravitropism. We screened 80 different ecotypes of Arabidopsis and found 2 that were partially resistant to the effects of TEnin1 at both whole plant and cellular level. This offers a way to use a genetic approach to identify the molecular target.

## Publications

Paudyal R., Jammaluddin A., Warren J. P., Doyle S. M., Robert S., Warriner S. L. & Baker A. (2014) Trafficking modulator TENin1 inhibits endocytosis, causes endomembrane protein accumulation at the prevacuolar compartment and impairs gravitropic response in *Arabidopsis thaliana*. *Biochem. J.* **460:**177-185.

## Funding

This work was funded by the BBSRC and the Leverhulme Trust

## Collaborators

***External:*** S. Robert (Umea University, Sweden)

# Phosphate Signalling and Transport

Tony Palmer, Wanjun (Catherine) Qi, S.A. Ceasar, Stephen Muench and Stephen Baldwin

## Introduction

Phosphorus (P) is an essential element for all cells as it is a non replaceable component of nucleic acids and phospholipids, a component of many key metabolic intermediates and plays a critical role in signal transduction and enzyme activity through protein phosphorylation. Animals acquire their P through their diet, plants from uptake from the soil. While P is a relatively abundant element its bioavailable form inorganic phosphate is not. In the environment it is complexed by metal ions in a pH dependent manner and bound by the soil particles rendering it immobile and inaccessible. Soil microorganisms compete with plants for inorganic phosphate. Indeed much soil P is locked in organic compounds. Sub optimal inorganic phosphate in soils limits crop production over much of the globe and consequently farmers apply inorganic fertiliser produced mainly from rock phosphate to boost yields. This is not a sustainable practice as rock phosphate reserves are finite, current predictions suggest depletion with 200 years, and much of what is applied is not taken up by crops but leaches into water bodies causing eutrophication. Plants have developed sophisticated sensing and signalling systems to detect and respond to phosphate deprivation. By understanding these we may be able to apply this knowledge to production of more P efficient crops by either transgenic or molecular marker assisted breeding approaches.

## Results

We focussed on foxtail millet (Setaria italica) as an experimental system for several reasons. Millets are a staple crop of millions of food insecure people in Asia and Sub-Saharan Africa. They are one of the most drought resistant crops known and as an orphan crop it has received little breeding improvement. Thus we reasoned that large gains would be possible for this crop. Foxtail millet is a model for the biofuel grasses switchgrass and Napier grass and has a completely sequenced genome. We identified all the members of the PHT1 family of phosphate transporters, 12 in total and characterised their expression in response to phosphate deprivation and response to root colonisation by arbuscular mycorrhizal forming fungi. We identified phosphate transporters that are candidates for Pi acquisition from the soil and those which may play a role in fungal colonisation. We are currently seeking to carry out functional characterisation of these transporters. In addition we have been investigating the role of SPX domain containing proteins in phosphate signalling and the structure and function of Aluminium activated malate transporters which secrete malate to sequester Aluminium and increase inorganic phosphate availability at low pH.

## Publications

Ceasar, S., Hodge, A., Baker, A. & Baldwin, S. (2014) Phosphate concentration and arbuscular mycorrhizal colonisation influence the growth, yield and expression of twelve PHT1 family phosphate transporters in foxtail millet (*Setaria italica*). *PLoS One* **9**: e108459.

## Funding

This work was funded by the BBSRC, the European Union, Yorkshire Agricultural Society, and a University of Leeds International Research Scholarship.

# Mechanistic insights into the role of lipid composition in the anticancer activity of an antimicrobial peptide

Anders Aufderhorst-Roberts, Simon Connell and Paul Beales.

## Introduction

Extracted from the Brazilian Wasp *Polybia paulista*, the host-defence peptide Polybia-MP1 (MP1) is known to have broad spectrum antimicrobial activity without being hemolytic or cytotoxic at relevant antibiotic concentrations. Intriguingly, MP1 has also be found to exhibit selective inhibition of cancer cells, including bladder and prostate cancer cells and multidrug resistant Leukemic cells. As a cationic peptide (net charge +2*e*), MP1's antimicrobial specificity is attributed to the high anionic potential of bacterial membranes. Similar, the anionic phopsholipid phosphatidylserine (PS) is more abundant in the membranes of cancer cells than normal, healthy cells and has therefore been attributed to the anticancer mechanism of MP1 peptides. However, it also known that phosphatidylethanolamine (PE) lipids, which form a major component of bacterial membranes, are coregulated with PS and similarly have a higher abundance in the plasma membranes of cancer cells. We sought to further investigate the role of PE and PS lipids in the interaction mechanism of MP1 with membranes, and hence their significance in MP1's anticancer mechanism. We applied a range of permeability assays and imaging techniques to investigate the interaction of MP1 with *in vitro* model membrane systems of four different compositions. The membrane compositions studied were phosphocholine (PC), the most abundant phospholipid of Eukaryotic plasma membranes, PC/PS (80:20), PC/PE (90:10) and PC/PE/PS (70:10:20).

## Results

Our primary experimental model systems were Giant Unilamellar Vesicles (GUVs) imaged by confocal microscopy. We developed a membrane permeability assay that could measure the permeability of GUVs at the single vesicle level simultaneously for 3 different sized molecular probes (0.37, 3.0 and 10 kDa). Dose-response curves for leakage of these dyes were constructed for the four GUV concentrations and the kinetics of dye influx was analyzed to quantify membrane permeabilities (Figure 1).

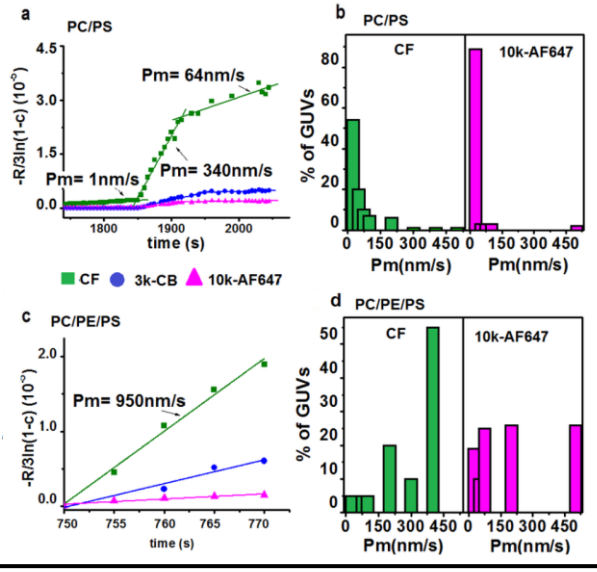


**Figure 1:** GUV membrane permeabilities. (a) Typical log-linear plot of time dependent dye influx: –R/3ln(1-c) *vs* time, for the three dyes in a single GUV of PC/PS. (b) Distributions of the obtained permeabilities in single GUVs composed of PC/PS. (c) Permeability plot showing time dependent dye influx for the three dyes in a single GUV of PC/PE/PS. (d) Distributions of the obtained permeabilities in single GUVs composed of PC/PE/PS.

To summarise the major findings of our GUV imaging studies, PE lipids were found to signifcantly increase the kinetics of the onset membrane permeabilisation and greater dye leakage

also occured at lower MP1 concentrations for PE-containing GUVs. Addition of PS lipids only showed a minor enhancement in these metrics. PE lipids also enhanced membrane permeability by an order of magnitude compared to GUVs without PE, indicating that the formation of larger membrane defects or pores by the activity of MP1 is facilitated by PE lipids. These results were corroborated by fluorescence leakage assays using LUVs, which give ensemble averaged leakage behaviour with greater statistics than GUV experiments but lack the sensitivity to the distribution of behaviours, transient intermediates and rare events. These fluorescence assays included an all-or-none leakage assay, which strongly indicated the membrane defects leading to permeabilisation were as a result of poration with pore lifetimes that are stable enough to result in the leakage of all dye contents of each LUV in a single permeabilisation event.

We further investigated the membrane poration mechanism using AFM imaging of supported lipid bilayers (Figure 2). Any pores that may have formed by MP1 action in PC membranes were too small to detect by this technique. PC/PS membranes contained small individual pores, while PC/PE and PC/PE/PS membranes contained large transmembranes pores, which were more prevailant in the latter. Time-resolved AFM imaging of the poration events revealed different mechanisms of membrane perturbation dependent on PE content. For PC/PS membranes, small blisters initially appeared on the surface of the membrane (possibly coinciding with similar structures observed on GUVs of this composition), which matured into transmembrane pores through an intermediate state of a hemibilayer defect. PC/PE and PC/PE/PS membrane pores grew in a step-wise fashion by the loss of lipid from the edges of pores through a lipid vesiculation mechansim.

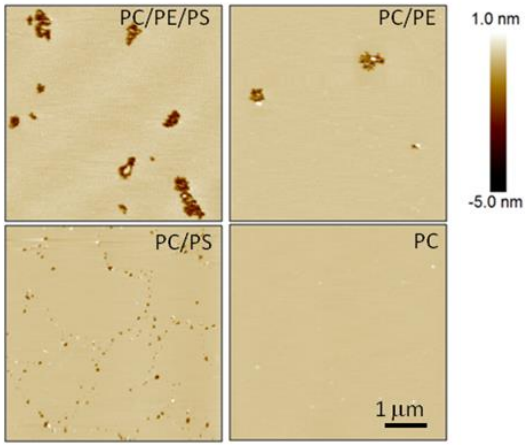


**Figure 2:** AFM images of pore formation. AFM images of the 4 different membrane compositions 2 hr. after the addition of 10 µM MP1. Large pores can clearly be seen in PC/PE/PS and PC/PE membranes with a larger number of pores in the former. PC/PS shown much smaller defects, while no membrane perturbation was resolvable by AFM for PC membranes.

In summary, our biophysical investigation shows that PE lipids are in fact more important than PS lipids for the mechanism of membrane disruption by MP1, contrary to established thinking. These insights will aid the development of peptide-based chemotherapeutic agents designed to target pathological changes in lipid composition. Such compounds could also be especially potent in combination therapies with drugs that have intracellular targets by synergistic enhancement of therapeutic efficacies.

**Funding**
This work was funded by an E.U. Marie Curie Career Integration Grant, EPSRC and FAPESP.

**Collaborators**
***External:*** M. Palma (Center of Studies of Social Insects and Department of Biology, São Paulo State University –UNESP, Brazil), N. Bueno Leite and J. Ruggiero Neto (Department of Physics, São Paulo State University –UNESP, Brazil).

# Peroxisome protein import

Tom Lanyon-Hogg, Nicola Skoulding, Rupesh Paudyal, Laura Cross, Andrew Cuming, Stuart Warriner, Alison Baker and Alan Berry

## Introduction

Peroxisomes are found in all eukaryotic cells and perform a diverse range of metabolic functions. The importance of peroxisomes is underscored by the severe developmental abnormalities seen in mullticellular organisms (animals, plants) that result from defects in peroxisome biogenesis or peroxisome metabolism. Peroxisomes import proteins post translationally from the cytosol. There are two amino acid sequences that act as signals for import into the matrix; a C terminal tripeptide PTS1, and PTS2 a more complex nonapeptide sequence found towards the N terminus of some peroxisomal proteins. Each of these import signals has a receptor protein; PEX5 in the case of PTS1 and PEX7 in the case of PTS2 that act as cycling receptors to shuttle the respective proteins to the peroxisome and deliver them to the protein import machinery. PEX5 is comprised of natively unstructured N terminal domain that binds the peroxisome membrane protein PEX14 and the C terminal TPR domain that binds the PTS1 containing cargo protein. In mammals and plants (but not yeasts) PEX5 also acts as co-receptor for PTS2 protein import by binding PEX7.

## Results

We expressed and purified recombinant full length and N terminally truncated Arabidopsis thaliana PEX5 and PEX14 soluble cytosolic domain. We studied the effect of PEX14 binding to PEX5 on cargo occupancy by fluorescence anisotropy and pull down assay. We showed that contrary to some prevailing models where cargo binding is proposed to trigger a conformational change in the receptor to allow docking, cargo free PEX5 is capable of binding to PEX14. Conversely PEX14 binding did not affect cargo occupancy of PEX5, contrary to the model that PEX14 binding causes cargo unloading from PEX5. This leads us to conclude that PEX14 cytosolic domain binding is insufficient to unload the receptor. Interestingly however we could never detect cargo loaded PEX7 after PEX14 binding to PEX5, suggesting PEX14 may have a role in PEX7 unloading.

We are also interested in affinity and specificity of PTS1 sequences. Although the C terminal tripeptide is a critical part of a PTS1 signal many experiments point to a role for amino acids immediately N terminal to the PTS1 playing an important role in regulating the affinity and efficiency of import. In vivo so called non-canonical PTS1 signals which do not fit the consensus of [small] [basic] [hydrophobic]-COOH have been shown to function to deliver reporter proteins to peroxisomes, or have been shown to be present on resident peroxisomal proteins identified in proteomic studies. Together with collaborators from the University of Stavanger, Norway we carried out a systematic analysis of a non canonical targeting signal which is classified as of very weak strength in vivo. We compared in vivo targeting of eYFP extended by the test sequence, in silico predictions of targeting strength and thermodynamic measurements of peptide binding to recombinant PEX5 by fluorescence anisotropy. We found that all three methods gave remarkably consistent results but that the efficiency of Tyr at the carboxy terminus was underestimated due to lack of examples in the training set for the targeting algorithm. We also found that some sequences that were capable of giving rise to specific peroxisome targeting in vivo had $K_d$s for interaction with PEX5 that were too high for detection by FA (<100μM). Since neither receptor nor cargo would be present at this concentration in vivo, this requires consideration of a non-equilibrium model for peroxisome protein import and also suggests how non-peroxisomal proteins can evolve PTS1 signals through random events that produce a ‘weak’ signal that is capable of subsequent selection to improve efficiency.

We are interested in understanding the 'design rules' for PEX5 PTS1 interaction. How can specificity arise from an apparently quire relaxed PTS1 consensus? To understand this better and to generate tools to measure protein import rates in vivo, which will be required along with measures of receptor-cargo binding affinity in order to develop mathematical models of import, we have been attempting to evolve an orthogonal receptor- PTS1 pair. This work has developed a number of different screens which are being applied towards this end. We have also been working on developing a line of the moss Physcomitrella patens, an excellent model system for genetics and cell biology, to allow switching of PEX5 receptor specificity *in vivo*.

**Publications**

Lanyon-Hogg, T., Hooper, J., Gunn, S., Warriner, S. & Baker, A. (2014) PEX14 binding to arabidopsis PEX5 has differential effects on PTS1 and PTS2 cargo occupancy of the receptor. *FEBS Lett.* **588**: 2223-2229.

**Funding**

This work was funded by the BBSRC and The Leverhulme Trust

**Collaborators**

***External:*** S. Reumann (Universities of Stavanger and Hamburg)

# Improving on Nature: protein engineering and design

Claire Windle, Christopher Rowley, Laura Cross, Marion Müller, Robert Smith,
Alex Moloney, Sasha Derrington, Adam Daniels, Chi Trinh, Adam Nelson and Alan Berry

## Introduction

We are using protein engineering and directed evolution in a wide range of projects. These methods are used to engineer both enzymes and protein-protein interactions.

## Modifying the activity of an enzyme using non-canonical amino acids

*N*-Acetylneuraminic acid lyase (NAL) catalyses the reversible aldol condensation of *N*-acetyl-D-mannosamine and pyruvate to form *N*-acetylneuraminic acid, through a mechanism that involves the formation of a Schiff base with a lysine residue at position 165. A chemical mutagenesis strategy, involving the formation of a dehydroalanine intermediate which then undergoes Michael addition with a thiol, has been used to incorporate non-canonical amino acids into the active site of NAL (Figure 1). This method has now been established, and a variety of non-natural amino acids have been inserted at various positions throughout the active site to create many different modified enzymes. These enzymes have then been screened for altered substrate specificity using a thiobarbituric acid assay.

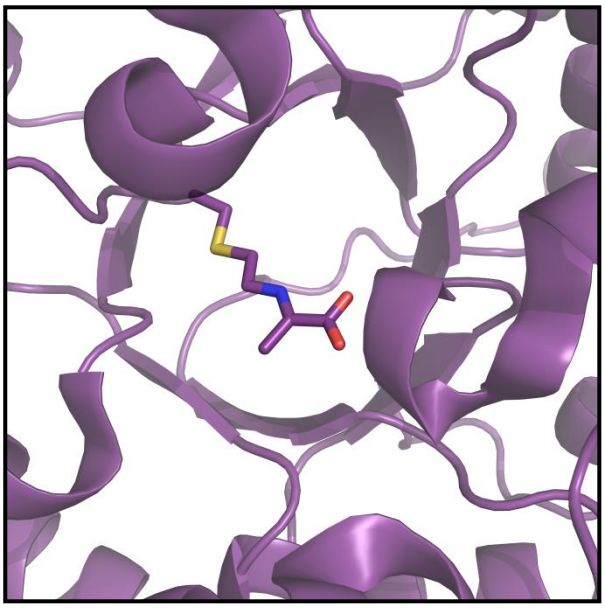

**Figure 1:** *S. aureus N*-acetylneuraminic acid lyase with the non-canonical amino acid γ-thialysine at position 165 in complex with pyruvate.

## mRNA display

mRNA display is a powerful technique for the exploration of large areas of sequence space in the search for functional peptides and proteins, and has recently proven an invaluable tool in the discovery of novel enzymes. mRNA display selection techniques are being explored as a method of engineering novel enzymes that catalyse the Diels-Alder reaction - a [4+2] cycloaddition that results in the generation of two new carbon-carbon bonds and up to four new stereogenic centres. Biologically catalysed Diels-Alder reactions are of great interest, as although it is an important reaction in synthetic organic chemistry, there are currently no known natural enzymes widely accepted to catalyse this powerful [4+2] cycloaddition.

## Creating novel binding motifs

The interaction between the peroxisomal receptor PEX5 and its signal sequence PTS1 (peroxisomal targeting signal 1) allows targeting of proteins to the peroxisome. We aim to generate an interaction between a mutated form of PEX5 (PEX5*) and a peptide representing a non-natural PTS1 (PTS1*). A selection of non PTS1-binding PEX5 variants (candidate PEX5* proteins) have been produced and are being screened against a library of candidate PTS1* peptides. A pull-down screen, using mass spectrometry to identify binding peptides (hits), has been developed this year (See Warriner group report “Creating novel binding motifs for orthogonal receptors”).

## Aldolases with fluorosubstrates

Aldolases catalyse carbon-carbon bond formation between a nucleophilic donor and an electrophilic aldehyde acceptor. As the resulting aldol product can have up to two new stereocentres, aldolases have become attractive biocatalysts for the synthesis of key chiral building blocks (Figure 2). Aldolases are generally quite flexible in their acceptance of different aldehyde acceptor substrate but changing the donor specificity is challenging because of the high specificity of aldolases for their donors. Despite this, we want to find aldolases which accept fluorinated donor substrates. The enzymatic aldol reaction with fluorinated substrates leads to organofluorine compounds which are widely used in industry, e.g. for the synthesis of pharmaceutical drugs. Organofluorine compounds are extremely rare in Nature and their chemical synthesis is difficult. Therefore, the use of aldolases could be a smart and environmentally friendly alternative. So far, we have identified, cloned, and expressed six different pyruvate-dependent aldolases and have demonstrated by $^{19}F$ NMR spectroscopy that at least two of them accept a fluorinated donor.

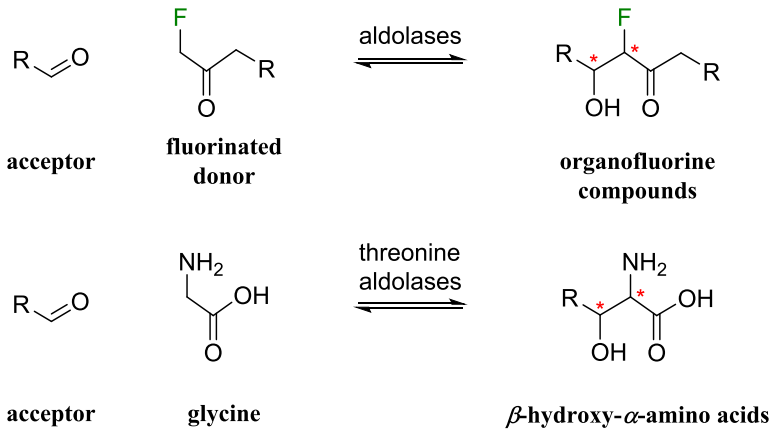


**Figure 2:** Exploiting aldolases in the synthesis of chiral building blocks. Top: The acceptance of fluorinated donors by aldolases allows the production of organofluorine compounds revealing a second stereocentre. Bottom: The aldol reaction catalysed by the pyridoxal phosphate (PLP)-dependent threonine aldolases naturally results into compounds containing two chiral centres (denoted by red asterisks).

## Threonine aldolases

Threonine aldolases are a family of homologous pyridoxal phosphate-dependent enzymes that catalyse the formation of *β*-hydroxy-*α*-amino acids. Using glycine and a wide range of aldehyde acceptor molecules as substrates, desired products containing two new stereocenters are formed (Figure 2). These products are of interest pharmaceutically as synthetic building blocks and precursor drug molecules. Rational and directed evolution studies can be implemented into shaping these enzymes to create the desired *β*-hydroxy-*α*-amino acid products providing faster, cheaper and more feasible routes for synthesis than the chemical production alternative.

## Publications

Daniels, A., Campeotto, I., Van Der Kamp, M., Bolt, A., Trinh, C., Phillips, S., Pearson, A., Nelson, A., Mulholland, A. & Berry, A. (2014) Reaction mechanism of n-acetylneuraminic acid lyase revealed by a combination of crystallography, QM/MM simulation, and mutagenesis. *ACS Chem. Biol.* **9**: 1025-1032.

Windle, C., Mueller, M., Nelson, A. & Berry, A. (2014) Engineering aldolases as biocatalysts. *Curr. Opin. Chem. Biol.* **19**: 25-33.

**Funding**
Our work is funded by BBSRC, the Wellcome Trust, The Leverhulme Trust, GlaxoSmithKline and Dr Reddy's Chirotech Technology.

**Collaborators**
***University of Leeds:*** S. Warriner, P. Stockley and A. Baker.
***External:*** J. Adams (GSK) and M. Bycroft (Dr Reddys).

# Targeted contrast agents for imaging of inflammatory markers

Martin Fisher, Daniel Williamson, Iain Manfield, Christian Tiede, Jeffrey Plante Richard Foster, Justin Ainscough, Mark Drinkhill, Louise Coletta, Sven Plein, Darren Tomlinson, Azhar Maqbool and Robin Bon

## Introduction

Molecular imaging allows the detection of key molecules or proteins that play a role in the development or progression of disease. Central to molecular imaging is the development of targeted imaging probes. We are interested in developing novel reagents to image, by magnetic resonance imaging (MRI), the hexameric matrix protein Tenascin C (TNC), which is a marker of inflammatory sites in cardiovascular disease and cancer.

Gadolinium (Gd) chelates are widely applied as contrast agents in magnetic resonance imaging (MRI). The development of hybrids of Gd chelates and ligands of proteins such as collagen and elastin has enabled the imaging of tissues that are enriched with these proteins. In this project we aim for the establishment of a chemical toolbox containing building blocks **1** for the modular synthesis of targeted Gd contrast agents **2**, and use these to label biomolecules that bind to TNC (Figure 1). In addition, we are developing Adhirons as novel TNC-targeting moieties for MRI.

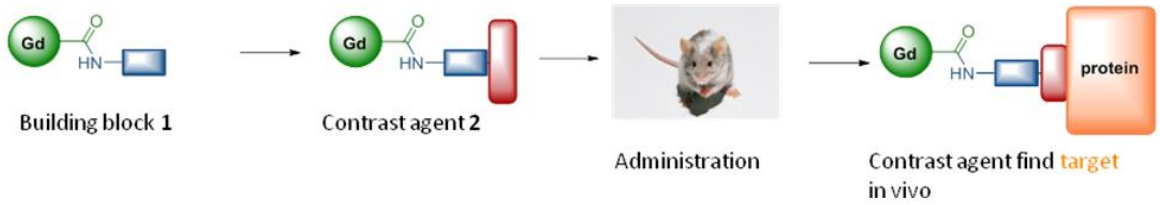


**Figure 1:** Strategy for the development of Gd-based contrast agents for MRI. Green: Gd chelate; blue: linker with handle for bioorthogonal ligations to biomolecular targeting moieties (red); orange: TNC.

## Results

We have recently completed the synthesis of trimeric Gd(III) chelates **3** with isothiocyanate (ITC; **3a**), maleimide (**3b**) and azide (**3c**) handles (Figure 2). We have used these reagents to label oligonucleotides and proteins through ITC ligations, maleimide ligations and strain-promoted alkyne-azide cycloadditions.

## Funding

This work was funded by the British Heart Foundation.

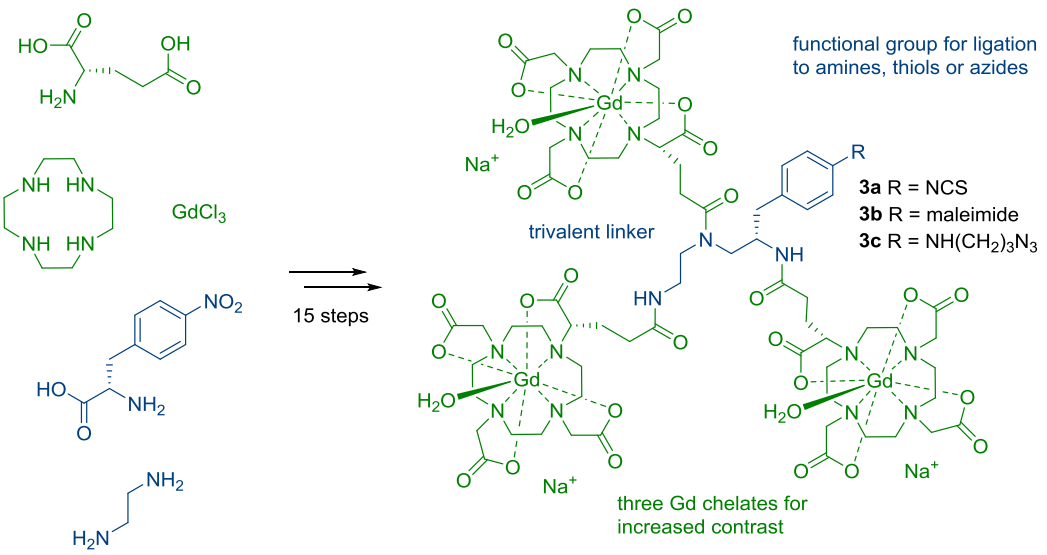


**Figure 2:** Synthesis of triple Gd chelate building blocks for biomolecule labelling

In addition, we have recently selected, sequenced and produced Adhirons that bind to TNC with dissociation constants of 10–50 nM (Figure 3A, B), but show no binding to the related protein Tenascin X (TNX) at 10 µM (not shown). In addition, we have demonstrated that a biotin-labelled version of one of our TNC-targeting Adhirons (Figure 3A) can be used to detect TNC in tumour slices with the same efficiency and selectivity as commercial TNC antibodies (Figure 3C). We are currently finalising the synthesis of TNC-targeted MRI contrast agents. In addition, we are currently evaluating dye-labelled TNC-targeting Adhirons as contrast agents for photoaccoustic imaging.

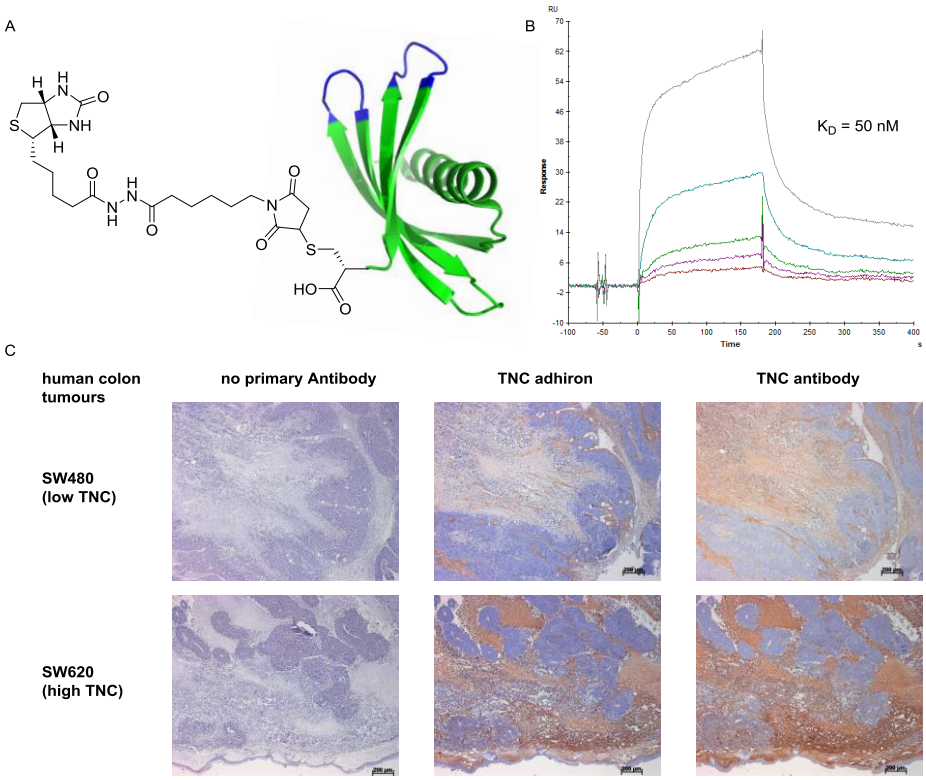


**Figure 3:** A biotin-labelled Adhiron (A) with a KD of 50 nM (B) was used to detect TNC in human colon tumour slices (C).

# Monitoring New Delhi Metallo-β-lactamase activity in live bacterial cells using NMR spectroscopy: new methods for antibacterials drug discovery

Alex Breeze

## Introduction

In the perpetual 'arms race' between pathogenic bacteria and their human and animal hosts, the microbes are once again gaining the upper hand, after close to three quarters of a century in retreat. A combination of factors that includes over-prescription of marketed antibiotics and a dearth of novel agents being brought into clinical use has contributed to the emergence of resistant strains, against which we currently have no effective therapies. Antibacterial drug discovery has been challenging, not least because inhibitors effective against isolated bacterial enzymes are often ineffective against whole bacterial cells; hence, new methods that permit measurement of enzyme activity in living bacteria are required. The β-lactam antibiotics that include the penicillins and cephalosporins have been among our most effective weapons against bacterial infection. Yet, their efficacy is waning as a result of the evolution of resistance mechanisms in the form of β-lactamases that disarm β-lactams through opening of the cyclic amide ring. New Delhi Metallo-β-lactamase (NDM-1) is a particularly alarming and rapidly disseminating resistance gene capable of cleaving even carbapenems, until recently considered the β-lactams of last resort because of their resistance to most β-lactamases. Development of new drug candidates that can inhibit the activity of these zinc-dependent β-lactamases, hence restoring the effectiveness of carbapenem antibiotics, is urgently needed.

## Results

In work performed with AstraZeneca, we have demonstrated that NMR spectroscopy can be used to monitor the effect of known inhibitors of NDM-1 on its β-lactamase activity in live bacterial cells. To demonstrate our ability to measure the enzymatic activity of NDM-1 in real time using

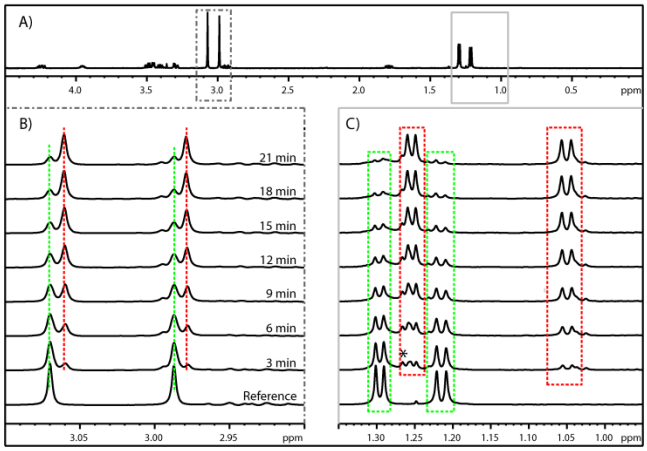


**Figure 1:** $^{1}$H NMR spectra (600 MHz) of meropenem hydrolysis in the presence of NDM-1 *E. coli* cells. A) The full $^{1}$H NMR spectrum of 100 μM meropenem in 50 mM sodium phosphate at pH 7.0. The hydrolysis of meropenem incubated with NDM-1 *E. coli* cells ($OD_{600}$ = 2.5) at different time points was monitored via the $^{1}$H NMR signals from B) the nitrogen-attached methyl groups and C) the carbon-attached ones. The green and red dotted lines/boxes represent the signals of substrate and product, respectively. The signals labelled with asterisks are from residual buffer contaminants.

NMR spectroscopy, we used a strain of *E. coli* that expresses the NDM-1 resistance gene. When we incubated the carbapenem antibiotic meropenem with NDM-1-expressing *E. coli* cells suspended in buffer in an NMR tube, we could clearly follow, in real time, the hydrolysis of the lactam ring using $^{1}$H NMR (Figure 1). Controls showed that this hydrolysis was not seen with non-NDM-1-expressing *E. coli* cells, nor was it due to cell lysis and release of NDM-1 into the medium, since hydrolysis was not observed in supernatants following centrifugation.

We next went on to examine whether we could observe inhibition of NDM-1 activity in the bacterial cell suspension using $^{1}$H NMR. There are very few documented inhibitors of Zn-dependent metallo-β-lactamases (hence the need for additional research in this area); however, although not suitable as an antibacterial drug, the marketed ACE inhibitor, L-captopril, has moderate inhibitory potency against a range of metallo-β-lactamases. Addition of captopril and another NDM-1 inhibitor, EDTA, to suspensions of NDM-1 *E. coli* cells in the presence of meropenem effectively inhibited the hydrolysis of the antibiotic in a dose-dependent fashion, as measured by the intensity of the $^{1}$H NMR resonances monitored in Figure 1. We were able to calculate half-maximal inhibition ($IC_{50}$) values of 175.0 μM and 1.6 μM, respectively, for L-captopril and EDTA (Figure 2), which are similar to literature values reported using isolated enzyme preparations and conventional enzyme inhibition assays.

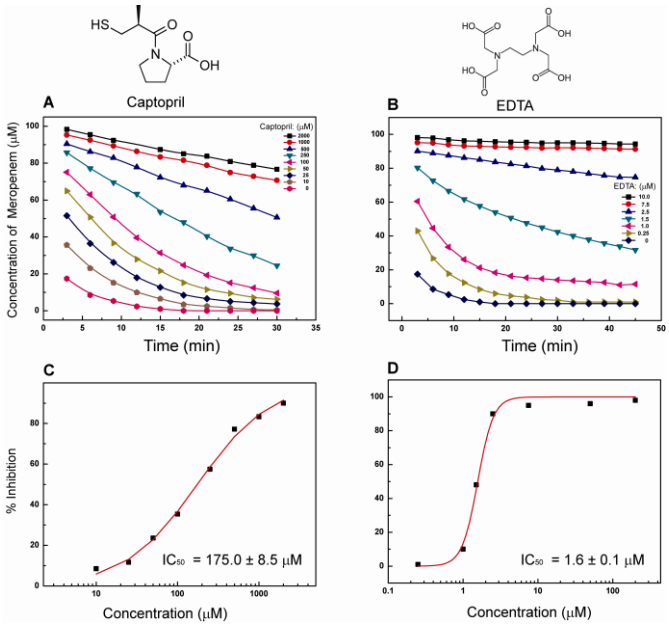


**Figure 2:** Inhibition of meropenem hydrolysis in the presence of NDM-1 *E. coli* cells by A) L-captopril and B) EDTA at various concentrations, and $IC_{50}$ measurements for L-captopril C) and EDTA D). For each experiment, the NDM-1 *E. coli* cells ($OD_{600}$ = 5.0) were first incubated with the inhibitor for 10 minutes before addition of 100 μM meropenem.

Our demonstration that $^{1}$H NMR can be used to monitor enzymatic activity in whole bacterial cell suspensions may open up new possibilities in drug discovery by bridging the gap between activity measured *in vitro* using isolated enzymes, and the desired activity against living cells – a gap that is often hard to cross in conventional antibacterials discovery approaches. We have subsequently gone on to show that we can use our NMR-based assay to screen compound collections against *E. coli* cells carrying the NDM-1 gene – an approach we are calling target-based whole cell NMR screening (Ma et al., *Angew. Chem. Int. Ed.*, in press).

**Publications**

Ma, J., Mcleod, S., Maccormack, K., Sriram, S., Gao, N., Breeze, A. & Hu, J. (2014) Real-time monitoring of New Delhi metallo-β-lactamase activity in living bacterial cells by $H^{1}$ NMR spectroscopy. *Angew. Chem. Int. Ed. Engl.* **53**: 2130-2133.

**Funding**

This work was funded by AstraZeneca PLC.

**Collaborators**

***External:*** J. Hu (AstraZeneca), G. Pielak (U. North Carolina)

# *In vitro* folding and remodelling of outer membrane proteins

Bob Schiffrin, Sam Hickman, Sheena Radford and David Brockwell

## Introduction

The outer membranes (OM) of Gram negative bacteria perform numerous essential and diverse functions, such as nutrient uptake (of vitamin $B_{12}$ by BtuB, for example), secretion of virulence factors and the maintenance of cell integrity. These functions are mediated by β-barrel outer membrane proteins (OMPs) which are found exclusively in the OM of bacteria, mitochondria and chloroplasts. We are currently investigating two aspects of OMP folding and dynamics: (i) the folding and assembly of a range of OMPs and the role associated assembly factors and (ii) the mechanical gating of the plugged lumen of an OMP by force-induced remodelling.

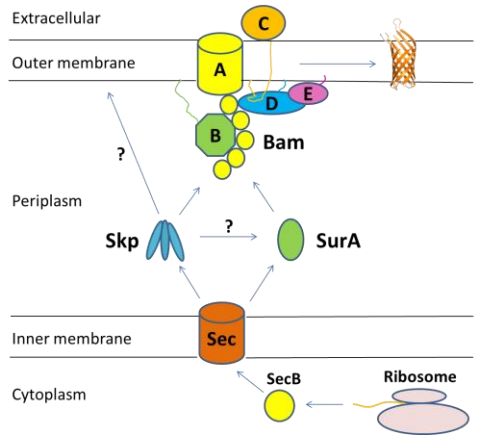


**Figure 1:** the OMP assembly pathway. Despite the availability of crystal structures for all proteins involved, very little is known at the molecular level about their role, function and interactions.

Key questions include: What is the molecular mechanism by which the Bam complex folds and inserts OMPs? What is the role of individual Bam components? How do periplasmic chaperones deliver OMP substrates to the Bam complex?

## Results

(i) The folding of OMPs *in vivo* is catalysed by the β-barrel Assembly Machinery (BAM) complex, a large hetero-oligomeric complex (Figure 1). BAM is an excellent potential antibiotic target given that it is essential, surface located and widely conserved across Gram negative species. Our work aims to gain insight into OMP assembly by recapitulating aspects of the

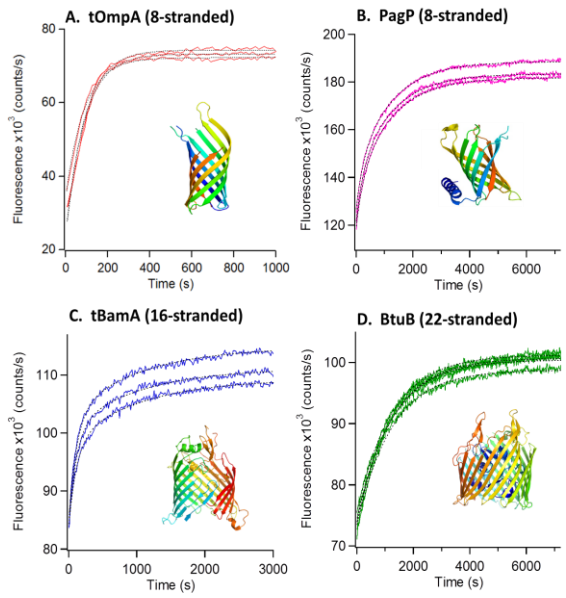


**Figure 2:** spectroscopic measurement of OMPs folding into liposomes.
(a) tOmpA: porin/adhesion, 19kDa.
(b) PagP: enzyme, 19 kDa.
(c) tBamA: insertase/secretase, 43 kDa.
(d) BtuB: transporter, 66 kDa.

All measurements carried out using 100 nm *di*$C_{11:0}$PC liposomes, in 0.24M urea, 50 mM glycine-NaOH, pH 9.5 at 25 °C. Inserts: crystal structures of tOmpA (PDB: 1QJP), PagP (PDB: 36P6), tBamA (PDB: 4C4V) and BtuB (PDB: 2GUF).

pathway using purified components. We have developed an *in vitro* assay to study the kinetics of chaperone-mediated folding of OMPs. We have shown that from an unfolded state in 8M urea, OMPs of different barrel sizes and structures can be folded into synthetic liposomes by rapid dilution, and the folding rate measured spectroscopically by monitoring changes in OMP intrinsic fluorescence (Figure 2). Work is now on going to dissect the effects of inclusion of folding factors in the assay on *in vitro* OMP folding. Using these kinetic assays, and a range of other biochemical and biophysical methods, we hope to provide new insights into the molecular mechanism of the BAM complex, chacterise its interactions with OMPs and periplasmic chaperones and assess how BAM modulates the OMP folding pathway.

(ii) Gram-negative bacteria use a specialised transport system to scavenge scarce essential nutrients, and actively transport them across the outer-membrane. How the interaction between the inner-membrane protein TonB and the Ton box of TonB-dependent receptors facilitates transport, however, remains unclear (Figure 3a). Our research has utilised atomic force microscopy (Figure 3b) to demonstrate that TonB is able to remodel the globular plug domain inside the core of the β-barrel using mechanical force before the non-covalent trans-membrane

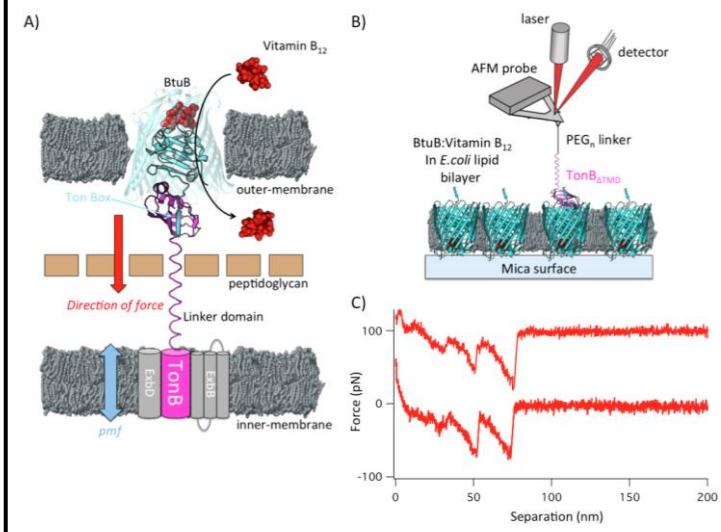


**Figure 3: (a)** the TonB-dependent transport system, TonB spans the periplasmic space and forms a 1:1 complex with BtuB by binding to the Ton Box. **(b)** the AFM experimental set up for investigating the BtuB plug remodelling when extended by mechanical force. **(c)** example traces showing the unfolding of the plug followed by the unbinding of TonB.

complex dissociates (Figure 3c). The remodelling is believed create a channel through the receptor that allows the passage of the bound substrate into the periplasmic space.

**Publications**

McMorran, L., Brockwell, D. & Radford, S. (2014) Mechanistic studies of the biogenesis and folding of outer membrane proteins *in vitro* and *in vivo*: what have we learned to date? *Arch. Biochem. Biophys.* **564**: 265-280.

**Funding**

This work was funded by the BBSRC and the Wellcome Trust.

# Cargo binding and regulation of kinesins

Joe Cockburn

## Introduction

Kinesins and cytoplasmic dyneins are molecular motors that use ATP hydrolysis to transport cellular cargoes along microtubules. Defects in these motors are associated with neurodegenerative diseases, developmental defects, ciliopathies and cancer. My research focuses on kinesins. The mammalian genome encodes around 45 different kinesin genes organised into 15 families. These molecules contain a motor domain related to those found in myosins, and generally associate into dimers via coiled-coil regions. In addition they usually harbour highly variable cargo-binding domains, reflecting the diversity in cellular cargoes that they transport. Similarly to myosins, most kinesins are believed to exist in an auto-inhibited state when not in use to avoid futile ATP hydrolysis; cargo binding must then lead to activation of processive motility. There are intriguing differences in how this is implemented in different kinesin families. For example, motors from kinesin families 1 and 2 "fold-up" so that their C-terminal cargo-binding regions inhibit microtubule binding and ATP hydrolysis by their motor domains, whilst kinesin-3 family motors exist in an inactive monomeric state when not bound to cargo, and are activated by cargo-induced dimerization. However, a detailed molecular description of kinesin recruitment and regulation by cargo is lacking. My research aims to obtain a structural and functional understanding how cellular cargoes (e.g. proteins, vesicles, organelles, viruses, mRNPs) recruit kinesin motors and how they regulate their motile activity. These questions are being tackled using a multidisciplinary approach involving extensive collaborations with other Astbury members, from structural techniques such as X-ray crystallography, electron microscopy and NMR to super-resolution live cell imaging and in-vivo studies. This will provide unique insights into the molecular mechanisms by which kinesins are regulated, and integrate this into output at the cellular and whole organism level.

## Funding

Startup funding from the Faculty of Biological Sciences (University of Leeds) is gratefuly acknowledged.

## Collaborators

***University of Leeds:*** M. Peckham, A. Breeze, N. Ranson, P. van Oosten-Hawle
***External:*** M. Way (CRUK, London Research Institute, London, UK)

# Physics of life in extreme environments

Matthew Batchelor, Toni Hoffmann, Megan Hughes, Katherine Ellen Kendrick, Natasha Rhys, James Towey, Katarzyna Tych, Danielle Walsh, Michael Wilson, David Brockwell and Lorna Dougan

## Introduction

Life has adapted to a vast range of environmental conditions and it is now difficult to find any place on Earth devoid of life. We are developing single molecule and neutron diffraction techniques to explore the physics of living systems under extreme conditions. These powerful techniques are used to study biomolecular self-assembly and the structure and dynamics of molecules in aqueous solutions, in both simple and complex systems.

## Research theme 1: Molecular mechanisms of cryoprotection

Cryopreservation of living cells and tissues has revolutionized areas of biotechnology, plant and animal breeding programmes and modern medicine. However, the molecular mechanisms by which cryoprotectants stabilise and protect molecules and cells, along with suppressing the formation of ice, are incompletely understood. We have completed neutron diffraction experiments with isotopic substitution and computational modelling to determine the atomistic level structure of the glycerol–water mixtures. Our aim is to find general rules for the action of cryoprotectants on water structure.

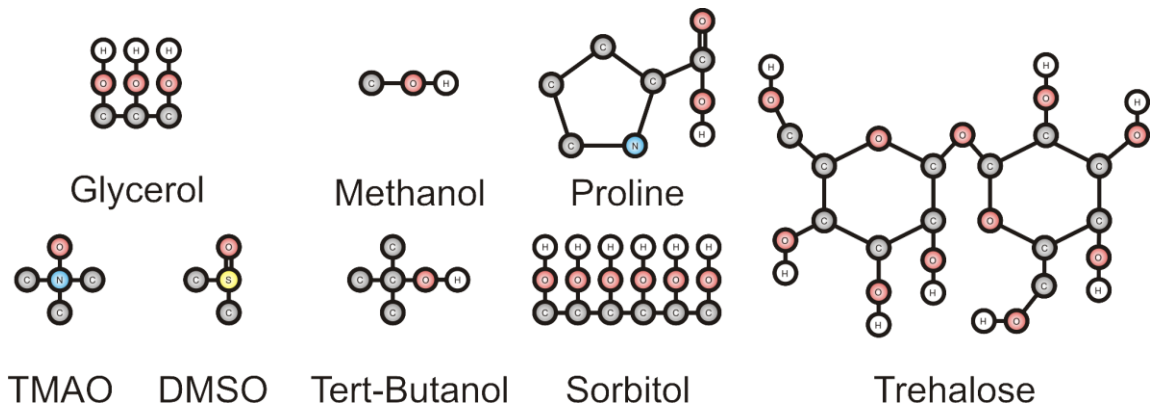


**Figure 1:** Schematic diagram of cryoprotectant molecules which have been examined using neutron diffraction and EPSR computational modelling. Carbon atoms are grey spheres labelled C, oxygen atoms are red spheres labelled O, hydroxyl hydrogens are white spheres labelled H, nitrogen are blue spheres labelled N and sulphur are yellow spheres labelled S.

## Research theme 2: Structural studies of self-assembly of biological molecules

Hydrogen bonding between glutamine residues has been identified as playing an important role in the intermolecular association and aggregation of proteins. To establish the molecular mechanisms of glutamine interactions, neutron diffraction coupled with hydrogen/deuterium isotopic substitution in combination with computational modeling has been used to investigate the structure and hydration of glutamine in aqueous solution.

## Research theme 3: Single molecule studies of proteins from extremophile organisms

Extremophiles are organisms which survive and thrive in extreme environments. The proteins from extremophilic single-celled organisms have received considerable attention as they are structurally stable and functionally active under extreme physical and chemical conditions. We have been developing single molecule force spectroscopy methods to mechanically manipulate

proteins from extremophilic organisms to gain information about their stability, flexibility and underlying energy landscapes.

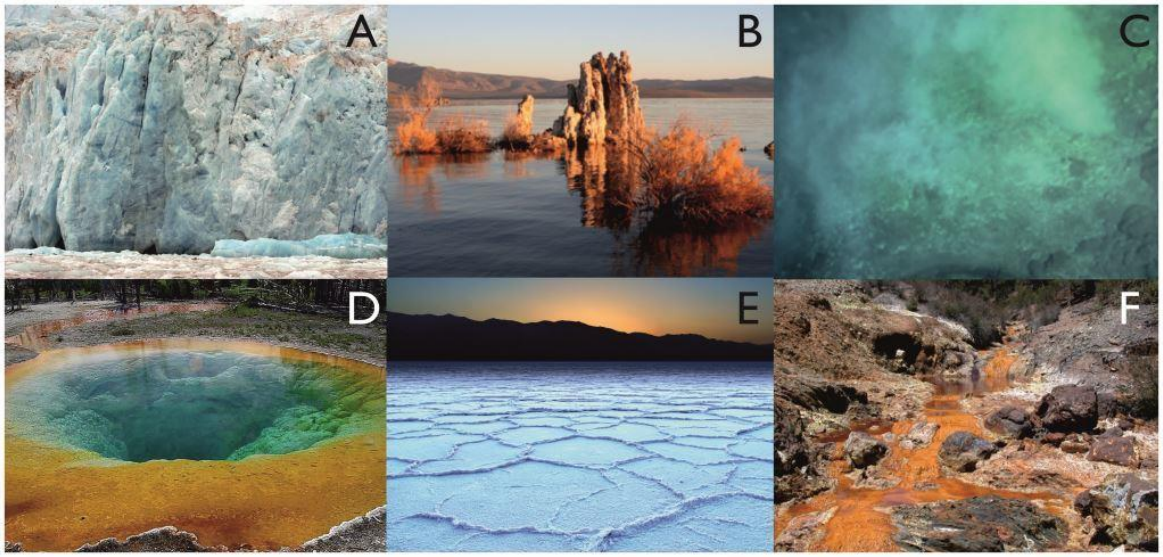


**Figure 2:** Examples of extreme environments (A) Chenega glacier, an active glacier in Alaska (image credit: U.S. Fish and Wildlife Service); (B) A calcium carbonate spire formed by the interaction of fresh spring water and the alkaline water of Mono Lake, California (image credit: Mila Zinkova); (C) Hot hydrothermal fluids and gases venting from the sea floor, Western Pacific Ocean (image credit: National Oceanic and Atmospheric Administration, U.S.A.); (D) Morning glory, acidic hot spring in Yellowstone National Park, U.S.A. (image credit: Jon Sullivan); (E) Badwater salt flats, California (image credit: Dave Toussaint); (F) The acidic Rio Tinto river in Spain (image credit: Carol Stoker, The National Aeronautics and Space Administration, U.S.A.).

**Publications**

Wolny, M., Batchelor, M., Knight, P., Paci, E., Dougan, L. & Peckham, M. (2014) Stable single alpha-helices are constant force springs in proteins. *J. Biol. Chem.* **289**: 27825-27835.

**Funding**

This work is being funded by the European Research Council, EPSRC and the BBSRC White Rose DTP in Mechanistic Biology

**Collaborators**

***External:*** A. Soper (Rutherford Appleton Laboratories,UK)

# The involvement of β-amyloid precursor protein proteolytic processing in neuronal iron homeostasis in dementia

Andrew Tsatsanis and James Duce

**Introduction.**

Iron is an essential element required as a cofactor in metabolic processes throughout the body and specifically in tissues of high oxygen consumption, such as the central nervous system. High levels of unbound iron are detrimental as this may catalyze the production of toxic reactive oxygen species. It is clear that increased cellular susceptibility to oxidative stress associated with iron accumulation leads to neurodegeneration. Age-related increases in neuronal iron, altered iron-related protein expression and increased susceptibility to oxidative stress have all been documented in neuropathological regions from patients with Alzheimer's disease (AD), Parkinson's disease and tauopathies.

One route in regulating cellular iron homeostasis is through proteins required to facilitate the efflux of iron from the cell. β-Amyloid precursor protein (APP), Ceruloplasmin and Hephaestin are all able to facilitate the movement of iron across the plasma membrane, partly through their ability to complex with the iron exporter ferroportin and promote its retention on the cell surface.

APP is a type 1 transmembrane protein more commonly known as the precursor to the toxic ß-amyloid peptide that accumulates in the AD brain. However, regulation of APP expression by iron regulatory protein implies a relationship with iron status. Our group strengthened this iron relationship through the discovery of the requirement for APP in promoting the efflux of iron via ferroportin in cells such as neurons. Prior to our discovery no mechanism was known for neuronal iron export as within the brain a membrane-associated form of Ceruloplasmin is only expressed on astrocytes and Hephaestin is only expressed in oligodendrocytes.

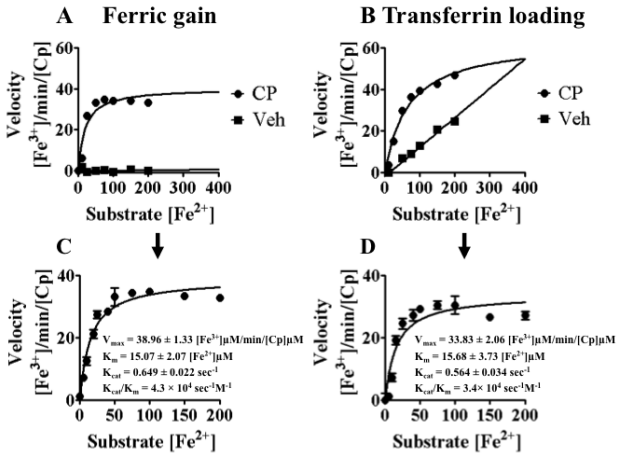


**Figure 1**. Characterizing the enzyme kinetics of ceruloplasmin. Plots representing raw kinetics blanked against 0 µM substrate of both CP activity and vehicle control auto-oxidation for (A) Ferric Gain, and (B) transferrin loading. Michaelis-Menten enzyme kinetics of CP blanked against auto-oxidation was measured by Ferric Gain (C) and TF loading (D). Conditions of the assays were as previously described at varying substrate concentrations ($FeSO_4$ 0-200µM). The individual data points shown are means ± S.E., n= 3 of a representative experiment, n=2.

**Results**

During the course of recent studies we have modified our original hypothesis in how APP is involved in neuronal iron efflux. Using a newly developed multiplex assay that is able to more accurately measure iron oxidation under physiological conditions, we have not only now published revised enzymatic kinetics for ceruloplasmin (Fig. 1), but also identified that in a normal physiological environment, ferric iron incorporation into transferrin is sufficiently enabled by the biological polyanions that are prevalent within extracellular fluids. Using this assay we have now determined that APP ferroxidase activity originates from phosphate. We

suggest that the presence of this physiologically abundant anion raises the possibility that APP facilitates the efflux of intraneuronal iron through an alternative mechanism to that previously reported; potentially either using the high anion, or soluble Ceruloplasmin, content within the surrounding extraneuronal environment. Biological evidence of a role for APP in iron efflux via ferroportin continues to be strengthened by our research illustrating; **(1)** correlation between surface presented APP and FPN in neurons, **(2)** evidence of altered iron homeostasis caused by α- and β-secretase cleavage of APP from the cell surface (Fig. 2 A&B), **(3)** altered iron levels caused by familial mutations in APP around the β-secretase cleavage site (Fig. 2 C&D), and **(4)** our previously published parallel work on tau requirement to transport APP to the cell surface to facilitate iron efflux. Findings on how the proteolytic processing of APP can regulate iron homeostasis have obvious implications for iron accumulation in familial AD as well as potentially hazardous side effects of β-secretase inhibitors currently being used as a therapeutic candidate in AD clinical trials.

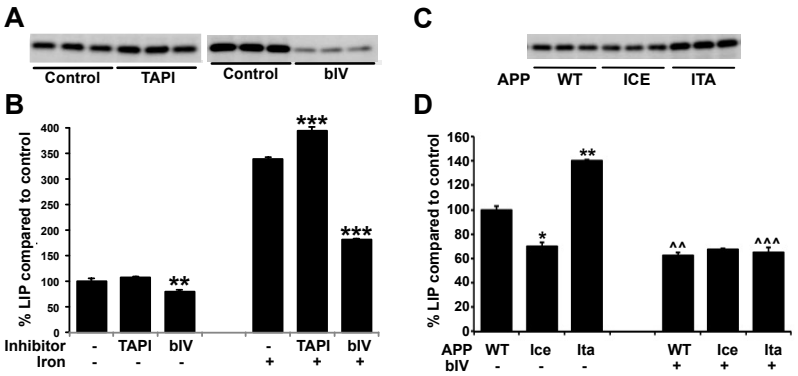


**Figure 2.** Neuronal iron homeostasis alterations caused by changes in APP proteolysis. **A & B.** SH-SY5Y neuroblastomas incubated with the α-secretase inhibitor TAPI increased ferritin expression (**A**) as well as intracellular labile iron pool as measured by Calcein-AM (see methods) (**B**). Inversely, β-secretase inhibition by bIV dramatically reduces ferritin expression (**A**) signifying a decreased labile iron pool (**B**). **C & D**. N2A neuroblastomas transfected with Icelandic-APP have reduced ferritin expression and decreased labile iron pool (LIP) but transfected with Italian-APP have increased ferritin and LIP compared to wt-APP overexpressing cells. The addition of bIV reduces the LIP to levels comparable to Icelandic-APP (**D**). Data are means ± SEM, N=3, *=p<0.05, **=p<0.01, ***=p<0.001 vs. control and in D ^^=p<0.01, ^^^=p<0.001 vs. non-treated samples by 2-tailed Ttest.

**Outlook.**

By continuing to support a novel candidate function for APP we now begin to explain the diverse trophic and morpho-regulatory activities of the protein and elucidate the vulnerability of the body to age-associated iron accumulation.

Current Aβ modulatory compounds such as β-secretase inhibitors attenuate Aβ production but also initiate a number of detrimental side effects, such as the iron dyshomeostasis suggested by our research, when administered at a dose that is too high. However, we propose that these drugs may still have therapeutic potential in AD if the administered dose is carefully monitored. Measuring iron in blood during β-secretase inhibitor administration may provide a more accurate biomarker for dose response in future clinical trials. Mediating the therapeutic dose of β-secretase inhibitor in response to plasma iron changes during administration could allow a better outcome for future clinical trials.

**Publications**

Wong, B.X., Tsatsanis, A., Lam, L.Q., Adlard, P.A., Bush, A.I & Duce, J.A. (2014) β-Amyloid Precursor Protein Does Not Possess Ferroxidase Activity but Does Stabilize the Cell Surface Ferrous Iron Exporter Ferroportin. *PLoS One* **9:** e114174.

Wong, B., Ayton, S., Lam, L., Lei, P., Adlard, P., Bush, A. & Duce, J. (2014) A comparison of ceruloplasmin to biological polyanions in promoting the oxidation of $Fe^{2+}$ under physiologically relevant conditions. *Biochim. Biophys. Acta* **1840**: 3299-3310.

Roberts, B., Lim, N., Mcallum, E., Donnelly, P., Hare, D., Doble, P., Turner, B., Price, K., Lim, S., Paterson, B., Hickey, J., Rhoads, T., Williams, J., Kanninen, K., Hung, L., Liddell, J., Grubman, A., Monty, J.-F., Llanos, R., Kramer, D., Mercer, J., Bush, A., Masters, C., Duce, J., Li, Q.-X., Beckman, J., Barnham, K., White, A. & Crouch, P. (2014) Oral treatment with $Cu^{ii}$(atsm) increases mutant SOD1 *in vivo* but protects motor neurons and improves the phenotype of a transgenic mouse model of amyotrophic lateral sclerosis. *J. Neurosci.* **34**: 8021-8031.

Wong, B. & Duce, J. (2014) The iron regulatory capability of the major protein participants in prevalent neurodegenerative disorders. *Front. Pharmacol.* **5**: 81.

Wong, B., Hung, Y., Bush, A. & Duce, J. (2014) Metals and cholesterol: two sides of the same coin in Alzheimer's disease pathology. *Front. Aging Neurosci.* **6**: 91.

Ayton, S., Zhang, M., Roberts, B., Lam, L., Lind, M., Mclean, C., Bush, A., Frugier, T., Crack, P. & Duce, J. (2014) Ceruloplasmin and beta-amyloid precursor protein confer neuroprotection in traumatic brain injury and lower neuronal iron. *Free Radic. Biol. Med.* **69**: 331-337.

**Funding**
This work was supported in the UK by a Senior Research Fellowship from Alzhiemer's Research UK, a Marie Curie Integration Grant from the European Commission and a Translational Project grant from Parkinson's UK. International support is also provided by the NHMRC, Australia.

**Collaborators**
***External:*** A.I. Bush (University of Melbourne, Australia), R. Cherny and D. Finkelstein (The Florey Institute, Australia), R. W. Evans (Brunel University, UK), D. Tetard and F. Lewis (Northumbria University, UK), D. Devos and J. C. Devedjian (Universite de Lille, France), I. Ganley and G. Allen (University of Dundee, UK), M. Ashford (University of Dundee, UK), D. Smith (Sheffield Hallam University, UK)

# Probing Bunyavirus N protein oligomerisation using mass spectrometry

Dale Shepherd, Antonio Ariza, Thomas Edwards, John Barr, Nicola Stonehouse and Alison Ashcroft

## Introduction

Bunyaviruses are becoming a major threat to both humans and livestock in Europe and the Americas. The nucleocapsid (N) protein of such viruses is key to the replication cycle and knowledge of this protein's oligomerisation is central to understanding the viral lifecycle and for development of therapeutic strategies.

## Results

Bunyamwera virus and Schmallenberg virus N proteins (BUNV-N and SBV-N) were expressed recombinantly in *E. coli* as SUMO-hexahistidine-tagged fusions. The tag was cleaved subsequently. Noncovalent nano-electrospray ionisation-mass spectrometry was conducted in the presence and absence of short RNA oligonucleotides. Conditions were optimised for the transmission of intact protein complexes into the gas-phase. The resulting protein-protein and protein-RNA complexes were identified and their stoichiometries verified by their mass. Collision-induced dissociation tandem mass spectrometry was used in cases of ambiguity.

Both BUNV-N and SBV-N proteins reassembled into N-RNA complexes in the presence of RNA; however, SBV-N formed a wider range of complexes with varying oligomeric states. The RNA-N oligomers observed were consistent with a model of assembly via step-wise addition of N proteins. Furthermore, upon mixing the two proteins in the presence of RNA no heteromeric complexes were observed, thus revealing insights into the specificity of oligomerisation.

Noncovalent mass spectrometry has provided the first detailed analysis of the co-populated oligomeric species formed by these important viral proteins and revealed insights into their assembly pathways. Using this technique has enabled comparisons to be made between the two N proteins.

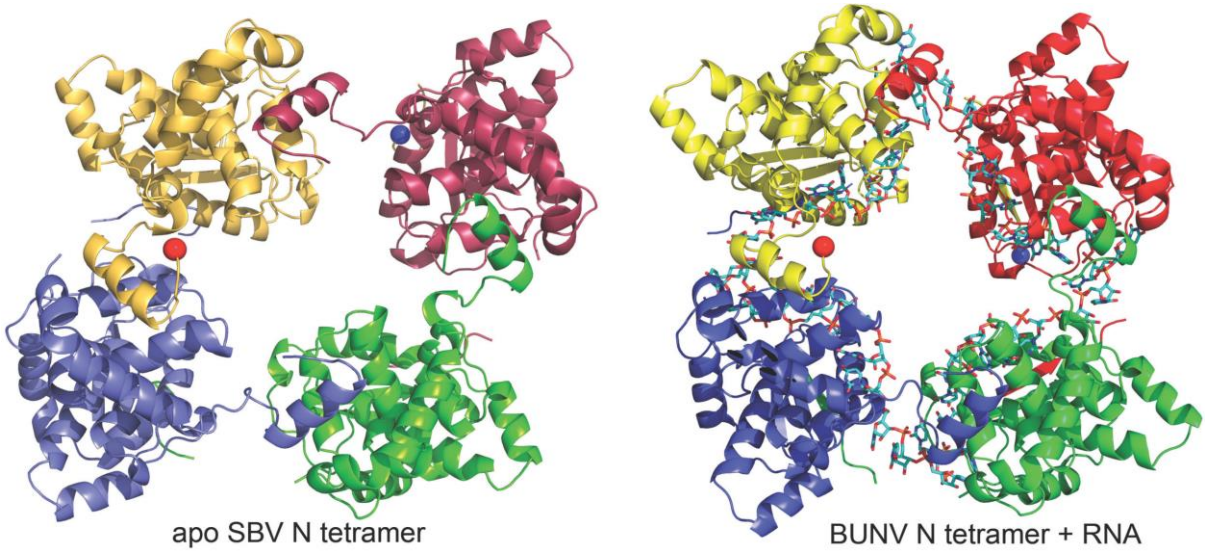


**Figure 1**: Tetrameric arrangement of proteins in the crystal structures. Apo Schmallenberg virus N to the left, and Bunyamwera virus N bound to RNA on the right. Larger complexes must form when the viral RNA genome is encapsidated by multiple N proteins.

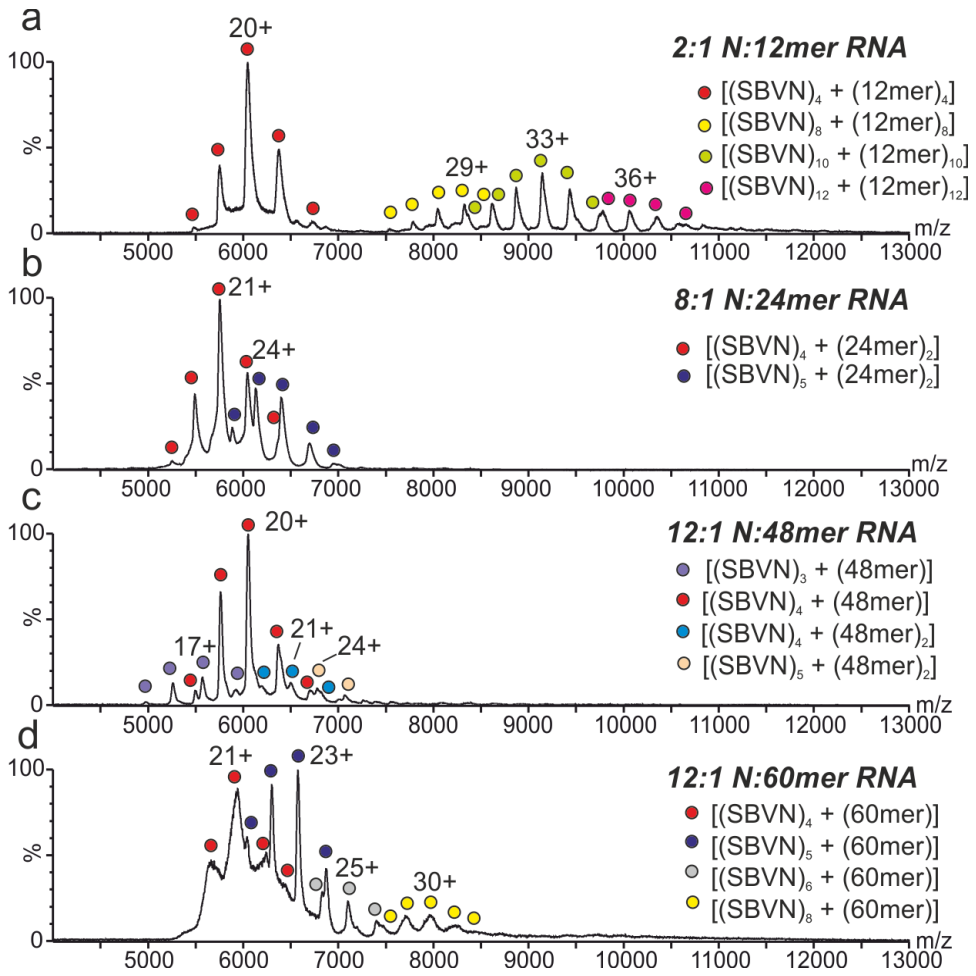


**Figure 2**: ESI-MS analysis of SBV N with synthetic RNAs. (a) SBV N in the presence of the 12-mer RNA forms complexes of $[(SBV)_4 + (12mer)_4]$ (red circles), $[(SBV)_8 + (12mer)_8]$ (yellow circles), $[(SBV)_{10} + (12mer)_{10}]$ (green circles) and $[(SBV)_{12} + (12mer)_{12}]$ (red circles); (b) SBV N in the presence of the 24-mer RNA forms complexes of $[(SBV)_4 + (24mer)_2]$ (red circles) and $[(SBV)_5 + (24mer)_2]$ (navy circles); (c) SBV N in the presence of the 48-mer RNA forms complexes of $[(SBV)_3 + (48mer)]$ (purple circles) and $[(SBV)_4 + (48mer)]$ (red circles) as well as small amounts of $[(SBV)_4 + (48mer)_2]$ (blue circles) and $[(SBV)_5 + (48mer)_2]$ (beige circles); (d) SBV N in the presence of the 60-mer RNA forms complexes of $[(SBV)_4 + (60mer)]$ (red circles), $[(SBV)_5 + (60mer)]$ (navy circles), $[(SBV)_6 + (60mer)]$ (grey circles) and $[(SBV)_8 + (60mer)]$ (yellow circles).

## Publications

Shepherd, D., Ariza, A., Edwards, T., Barr, J., Stonehouse, N. & Ashcroft, A. (2014) Probing bunyavirus N protein oligomerisation using mass spectrometry. *Rapid Commun. Mass Spectrom.* **28**: 793-800.

## Funding

This work was funded by the BBSRC and the Wellcome Trust.

# The crystal structure of the M2-1 protein from human respiratory syncytial virus (HRSV) and its function as an anti-terminator

Sian Tanner, Rachel Dods, Kavestri Yegambaram, Hannah Kyle, Antonio Ariza, Chi Trinh, John Barr and Thomas Edwards

## Introduction

Human respiratory syncytial virus (HRSV) is the leading cause of lower respiratory tract illness in young children and the immunocompromised. HRSV is a non- segmented negative-strand RNA virus from the Pnuemovirinae sub-family. The M2-1 protein of HRSV is a zinc-binding transcription antiterminator with an essential role in viral gene expression. M2-1 prevents premature transcription both intra and intergenically, however the exact mechanism by which M2-1 facilitates complete transcription is poorly understood. M2-1 interacts with other viral components including the phosphoprotein (P), matrix protein (M) and RNA further complicating attempts to understand the anti-termination activity of the M2-1 protein. Our work aims to elucidate the structure of the M2-1 protein and its function as an anti-terminator in addition to understanding the interactions of M2-1 with other viral components.

## Results

The crystal structure of HRSV M2-1 was solved to a resolution of 2.4 Å. M2-1 crystallized as a tetramer in all cases (Figure 1.A). This is consistent with experiments in solution where the protein has only been observed in the tetrameric state. Each M2-1 monomer forms three distinct regions linked by unstructured or flexible sequences (Figure 1.B). These regions are the zinc binding domain (ZBD) (residues 7–25) and tetramerization helix (residues 32–49), extending on an N-terminal arm, and the core domain (residues 69–172). The C-terminal 20 residues were not resolved as they are unstructured. The tetramer has a highly positively charged surface, which is consistent with its ability to bind RNA.

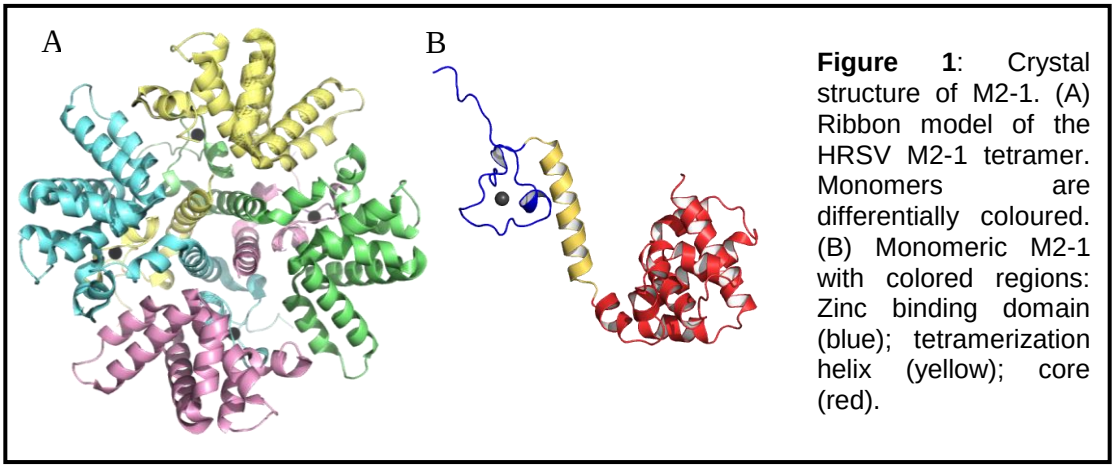


**Figure 1**: Crystal structure of M2-1. (A) Ribbon model of the HRSV M2-1 tetramer. Monomers are differentially coloured. (B) Monomeric M2-1 with colored regions: Zinc binding domain (blue); tetramerization helix (yellow); core (red).

M2-1 binds RNA, and mutants with compromised RNA binding *in vitro* also lose antitermination ability in cells, suggesting RNA binding is critical to M2-1 function. Conflicting data exists as to whether M2-1 binds viral mRNAs or viral genomic RNA. The binding affinities of a variety of 13mer RNA oligos were determined by fluorescence anisotropy. RNAs were 3' Fluorescein-tagged and included cis-acting signals from the HRSV genome, mRNAs and poly-G, -A, -U or –C homo-oligomers.

Of the four homo-oligomeric RNAs, poly-A bound with highest affinity ($K_d$ = 19.1 nM) (Figure 2.A). When examining the binding specificity for HRSV specific sequences, gene end sequences

were chosen as termination is signaled by conserved gene ends alone and M2-1 functions as a transcription antiterminator. Higher affinities were seen for mRNA transcripts than the viral genome sequences (Figure 2.B). As mRNA sense gene end sequences are more A-rich than their complementary sequence, this finding is consistent with our results for the homo-oligomers, in that M2-1 preferentially binds A-rich sequences.

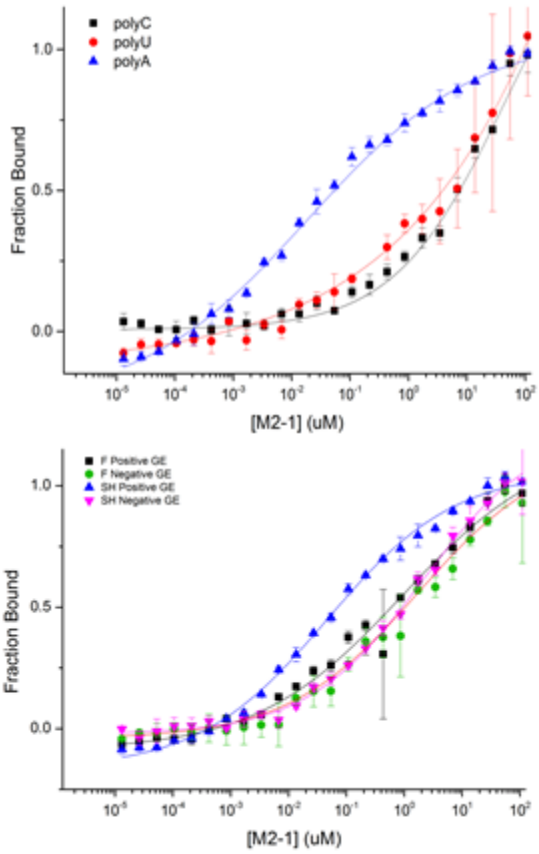


**Figure 2**: M2-1 binding to various RNAs. Fluorescence anisotropy binding isotherms for (A) homo-oligomers –pA, pC and pU (pG not fitted). (B) HRSV specific mRNA and viral genome sequences. All RNAs were 3'Fl labeled and 13 nucleotides in length.

There are still many unanswered questions surrounding the anti-termination activity of M2-1 including the exact mechanism of anti-termination, RNA specificity, and the interactions surfaces of M2-1 with other viral components. Current work aims to determine the structure of M2-1 bound to RNA and the P protein using X-ray crystallography. Structural insights into the surfaces involved in RNA or P binding will allow structure based anti-viral drug design directed against the M2-1 protein, another avenue currently under exploration.

**Publications**

Tanner, S., Ariza, A., Richard, C.-A., Kyle, H., Dods, R., Blondot, M.-L., Wu, W., Trincao, J., Trinh, C., Hiscox, J., Carroll, M., Silman, N., Eleouet, J.-F., Edwards, T. & Barr, J. (2014) Crystal structure of the essential transcription antiterminator M2-1 protein of human respiratory syncytial virus and implications of its phosphorylation. *Proc. Natl Acad. Sci USA* **111**: 1580-1585.

**Funding**
Funding for this work from the MRC and BBSRC is much appreciated.

**Collaborators**
***External:*** J. Eléouët (Unité de Virologie et Immunologie Moléculaires, Institut National de la Recherche Agronomique, F-78352 Jouy-en-Josas, France), J. Hiscox (Univeristy of Liverpool, UK), M. Carroll and N. Silman (Public Health England, UK), J. Trincao (Diamond Light Source, UK)

# Identification and optimisation of small molecule inhibitors as chemical tools

Roger Taylor, Lewis Turner, Aidan France, Rajendra Gosain, Syikin Hamzah, Rachel Trowbridge, Charlotte Revill and Richard Foster

## Introduction

Our group is interested in the design, synthesis and optimisation of small molecules for therapeutic application or their use in the elucidation of biological function. By combining tools and techniques in medicinal chemistry, computer-aided drug design and chemical genetics we identify and optimise small molecules as key modulators of specific biological function to support both basic target validation of proteins implicated in disease and as potential starting points for future drug discovery.

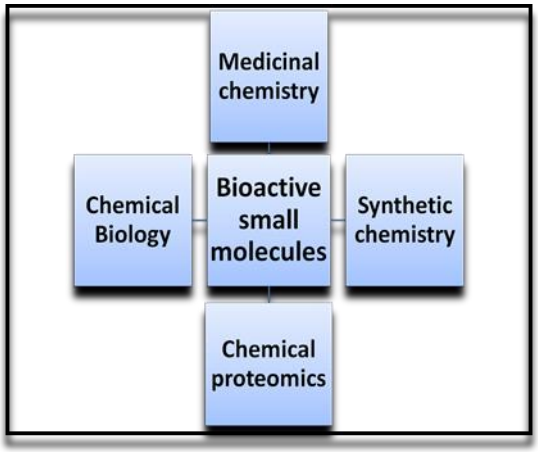


The group has capabilities in a number of areas for which bioactive molecules may be identified, optimised and/or targeted, including:

Medicinal chemistry, probe synthesis and chemical genetics

- Bio-targeted small molecules
- Targeted imaging agents
- Small molecule microarrays

Computational-aided drug design

- Ligand- and structure-based design
- Virtual screening

High-throughput screening

- 36k member diverse lead-like small molecule library
- 4k drug library for repurposing of chemical leads
- Fragment library
- Assay transfer/assay development expertise – to 384-well format incorporating a variety of assay formats and readouts

The activities are managed through the Medicinal Chemistry and Chemical Biology (MCCB) Technology Group as part of the Biomedical Health Research Centre (BHRC) at Leeds. Several projects in the cardiovascular and cancer disease areas have been progressed during 2014.

## Development of a novel anticoagulant with minimal bleeding risk

We have identified potent, novel small molecule inhibitors of a key enzyme involved in regulation of the coagulation cascade with exceptional *in vivo* efficacy. The inhibitors have been

identified by a number of parallel approaches incorporating virtual drug design, chemical synthesis and HTS of drug-like small molecule libraries and fragments. Presently, we are optimising the inhibitors for target potency, specificity and drug-like physicochemical properties using iterative rounds of medicinal chemistry development and screening using a panel of orthogonal bioassays. *with Helen Philippou, Robert Ariens, Colin Fishwick*

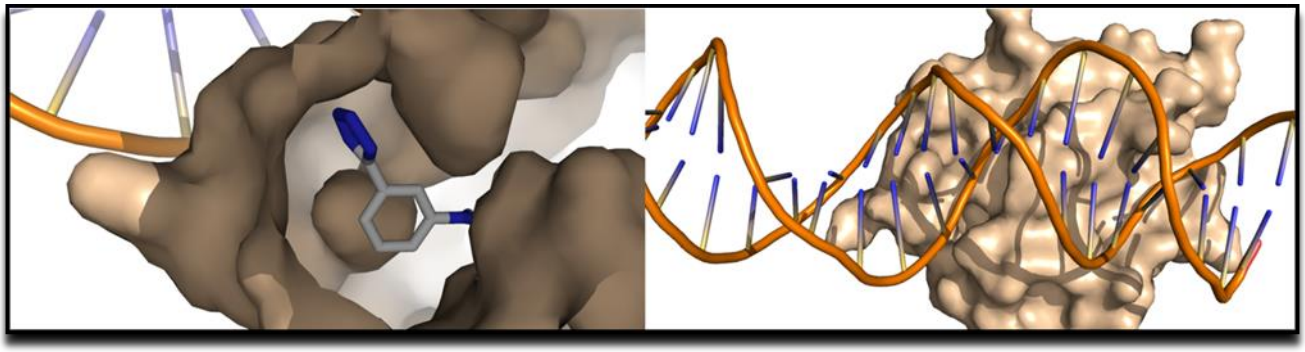

**Identification of novel inhibitors of TRP ion channel function as potential therapeutics**
We have identified a series of novel inhibitors of a number of TRP ion channels implicated in cardioprotection. The compounds have been developed as agents to support detailed understanding of the role of the protein target and its relevance in disease as well for future development of small molecule-based therapeutics. These dual aims are being achieved through iterations of directed chemical synthesis aided by pharmacophore-based design and screening *via* a panel of orthogonal assays. The current inhibitors are novel, potent and selective and demonstrate lead-like properties consistent with the potential for further development. *with Lin-Hua Jiang, David Beech, Rao Sivaprasadarao*

**Funding:**
Our work was funded by the MRC, EPSRC, BBSRC, AICR, CRUK, BHF and BHRC.

# Viruses as combined anti-cancer and antiviral immunotherapies

Adel Jebar, Matthew Bentham, Fiona Errington-Mais, Karen Scott, Adam Peckham-Cooper, Rajiv Dave, Giles Toogood, Daniel Swinson, Peter Selby, Alan Melcher and Stephen Griffin.

## Introduction

Hepatocellular Carcinoma (HCC) is the 4th most common, and 2nd deadliest malignancy worldwide. Over 70 % of HCC is caused by underlying infection with hepatitis B, or hepatitis C viruses (HBV, HCV), and the majority of cases are inoperable, with average survival measured in months. Current anti-HCC therapies such as Sorafenib are ineffective, extending life by only a few months at most, and have significant side-effects. Furthermore, the majority of treatments are immunosuppressive and can exacerbate underlying virus infections, further complicating HCC disease. Oncolytic viruses represent a burgeoning class of anti-cancer therapies. Whilst these were originally developed as direct cytotoxics, specifically eliminating tumour cells by virtue of preferential replication in this context, it is increasingly accepted that these agents mediate anti-cancer effects via the stimulation of host immune responses, rather than direct tumour lysis. We hypothesised that this pro-inflammatory mode of action might be particularly effective in the context of HBV/HCV positive HCC, simultaneously targeting both the tumour, as well as the underlying oncogenic virus infection.

## Results

We assessed whether clinical grade oncolytic orthoreovirus, also known as "Reolysin", provided effective treatment in pre-clinical models of HCC. Reovirus has demonstrated consistently safe administration in cancer patients, and, unlike other pro-inflammatory immunotherapies, has yet to reach a dose-limiting toxicity in clinical studies.

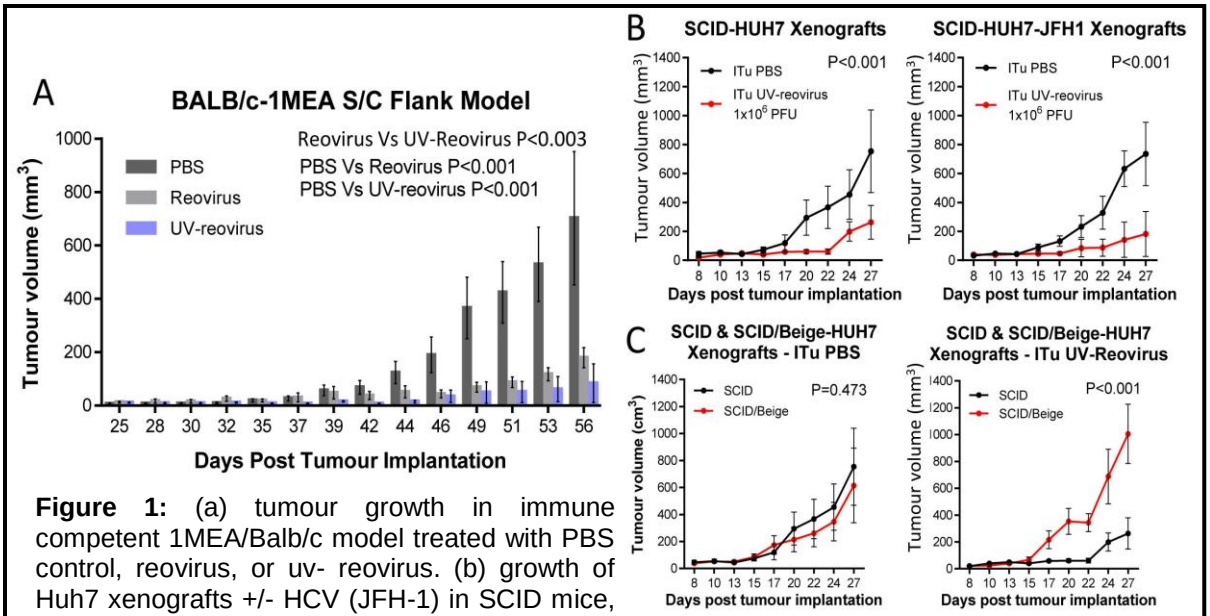


**Figure 1:** (a) tumour growth in immune competent 1MEA/Balb/c model treated with PBS control, reovirus, or uv- reovirus. (b) growth of Huh7 xenografts +/- HCV (JFH-1) in SCID mice, treated with uv- reovirus. (c) as (b), comparing SCID and SCID beige mice.

Both replication competent and *uv*-inactivated reovirus resulted in significant retardation of tumour growth in an immune-competent, syngeneic HCC model (1MEA flank xenografts in BALB/c mice, **Fig1A**), which translated to a significant survival advantage (not shown). This illustrated that the immune response to reovirus was sufficient to drive an anti-tumour response, independent of the virus completing its full infectious life cycle. Furthermore, treatment of immune-deficient models of HCV positive HCC with *uv*-inactivated reovirus (Huh7+/- HCV

JFH-1 xenografts in SCID) again resulted in therapy, whilst no therapeutic effect was observed in SCID/Beige mice, supporting that innate immune responses were critical for the anti-tumour effect, and that NK, or other degranulating immune cells, played a critical role in tumour clearance (**Fig1b/c**). *uv*-inactivated reovirus induced a potent inflammatory cytokine response,

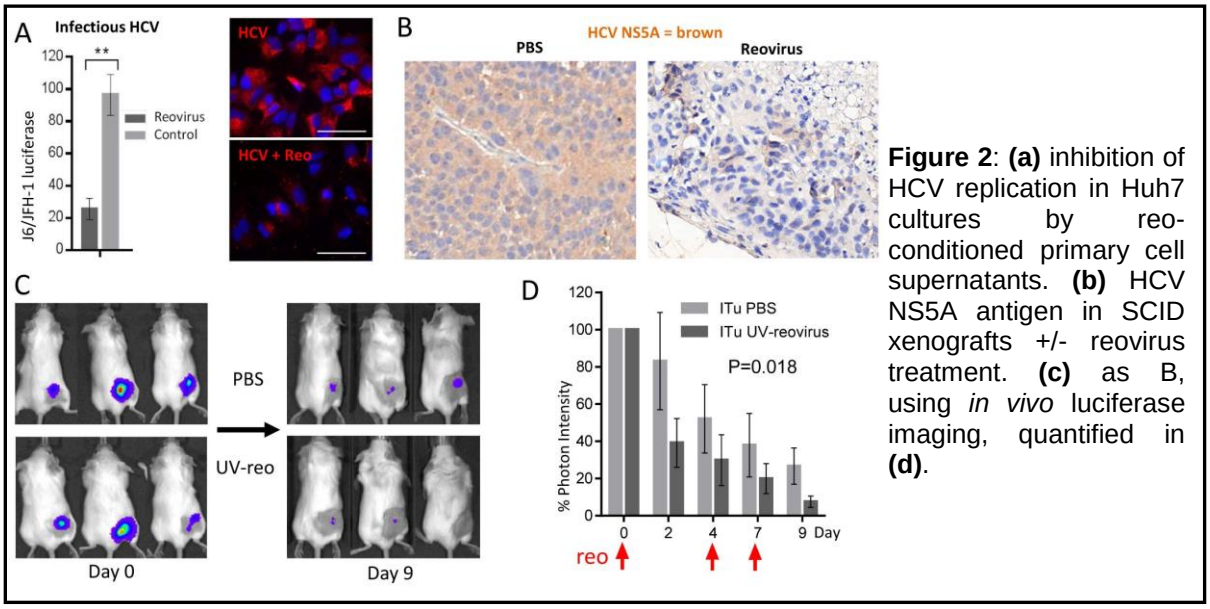


**Figure 2**: **(a)** inhibition of HCV replication in Huh7 cultures by reo-conditioned primary cell supernatants. **(b)** HCV NS5A antigen in SCID xenografts +/- reovirus treatment. **(c)** as B, using *in vivo* luciferase imaging, quantified in **(d)**.

primarily involving interferon (IFN) β, and that this could be recapitulated in primary explant cultures of human liver cells, including both hepatocytes and mononuclear cells. This IFN response was required for the activation of primary immune effector cells, and promoting their ability to kill tumour targets *ex vivo*. Finally, we showed that this same IFN-mediated response resulted in a simultaneous antiviral, as well as anti-tumour effect. This was observable both in cell culture models of HCV (and also HBV, not shown) HCC lines, as well as by *in vivo* imaging of HCV replication within the Huh7/SCID model. In conclusion, reovirus represents a potentially safe and effective treatment for HCC in the context of underlying oncogenic virus infection, and we are currently pursuing clinical studies combining this agent with standard of care in HCC patients.

**Publications**

Griffin, S. (2014) 'Too little, too late?' Will inhibitors of the hepatitis C virus p7 ion channel ever be used in the clinic? *Future Med. Chem.* **6**: 1893-1907.

Bentham, M., Marraiki, N., Mccormick, C., Rowlands, D. & Griffin, S. (2014) Ns2 is dispensable for efficient assembly of hepatitis C virus-like particles in a bipartite trans-encapsidation system. *J. Gen. Virol.* **95**: 2427-2441.

Foster, T., Thompson, G., Kalverda, A., Kankanala, J., Bentham, M., Wetherill, L., Thompson, J., Barker, A., Clarke, D., Noerenberg, M., Pearson, A., Rowlands, D., Homans, S., Harris, M., Foster, R. & Griffin, S. (2014) Structure-guided design affirms inhibitors of hepatitis C virus p7 as a viable class of antivirals targeting virion release. *Hepatology* **59**: 408-422.

**Funding**

Leeds CRUK Clinical Centre.

**Collaborators**

***External:*** R. Vile (Mayo Clinic, Rochester, USA), G. Nuovo and M. Coffey (Oncolytics Biotech, Canada).

# Studies on hepatitis C virus replication and pathogenesis

Hazel Stewart, Zsofia Igloi, Chris Bartlett, Joe Lattimer, Lorna Kelly, Chunhong Yin, Niluka Goonarwardane, Carsten Zothner, Nicola Stonehouse and Mark Harris

## Introduction

Hepatitis C virus (HCV) infects 170 million individuals and is a major cause of chronic liver disease, including fibrosis, cirrhosis and hepatocellular carcinoma. The virus has a single stranded positive sense RNA genome of 9.5kb that contains a long open reading frame encoding a single polyprotein of 3000 amino acids which is cleaved into 10 individual polypeptides by a combination of host cell and virus specific proteases. We are interested in understanding the molecular mechanisms of viral genome replication and assembly, with a particular focus on the virus-host interactions that underpin these processes. The ultimate goal of this research is to identify new targets for the development of novel antivirals.

A major focus of work is NS5A, a pleiotropic phosphoprotein with multiple roles in the virus lifecycle. We are investigating the roles of NS5A in virus replication and assembly, as well as its interactions with cellular factors. For example, we are following our mass spectrometric analysis of sites of phosphorylation (1) with a functional analysis of the role of this post-translational modification in virus replication. We are also investigating the interactions of NS5A and the Core (capsid) protein with RNA, both *in vitro* and *in vivo,* using the techniques of SELEX and CLIP.

In separate studies we are using imaging techniques to probe the multiprotein complex that replicates the viral genome. For example, genetically tagging the virus to enable either high resolution EM or fluorescent imaging, in collaboration with Michelle Peckham and Jamel Mankouri (Leeds) we are utilising both super-resolution and confocal microscopy, the latter located within a category III containment facility – a unique resource within the UK for the study of HCV. We are also developing adhirons (non-antibody binding reagents) to HCV proteins to facilitate this analysis (collaboration with Darren Tomlinson).

In collaboration with Colin Fishwick (Leeds) we are applying structure-based drug design methodology to the NS2 protein, a key protease involved in the cleavage of the viral polyprotein. We have established a robust cell-based assay to identify small molecules with the ability to block NS2 mediated cleavage. We hope that these may form the basis for a novel future therapeutic approach. An alternative approach to development of antivirals comes from a collaboration with colleagues in Brazil (Carol Jardim and Paula Rahal) to exploit the unique flora of that country for potential pharmacologically active compounds. Recent publications have exemplified both of these antiviral strategies.

Recently, homologues of HCV have been identified in other species, the closest relative is the non-primate hepacivirus (NPHV) identified in both dogs and horses. We have begun a programme of work on this virus, both as a model system to study HCV but also for comparative studies – although closely genetically related to HCV, NPHV does not appear to cause disease and this difference may shed light on some of the pathogenic mechanisms specific to HCV.

## Publications

Ross-Thriepland, D. & Harris, M. (2014) Insights into the complexity and functionality of hepatitis C virus NS5A phosphorylation. *J. Virol.* **88**: 1421-1432.

## Funding

Chris Bartlett is a student on the Wellcome Trust programme ‘The Molecular Basis of Biological Mechanisms’. This work is funded by a Wellcome Trust Senior Investigator Award.

**Collaborators**

***University of Leeds:*** J. Mankouri, M. Peckham, S. Griffin, C. Fishwick,

***External:*** T. Mbisa (Public Health England, UK), P. Simmonds (Roslin Institute, UK), J. McLauchlan (Centre for Virology Research, UK), K. Saksela (University of Helsinki, Sweden) C. Jardim (Federal University of Uberlandia, Brazil), P. Rahal (Sao Paolo State University, Brazil)

# Computational Biophysics

Glenn Carrington, Ben Hanson, Outi Kamaradin, Thana Suthibuttpong, Agnes Noy, Albert Solernou and Sarah Anne Harris

## Introduction

We use high performance supercomputing to understand biomacromolecules and their interactions. While there is a strong emphasis on addressing biological questions, we have the philosophy that understanding the physics of macromolecules is central to describing aspects of biomolecular function. Our research projects maintain a balance between applying existing methods, such as atomistic molecular dynamics (MD), and developing new approaches to improve on current theories, such as our new mesoscale modelling tool Fluctuating Finite Element Analysis (FFEA).

***Developing novel mesoscale modeling methods:*** Much of biophysics occurs at mesoscopic length-scales inaccessible to conventional atomistic calculations due to the computational expense of the calculations. We are developing a new meso-modeling method that extends finite element analysis from macroscopic length-scales down into the nanoscale by including thermal fluctuations, which is known as Fluctutating Finite Element Analysis (FFEA) (with Oliver Harlen and Daniel Read). These meso-simulations use bespoke code that we have developed and tested. Typically, the intermolecular interactions in the model are parameterised by calculating the surface potentials from atomistic information, and the flexibility is obtained from negative stain EM.

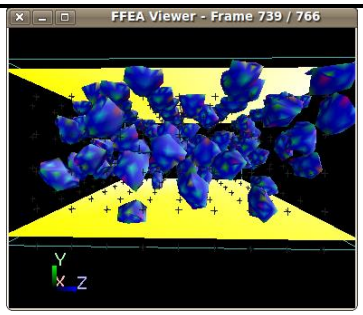


FFEA of multiple interacting proteins (blue) with two sticky surfaces (yellow).

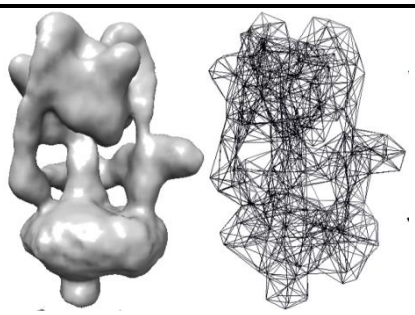

3D cryo (left) and FFEA mesh (right) for the rotary ATPase motor

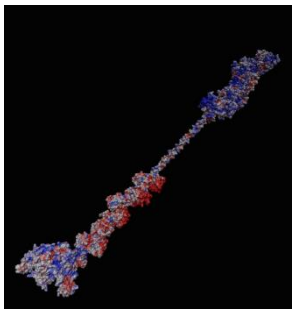

Atomistic structure of Myosin VII showing the electrostatic potential (blue is positive and red is negative).

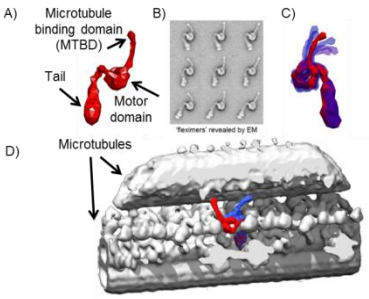


Flagellar dynein from cryoEM (top left), conformers showing the structural diversity of dynein from negative stain EM (top centre) and FFEA (top right), and FFEA of dynein within the axoneme (bottom).

The model has enabled us to study protein dynamics based on low resolution structural data from cryo-EM experiments on the dynein (with Stan Burgess), myosin (with Michelle Peckham) and rotary ATPase molecular motors (with Ste Muench). We are now also using FFEA to model fibrin aggregation during blood clotting (with Kerrie Smith).

***Atomistic MD simulations of supercoiled DNA:*** It is becoming increasing clear that the spatial and temporal organization of the genome, as well as the chemical sequence of the DNA bases, plays an important role in the storage and transfer of biological information. Bacterial DNA is compacted by supercoiling the long biopolymer into plectonemic loops. Through a joint computational/ experimental research grant (BBSRC with Tony Maxwell (John Innes Centre)) we have been testing the predictions of atomistic models of the structure and dynamics of supercoiled DNA minicircles, and investigating how supercoiling affects their recognition by other molecules.

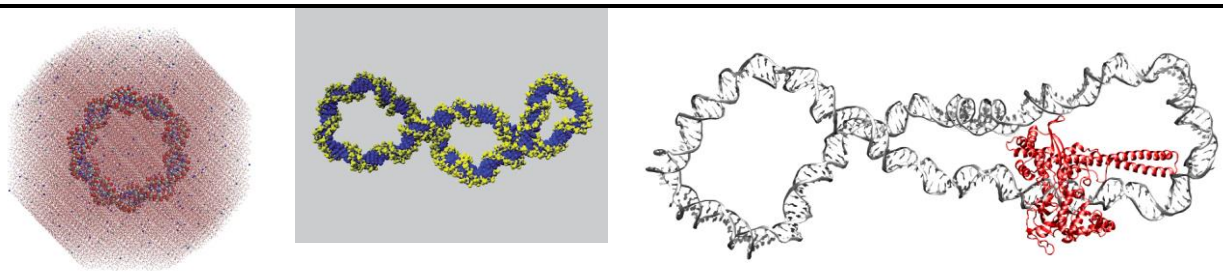

Atomistic MD simulations of supercoiled DNA showing a 90 base pair circle in explicit solvent (left), a plectonemically supercoiled 178 base pair over-wound circle (centre) and a 178 supercoiled minicircle interacting with human topoisomerase I (right).

***MD calculations of the entropic contribution during biomolecular recognition:*** Most rational drug design strategies use structure based methods to assess the chemical complementary of the ligand and its target. However, these techniques frequently neglect the contribution made by changes in entropy to biomolecular affinities, primarily because of the computational expense required to sample large regions of conformational space, but also because of the need for new quantitative physics based models of protein dynamics of flexibility.

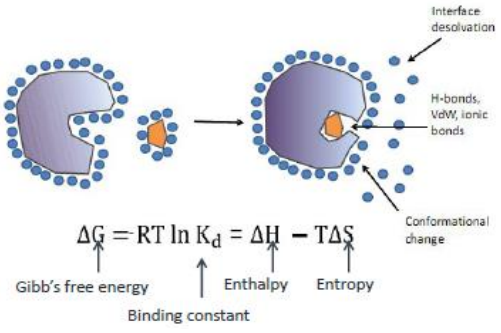


Schematic of thermodynamics changes during ligand/protein binding.

We are using atomistic MD, NMR and ITC (with Anastasia Zhurleva and Geoff Holdgate (AstraZeneca)) to measure the change in dynamics when the HSP90 chaperone binds a panel of

related inhibitory ligands. The aim is to provide new physical insight that will assist in the design of protocols for improving biomolecular affinities.

**Publications**

Richardson, R., Papachristos, K., Read, D., Harlen, O., Harrison, M., Paci, E., Muench, S. & Harris, S. (2014) Understanding the apparent stator-rotor connections in the rotary ATPase family using coarse-grained computer modeling. *Proteins* **82**: 3298-3311.

Kato, Y., Yagi, T., Harris, S., Ohki, S.-Y., Yura, K., Shimizu, Y., Honda, S., Kamiya, R., Burgess, S. & Tanokura, M. (2014) Structure of the microtubule-binding domain of flagellar dynein. *Structure* **22**: 1628-1638.

Toroz, D., Hammond, R., Roberts, K., Harris, S. & Ridley, T. (2014) Molecular dynamics simulations of organic crystal dissolution: The lifetime and stability of the polymorphic forms of para-amino benzoic acid in aqueous environment. *J. Cryst. Growth* **401**: 38-43.

D'annessa, I., Coletta, A., Sutthibutpong, T., Mitchell, J., Chillemi, G., Harris, S. & Desideri, A. (2014) Simulations of DNA topoisomerase 1b bound to supercoiled DNA reveal changes in the flexibility pattern of the enzyme and a secondary protein-DNA binding site. *Nucleic Acids Res.* **42**: 9304-9312.

Shoura, M., Ranatunga, R., Harris, S., Nielsen, S. & Levene, S. (2014) Contribution of fluorophore dynamics and solvation to resonant energy transfer in protein-DNA complexes: a molecular-dynamics study. *Biophys. J.* **107**: 700-710.

Elsheshiny, A., Ashcroft, A. & Harris, S. (2014) A comparison of the electromechanical properties of structurally diverse proteins by molecular dynamics simulation. *J. Biomol. Struct. Dyn.* **32**: 1734-1741.

**Funding**

This work was funded by the Thai and Egyptian governments, the EU PRACE supercomputing consortium, AstraZeneca, the BBSRC and the EPSRC.

# Kinetic dissection of the $Na^+$-coupled binding of hydantoin to purified Mhp1

Scott Jackson, Ekaterina Ivanova, David Sharples and Peter Henderson

## Introduction

The Mhp1 membrane protein from *Microbacterium liquefaciens* implements transport of compounds like 5-L-benzylhydantoin (BH), a product formed from nucleobases during death and decay of plants, into cells of bacteria. We have purified the protein, and its 3d structure has been determined in several conformations with and without bound substrate. When BH binds to the protein there is a quenching of tryptophan fluorescence. Here we show how measuring these fluorescence changes reveals the synergy and stoichiometry of $Na^+$ and BH binding to Mhp1.

## Results

Titrations of Mhp1 with benzylhydantoin (0-2mM) were repeated with different fixed [$Na^+$] over a wide range 0.33-125mM (Fig. 1A), keeping the ionic composition of the medium constant by complementing the increase of [NaCl] with decrease in [choline Cl].

$$Eq.1 \qquad \Delta F = \frac{\Delta F_{MAX} \times [L]}{(K_M + [L])}$$

The values of $K_M^{BH}(app)$ obtained by fitting each curve to the equation (1) were strongly dependent on the concentration of NaCl (Fig. 1A). This was analysed using eq. 2, where $K_M^{BH}(app)$ is considered to be an hyperbolic function of sodium concentration.

$$Eq.2 \qquad K_M^{BH}(app) = K_M^{BH} \times \left(1 + \frac{K_M^{Na^+}}{[Na^+]}\right)$$

With the increase of $Na^+$ concentration the values of the apparent $K_M^{BH}(app)$ asymptotically tend towards a 'true' $K_M^{BH}$ value (Fig. 1C), i.e. its thermodynamic dissociation constant. When each apparent $K_M^{Na^+}(app)$ is similarly determined by replotting the data in the form of titrations with $Na^+$ at different fixed [BH] a complementary series of hyperbolic curves is observed (Fig. 1B), also with an hyperbolic dependence of the apparent $K_M^{Na^+}$ on [BH] (Fig. 1D). Hence, as predicted by eq. 2, in the absence of either $Na^+$ or BH the apparent $K_M^{BH}$ or $K_M^{Na^+}$ increases towards infinity. This suggests that neither binds to Mhp1 in the complete absence of the other, which could mean that in the absence of both $Na^+$ and BH the great majority of Mhp1 molecules are in a closed form that does not bind either. The obvious candidate for this is the closed unloaded form of the protein, though it is possible that it is the open-inwards form, which we know from structural data and simulations has an extremely low affinity for $Na^+$.

When the log of the apparent $K_M^{BH}$ value was plotted against the log [$Na^+$] a reasonably linear plot with a slope of 0.83 was obtained. Similarly, when log $K_M^{Na^+}$ was plotted against log[BH] the slope was 1.06 implying that the ratio of Na:BH binding to Mhp1 is 1:1. This conclusion is reinforced when all the points are plotted on the same graph, when the unweighted fit to a straight line yields a slope/stoichiometry of 0.97 (Fig. 1E).

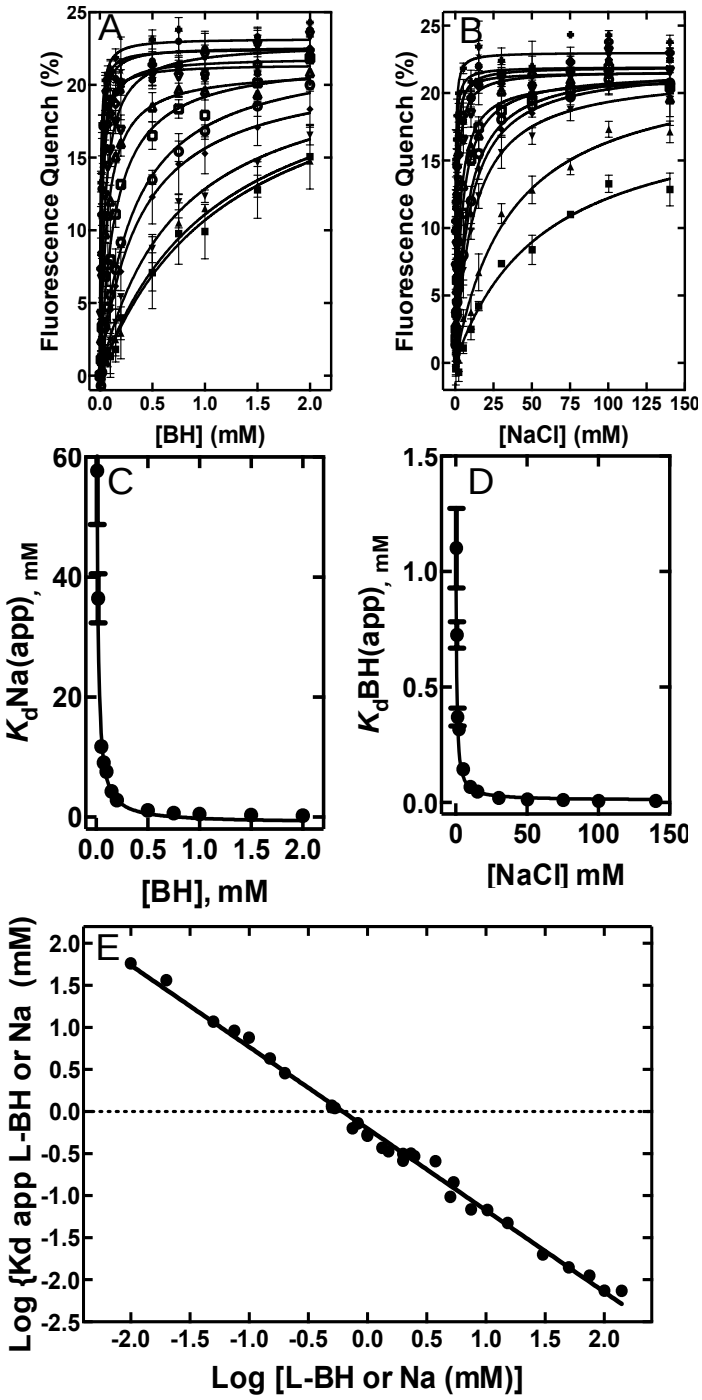


**Figure 1**: Synergistic interactions of BH and $Na^+$ with the Mhp1 protein deduced from steady state fluorescence measurements. **A.** Mhp1 (2.57□M) in 140mM cholineCl 10mM TrisCl pH 7.6, 0.02% DDM was mixed with increasing concentrations of BH (0.0, 0.1, 0.2, 0.5, 0.75, 1.0, 1.5, 2.0 mM) initially in the absence of added $Na^+$., and then the titrations repeated in the presence of different fixed concentrations of Na+ (0.0, 0.5, 0.8, 1.3, 2.3, 5.3, 10.3, 15.3, 30.3, 50.3, 75.3, 100.3, 140.3 mM), with the [cholineCl] adjusted downwards so that the overall osmolarity remained equivalent to 140mM salt. Each mixture was incubated with stirring for 1.5min at 18$^o$C, the spectrum was measured and the percentage change in the peak heights (fluorescence quench) was recorded. **B.** The same experiment as in A but plotted to show variation in the Kd(app) for $Na^+$ at the different fixed concentrations of BH given above. In both A and B the best fit lines were calculated by fitting the data to equation 1 in the text. **C**. The apparent Kd for Na+ at increasing [BH]. **D**. Apparent Kd for BH at increasing [Na+]. In both C and D the best fit lines were calculated by fitting the data to equation 2 in the text. **E**. Replot of log Kd(app) for either BH or Na+ vs log[BH] and log [Na+].

**Publications**

Simmons, K., Jackson, S., Brueckner, F., Patching, S., Beckstein, O., Ivanova, E., Geng, T., Weyand, S., Drew, D., Lanigan, J., Sharples, D.J, Sansom, M., Iwata, S., Fishwick, C., Johnson, A., Cameron, A. & Henderson, P. (2014) Molecular mechanism of ligand recognition by membrane transport protein, MHP1. *EMBO J.* **33**: 1831-1844.

**Funding**

Funding was from the BBSRC, Wellcome Trust and the EC

# β2-microglobulin amyloid fibrils disrupt membranes enriched in endosomal lipids and inhibit protein degradation by lysosomes

Sophia Goodchild, Toral Jakhira, Andrew Hellewell, Tania Sheynis, Matthew Jackson, Morwenna Porter, Rebecca Thompson, Kevin Tipping, Wei-Feng Xue, Neil Ranson, Paul Beales, Sheena Radford and Eric Hewitt

## Introduction

The formation of insoluble amyloid fibrils is associated with a spectrum of human disorders, including Alzheimer's, Parkinson's, type 2 diabetes and dialysis related amyloidosis (DRA). In these disorders the formation of amyloid fibrils is associated with cellular dysfunction and tissue destruction. Yet despite decades of research the culprit species and mechanisms of amyloid toxicity remain poorly understood. We use $\beta_2$-mircoglobulin ($\beta_2$m), which forms amyloid in DRA, as a model to study the pathological effects of amyloid fibrils. Our previous work demonstrated that $\beta_2$m amyloid fibrils, but not monomeric $\beta_2$m, disrupt purified lipid membranes and are toxic to cells. Moreover, nanoscale fibrils produced by fragmentation cause more membrane damage and are more toxic than their unfragmented precursors. In our recent work we examined in more detail the effect of $\beta_2$m amyloid fibrils on lipid membranes and cellular function.

## Results

A carboxyflorescein (CF) dye-release assay was used to investigate membrane damage resulting from the interaction between $\beta_2$m and membranes containing different anionic lipids. Recombinant $\beta_2$m monomer was incubated quiescently at pH 2 to produce unfragmented fibrils (length 1.30 ± 0.05 μm). These $\beta_2$m fibrils were subsequently agitated with a precision stirrer to produce fragmented fibrils (length 0.30 ± 0.01 μm). $\beta_2$m monomers and fibrils were incubated with lipid vesicles loaded with CF. Despite all species interacting with the liposomes, $\beta_2$m fibrils, but not monomeric $\beta_2$m, caused significant membrane damage that resulted in CF release (Fig. 1). Membrane damage conferred by fibrils was shown to occur primarily at acidic pH and to require an anionic lipid mix, although the degree of membrane disruption depended on the identity of anionic lipid component present (Fig. 1). Most strikingly, greatest membrane disruption was observed for lipids containing 50% bis(monoacylglycero)phosphate (BMP) liposomes at acidic pH (Fig. 1), conditions likely to be encountered in the endocytotic pathway.

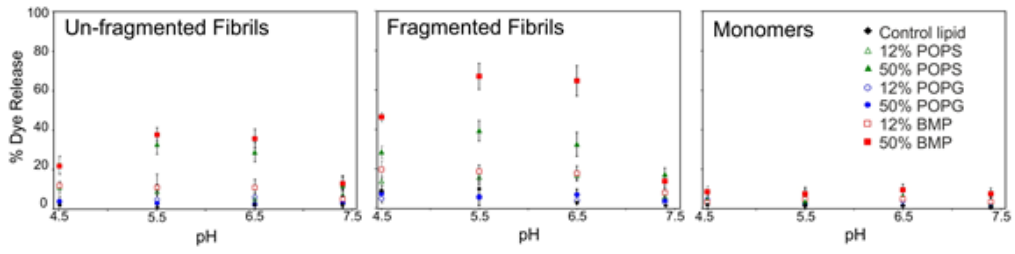


**Figure 1**: Relative CF dye release from LUVs containing 36 POPC: 20 POPE: 7 sphingomyleiln: 25 cholesterol (mol/mol) (control) plus 12 or 50 mol% POPS, POPG or BMP at pH 4.5-7.4. Errors: SD from n=3.

In order to determine the effect of $\beta_2$m amyloid fibrils on cells, the uptake and trafficking of $\beta_2$m amyloid fibrils was examined using confocal microscopy. This revealed that whereas unfragmented $\beta_2$m amyloid fibrils are predominantly located on the extracellular side of the plasma membrane, fragmented $\beta_2$m amyloid fibrils are endocytosed and trafficked to lysosomes (Fig. 2A). Despite being able to disrupt purified lipid membranes, fragmented $\beta_2$m amyloid fibrils did not increase lysosomal membrane permeability. However, incubation of cells with fragmented $\beta_2$m amyloid fibrils did cause missorting of the lysosomal membrane proteins LAMP-1 and CD63 to the plasma membrane and result in the inhibition of the degradation of endocytosed ovalbumin by lysosomes (Fig. 2B).

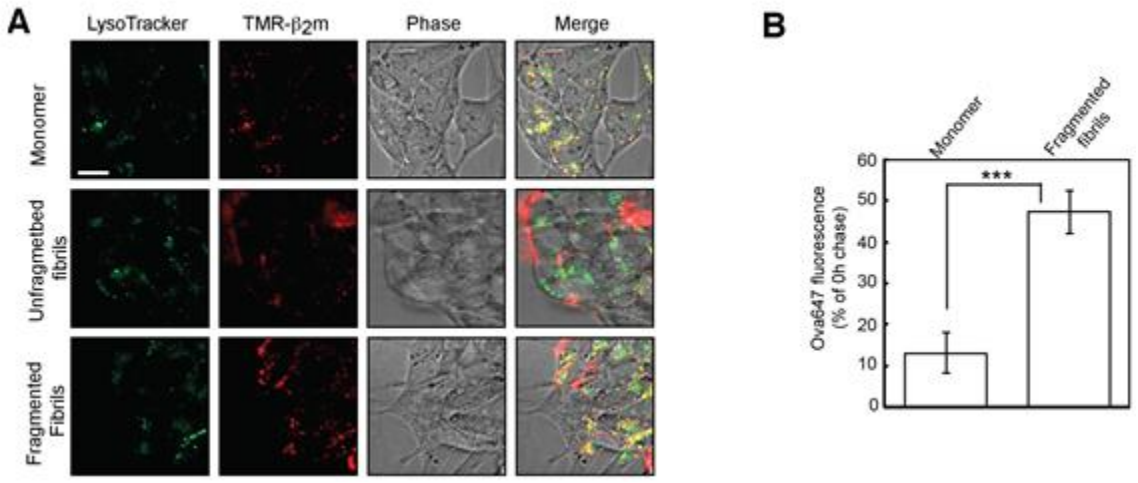


**Figure 2**: A. SH-SY5Y cells were incubated with TMR-labelled (red) monomeric β2m, or with either or unfragmented or fragmented TMR-labelled β2m fibrils for 4h. Acidic compartments were labelled with Lysotracker green. B. Cells were preinubated with either monomeric β2m or fragmented β2m fibrils. The capacity of lysosomes to degrade proteins was then assayed by incubating the cells with a fluorescently labelled ovalbumin (Ova-647). The % of Ova-647 remaining after a 24h chase in the absence of Ova-647 is plotted. Error bars indicate mean ± 1 SE.

In summary $\beta_2$m fibrils disrupt lipid membranes enriched in the endosomal lipid BMP at acidic and inhibit protein degradation by lysosomes.

**Publications**

Goodchild, S., Sheynis, T., Thompson, R., Tipping, K., Xue, W.-F., Ranson, N., Beales, P., Hewitt, E. & Radford, S. (2014) $\beta_2$-microglobulin amyloid fibril-induced membrane disruption is enhanced by endosomal lipids and acidic pH. *PLoS One* **9**: e104492.

Jakhria, T., Hellewell, A., Porter, M., Jackson, M., Tipping, K., Xue, W.-F., Radford, S. & Hewitt, E. (2014) $\beta_2$-microglobulin amyloid fibrils are nanoparticles that disrupt lysosomal membrane protein trafficking and inhibit protein degradation by lysosomes. *J. Biol. Chem.* **289**: 35781-35794.

**Funding**

This work was supported by the BBSRC, the European Research Council, the European Union (IEF fellowship), Yorkshire Kidney Research Fund and the Wellcome Trust.

# Hybrid protein-nanoparticle layers for photovoltaics

Ee Taek Hwang, Khizar Sheikh, Valentin Radu and Lars Jeuken.

## Introduction

As global energy consumption increases, the development of biological or bio-inspired systems for solar energy conversion has received intense interest. Sunlight is the most abundant renewable energy source and readily utilized by photosynthetic organisms through a complex cascade of photoinduced energy and electron transfer steps, leading to efficient charge separation and high quantum yields. The elegant way nature converts solar energy has inspired scientists to create synthetic photo-electrochemical cells in which biomimetic conversion systems generate electrical power or photofuels (ethanol, H2, etc.). Many studies aim to integrate nature's light-harvesting systems such as chloroplasts, thylakoids, photosynthetic reaction centres of bacteria and photosystems (photosystems I and II) with synthetic systems.

Besides using biosystems for light harvesting, many studies have been performed with inorganic systems such as semi-conducting nanoparticles or quantum dots. Although inorganic materials do not suffer the generally short lifespan of their biological counterparts, they often suffer in their quantum yield as they are not as efficient in charge separation. In biology, charge separation proceeds by a series of fast electron-transfer steps along a chain or wire of redox centres. In 2014, we developed a hybrid system where we have coupled a dye-sensitized $TiO_2$ nanocrystal to a decaheme protein from *Shewanella oneidensis* MR-1, known as MtrC, Figure 1. In this biomimetic system, the dye-sensitized nanocrystal functions as the light harvesting centre and MtrC provides a long redox chain for charge separation. Electron transfer across the ten hemes in MtrC will spatially separate the photo-induced charge from the nanocrystal, potentially reducing charge recombination. The successful construction of the biohybrid system is confirmed by a photoswitching behaviour where the photocurrent depends on the redox state of the MtrC electrical bridge.

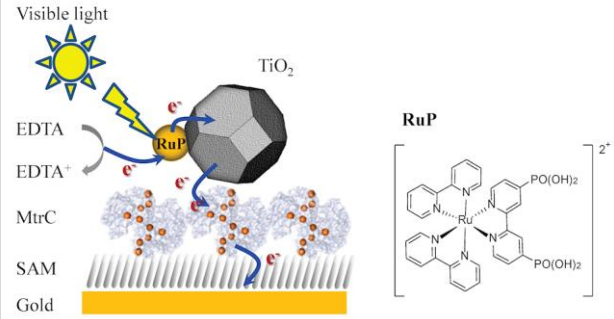


**Figure 1**: (Left) Schematic representation of the layered MtrC/$TiO_2$ system on gold electrode modified with a self-assembled monolayer (SAM). The interfacial electron transfer step required for the generation of a photocurrent. (Right) The molecular structure of the cation $Ru(bpy)_2(4,4'\text{-}(PO_3H_2)_2bpy)](Br)_2$ (**RuP)**

## Results

To optimize construction of the photoanode comprised of **RuP**-$TiO_2$ and MtrC on a gold electrode, ultra-flat template-stripped gold surfaces were modified with a range of different self-assembled monolayers (SAMs), made up of various mixtures of alkanethiols with positive (amine), negative (carboxylic acid) and uncharged (hydroxyl) 'headgroups'. MtrC redox signals, indicating interfacial electron transfer, were only detected for SAMs with positively charged surfaces and the highest electroactive coverage was obtained with a SAM consisting of 8-mercaptooctanol (8-OH) and 8-amino-1-octanethiol (8-$NH_3^+$) in an 80/20 ratio.

$TiO_2$ has a high affinity for the carboxylates in Glu/Asp side chains and we previously used this propensity to couple P25 **RuP**-$TiO_2$ nanoparticles to redox enzymes in solution. However and unexpectedly, we did not observe immobilization of P25 $TiO_2$ or **RuP**-$TiO_2$ on either MtrC films or bare gold electrodes modified with SAMs (either pure or mixtures of 8-OH, 8-$NH_3^+$ and/or 8-

mercapto-octanoic acid). In contrast, when we incubated the electrode surfaces with the mono-disperse synthesized 3,4-dihydroxybenzoic acid-modified $TiO_2$ nanocrystals (0.2-0.5 mg $mL^{-1}$) of 6.7 nm, a densely-packed $TiO_2$ monolayer was formed on either MtrC films or bare SAM surfaces within 5 minutes, as monitored with QCM-D and AFM.

In the presence of EDTA as a sacrificial electron donor, photocurrents are readily observed upon excitation of the **RuP**-TiO2 nanocrystals with visible light. Control experiments without each of the components (**RuP**, $TiO_2$ or EDTA) gave no observable photocurrent, indicating that **RuP** does not directly interact with MtrC. Furthermore, in the presence of $TiO_2$, but absence of **RuP**, photocurrents were observed under UV light, confirming that electron transfer proceeds from $TiO_2$ to MtrC (Figure 1).
Since MtrC is a redox protein that exists in oxidized and reduced states, it can also operate as an electrical diode or on/off switch for photocurrent. When MtrC is reduced at potentials below -0.3 V, no oxidative photocurrents are observed and the system behaves the same as without the sacrificial electron donor EDTA (Figure 2A). This switch is clearly distinct from the behaviour of **RuP**-TiO2 without MtrC (when $TiO_2$ is directly adsorbed on the SAM-modified electrode). In Figure 2B, differences in photocurrent with and without EDTA are plotted, where the switch in oxidative photocurrent is more clearly visible upon reduction of MtrC. When MtrC is reduced (i.e. at potentials below 0 V), the electron transfer from **RuP**-$TiO_2$ to MtrC is impaired, explaining the observed switch in photocurrent. The switch thus provides direct proof that for the MtrC/$TiO_2$ hybrid system the majority of electron transfer proceeds via MtrC and that the densely-packed monolayer of MtrC prevents direct interaction between the gold electrode and the **RuP**-$TiO_2$ layer, confirming the formation of the layered structure schematically depicted in Figure 1.

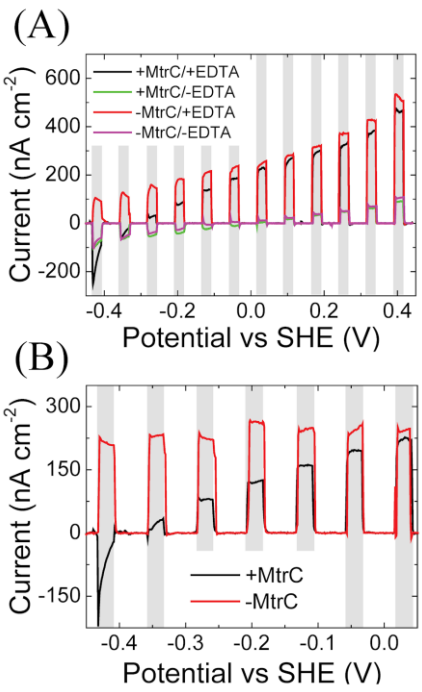


**Figure 2**: (A) Effect of applied bias potential on the photocurrent of MtrC/$TiO_2$ (+MtrC) and $TiO_2$ only (- MtrC) measured w ith EDTA (+ EDTA) and without EDTA (-EDTA). The response was measured by linear sweep voltammetry (LSV) at 5 mV $s^{-1}$. (B) Normalized photocurrent (the difference between photocurrent generalized with and without the sacrificial electron donor EDTA). The grey bars represent the times during with the photoanodes are illuminated.

**Funding**
This work was funded by the BBSRC.

**Collaborators**
***External:*** M. Gross, K. Orchards, C.-Y. Lee, E. Reisner (University of Cambridge, UK); D. Hojo, T. Adschiri (Tohoku University, Japan); E. Ainsworth, C. Lockwood, J. Butt (University of East Angla, UK).

# Flexibility within the heads of muscle myosin-2 molecules

Neil Billington, Derek Revill, Stan Burgess and Peter Knight

## Introduction

The heads of muscle myosin molecules generate the force and movement for muscle contraction, but their mechanical properties are controversial. Myosin forms the thick filaments of muscle, generating an axial force through the heads binding to actin subunits of the thin filaments and producing sliding of the filaments past one another. The heads comprise a motor domain which hydrolyses ATP to power movement, and the changes in motor conformation are amplified by a lever that extends from the motor and connects to the thick filament backbone. This lever is an α-helix that is stabilised by the attachment of two calmodulin-like light chains that wrap around it. X-ray crystallography has shown variation in lever shape and more strikingly a diversity of angles of attachment of the lever to the motor that arise from differences in the conformation of the polypeptide at the junction between motor and lever. However, crystallography is not the best way to determine the origins of this diversity, since flexibility in solution has to be suppressed when crystals form. Electron microscopy of individual molecules offers an alternative approach, because diversity within a large number of images of molecules can represent the diversity of conformations adopted by each molecule over time through thermal excitation. Quantitative analysis of this diversity can then yield estimates of mechanical properties.

## Results

Atomic structures of chicken skeletal and scallop cross-striated muscle myosin heads isolated by proteolysis have been deduced previously by X-ray crystallography, so we collected images of these heads by negative stain electron microscopy and also from rabbit skeletal muscle myosin which is commonly studied. In addition to native chicken myosin heads we studied the product of reductive methylation, since this procedure was used to induce the chicken protein to crystallise, and we wanted to test whether this had modified its structural characteristics.

Aligning and averaging thousands of images of individual heads allows consistent features to be reinforced while noise is suppressed (Fig. 1). The heads are usually oriented in a specific way so we see a particular outline for the motor domain that fits well with a view of the crystal structure. In addition the lever shows detail that is recognisable as the light chains. Further classification of the images based on just the pixels in the lever region of the images, shows the diversity of lever position relative to the fixed motor domain (Fig. 1). The lever appears flexible, mainly about a fulcrum situated at the junction between the motor and lever domains. This coincides with a site at which the head can flex in forming a specific, shut down conformation when muscle myosin molecules are enzymatically inactive.

A quantitative assessment of the characteristics of the lever flexibility was obtained by measuring lever angles in a large dataset of head images classified into many lever classes. For all four different myosin head species, the data are well fitted by a Gaussian distribution Fig. 1). This strongly suggests that the variation in lever angle seen in the data derives from thermal excitation of an elastic protein conformation, acting as a torsion spring, as goverened by the Equipartition Theorem. The variance value obtained from the fitted Gaussian distribution is thereby related to the mechanical compliance of the elastic element. The torsional stiffnesses of the four types of heads is similar and averages about 25 pN.nm/rad$^2$. For a muscle myosin head working as part of the thick filament, this torsional stiffness is manifested in the resistance of the tip of the lever to axial movements along the muscle fibre, *i.e.* as if the lever was a bending cantilever. This cantilever stiffness is estimated at about 0.4 pN/nm. This value is lower than recent estimates for

the stiffness of crossbridges in muscle, and we therefore suggest that attachment of the head to actin increases the stiffness of the motor-lever junction.

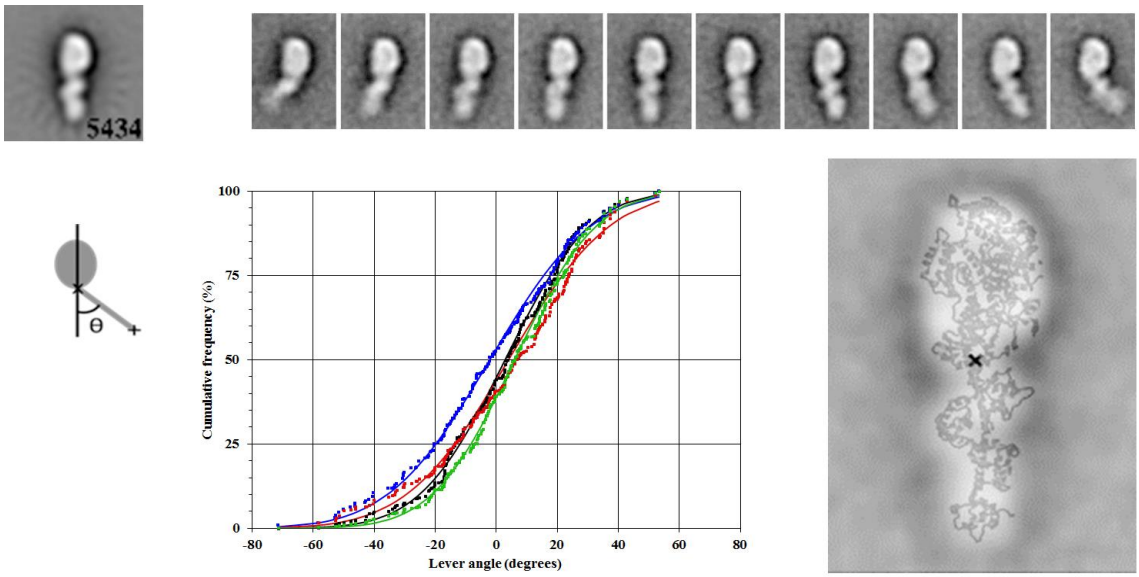


**Figure 1**: Flexibility in myosin heads. Top left global average of 5,434 motor-aligned head images. Top right shows classification of images into 10 classes based on lever angle. Lower left shows lever angle definition. Centre shows the distribution of lever angle for 4 types of head, together with fitted Gaussians. Blue denotes scallop heads, black is methylated chicken, green is chicken and red is rabbit. Right shows scallop head crystal structure backbone ribbon superposed on an image average from the centre of the distribution, with the flexion fulcrum as an **x**.

All four types of myosin head examined showed similar shapes, including the median (unstrained) angle between the lever and motor domains. Thus reductive methylation of the chicken heads prior to crystallisation has no obvious effect on the head shape. The good fit of that shape to the scallop crystal structure for all the types of head indicates that the scallop structure more closely resembles the structure of the myosin head in solution, and the more bent shape of the chicken crystal structure suggests that the forces between molecules during crystallisation of the chicken heads has favoured a conformer containing some internal strain.

**Publications**

Billington, N., Revill, D., Burgess, S., Chantler, P. & Knight, P. (2014) Flexibility within the heads of muscle myosin-2 molecules. *J. Mol. Biol.* **426**: 894-907.

**Funding**

This work was funded by the BBSRC and Wellcome Trust.

**Collaborators**

***External:*** P. Chantler (Royal Veterinary College, University of London, UK)

# Fep1d: a script for the analysis of reaction coordinates

Polina Banushkina and Sergei Krivov

## Introduction

With the growing number of experiments and the steady progress in the simulations of different biological, physical and chemical processes the rigorous quantitative analysis of the obtained data becomes all the more important. The complex nature of the processes and the large size of data sets generated by simulation and experiment make the development of automated analysis tools very important, practically and conceptually.

One popular method of such a data analysis is the projection of multidimensional coordinate space to a one dimensional reaction coordinate (RC). During such a dimensionality reduction some information is inevitably lost. The optimal RC should absorb all the important dynamical information contained in the other degrees of freedom, so they can be neglected. Then the free energy profile (FEP) constructed along the optimal coordinate together with the determined diffusion coefficient can give an accurate description of the system dynamics as diffusion on this free energy surface. Examples of such dimensionality reduction can be found in different fields: physically based reaction coordinate in single molecular experiments, molecular dynamics simulations, and biomarkers in medicine [1].

In protein folding simulations the following RCs are frequently chosen: the root mean square distance (rmsd) from the native structure, the number of native contacts, and the radius of gyration. In many cases, however, such coordinates can hide the complexity of the dynamics, in particular the barriers between states. For example, Figure 1 shows the free energy profiles determined along two different reaction coordinates describing the folding dynamics of HP35 protein. Accordingly to the rmsd coordinate, folding proceed through a single transition state, while the FEP along the optimized coordinate shows 2 transition states with an intermediate state between them. Which of these two coordinates describes the dynamics of the protein correctly?

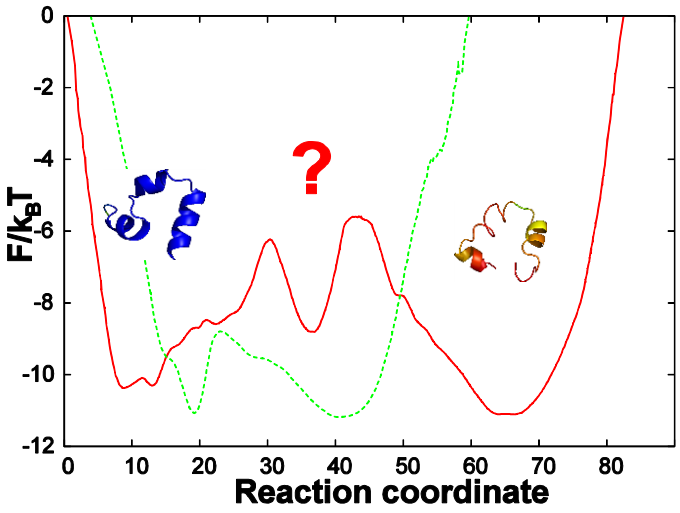


**Figure 1**: Free energy profiles along the rmsd coordinate (green line) and the optimized coordinate (red line) determined for a folding trajectory of HP35 protein.

In general, during such a free energy landscape analysis the following problems/questions often appear and are to be solved: determination of the free energy profile and the diffusion coefficient, which provide complete description of diffusive dynamics; establishing that the reaction coordinate is optimal and/or that the dynamics projected on such a coordinate is diffusive, rather than sub or super diffusive; transformation of the putative reaction coordinate to

another, more convenient one, for example, to the one with the constant diffusion coefficient; computation of various properties associated with stochastic dynamics, such as, the mean first passage time (mfpt), the mean transition path times (mtpt).

While some of the tasks are rather trivial (such as the computation of the conventional histogram free energy profile), other (such as the computation of the cut profile using transition path segments with different sampling intervals) are not. We have developed a python script fep1d.py -- a simple tool for the analysis of the reaction coordinates and the projected dynamics -- which allows one to readily perform the described tasks [2]. Being a python script, the code can be easily read, adapted and modified to extend the functionality.

The command line contains the list of the data files with the RC time series (the mandatory arguments), and a list of optional arguments starting with --. For example,
*fep1d.py rc1.dat rc2.dat --transformto=natural --hfep=1* will transform two different reaction coordinates rc1 and rc2 to the "natural" reaction coordinates with the constant diffusion coefficient (optional argument *transformto*) and will construct and plot the histogram based free energy profiles (the optional argument *hfep*) along the transformed RCs. For a protein folding trajectory these can be the root mean square distance from the native structure and the number of native contacts reaction coordinates. The command then can be used to compare which of the two putative coordinates is more optimal or better describes the dynamics: it is the one with the highest profile (Figure 1).

The script, invoked without arguments, lists all the options. The gnuplot library is used to plot the graphs. The plots can be saved as postscripts files, or as data files to be plotted using other software. The transformed coordinates can be saved as well. However, the unique functionality of the script is the ability to assess the optimality of a putative reaction coordinate and to inspect whether the dynamics projected on such a coordinate is diffusive, rather than sub or super diffusive. We hope that it will make a rigorous analysis of increasingly available large amount of complex data less involved. The fep1d.py program can be downloaded from http://sourceforge.net/projects/fep1d/.

**Publications**

Krivov, S., Fenton, H., Goldsmith, P., Prasad, R., Fisher, J. & Paci, E. (2014) Optimal reaction coordinate as a biomarker for the dynamics of recovery from kidney transplant. *PLoS Comput. Biol.* **10**: e1003685.

**Funding.**

This work was supported in part by an RCUK fellowship and a BBSRC grant**.**

# Studies of small DNA tumour viruses that cause disease in humans

Christopher Wasson, Hussein Abdul-Sada, Emma Prescott, Rajni Bhardwaj, Gemma Swinscoe, Sam Dobson, Margarita Panou, Daniel Hurdiss, Ethan Morgan and Andrew Macdonald

## Introduction

Members of the *Papovaviridae*, which includes the Papillomaviruses and Polyomaviruses, are the causative agents of a number of severe diseases in humans. Notable examples include cervical cancer, which is exclusively associated with infection with human papillomaviruses, and polyomavirus-associated nephropathy (PVAN) and progressive multifocal leukoencephalopathy (PML) caused by the BK and JC polyomaviruses, respectively. Current therapeutic strategies to treat these virus-associated maladies are lacking. We undertake a broad ranging analysis of these viruses in an effort to identify new targets for therapeutic intervention. These studies have revealed novel information about these viruses.

## Results

Human papillomavirus: We use an integrated approach to understand the roles of the least understood virus encoded proteins in the HPV life cycle and in cancer development. In particular we have focussed on the E5 oncoprotein. This highly hydrophobic membrane protein is expressed by all cancer-associated HPV isolates but its role in transformation and the life cycle is not clear. In 2012 we developed the first system to study recombinant E5 and subsequently demonstrated that it was a novel member of the viroporin family of virus encoded ion channels. This has opened up the possibility of developing small molecule inhibitors targeting the channel function of E5. In addition, we study the host pathways deregulated by E5, including growth factor receptor pathways, which we now understand are essential both for transformation and the HPV life cycle. Using three-dimensional organotypic raft culture models – we grow skin in a dish – we have shown that E5 manipulates growth factor pathways to enhance keratinocyte proliferation and to delay terminal differentiation, both of which are essential for the HPV life cycle. Current projects include studying novel E5 binding partners and understanding how these contribute to HPV infection and pathogenesis. In addition we have embarked on a novel study to ascertain the global changes to the host proteome upon HPV infection.

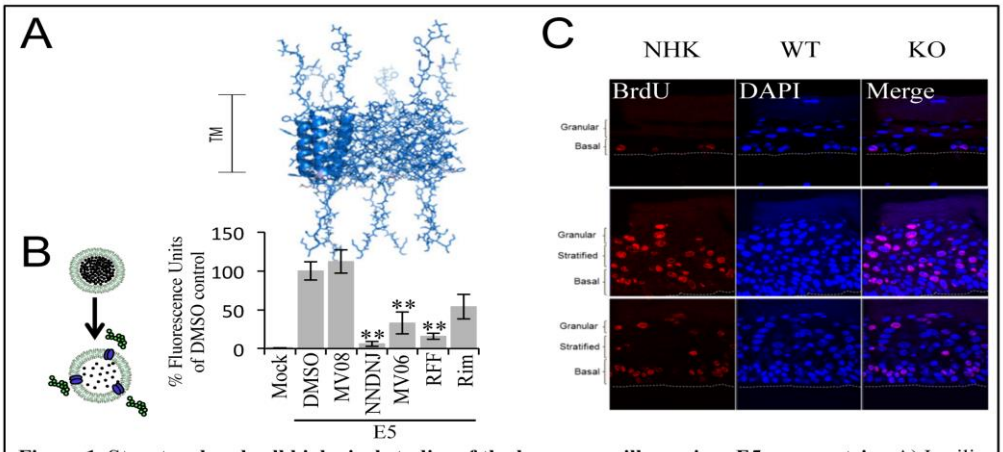


**Figure 1. Structural and cell biological studies of the human papillomavirus E5 oncoprotein**. A) In silico modeling the HPV16 E5 proteins. Energy minimisation models depicting a hexameric channel structure (Wetherill et al., 2012). B) Screen for novel inhibitors of E5 viroporin activity. Panel of known viroporin inhibitors and bespoke compounds generated from the insilico model were tested for ability to prevent E5-mediated dye release. C) Genetic studies of E5 function during the HPV18 life cycle using E5-knockout viruses in primary three dimensional organotypic raft culture models. BrdU incorporation measures the levels of unscheduled DNA replication in the suprabasal layers of the epithelium (red stain) in normal human keratinocytes (NHK), cells infected with wild type HPV18 (WT) and cells infected with an HPV18 genome lacking E5 expression (KO). Loss of E5 results in a significant reduction in DNA replication.

Human polyomaviruses: Members of this family, including BK, JC and Merkel cell polyomavirus, are associated with disease in humans. Despite their clear association with disease there is a paucity of understanding of their basic biology and as such we are using a wide ranging series of experiments to understand their life cycles and to identify novel targets for antiviral therapeutics. We have identified a novel immune evasion strategy for the Merkel cell polyomavirus and are uncovering the roles of the enigmatic agnoprotein in the polyomavirus life cycle. We are also using the latest advances in structural biology to gain an unprecedented understanding of the fundamental make-up of polyomavirus particles. This information may herald crucial advances in anti-viral drug design.

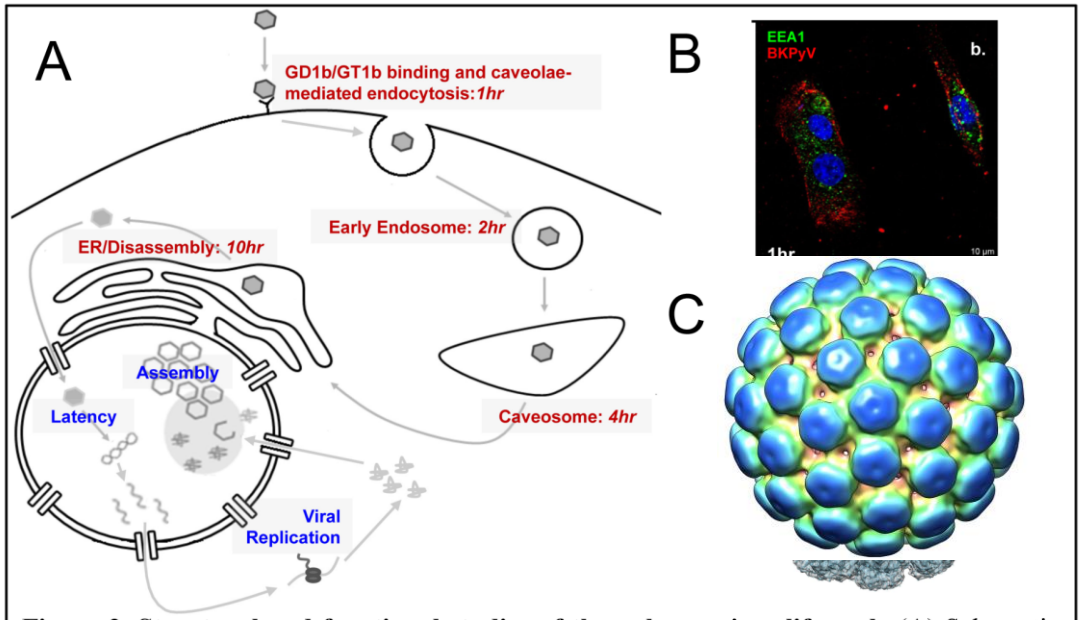


**Figure 2. Structural and functional studies of the polyomavirus life cycle** (A) Schematic of the current understanding of BK polyomavirus (BKPyV) life cycle. (B) Immunofluorescence with Alexafluor954 labelled BKPyV infected human renal proximal tubular epithelial (RPTE) cells. (C) Cryo electron microscopy structure determination of the native BKPyV virion.

**Publications**

Stakaityte, G., Wood, J., Knight, L., Abdul-Sada, H., Adzahar, N., Nwogu, N., Macdonald, A. & Whitehouse, A. (2014) Merkel cell polyomavirus: molecular insights into the most recently discovered human tumour virus. *Cancers* **6**: 1267-1297.

Richards, K., Doble, R., Wasson, C., Haider, M., Blair, G., Wittmann, M. & Macdonald, A. (2014) Human papillomavirus e7 oncoprotein increases production of the anti-inflammatory interleukin-18 binding protein in keratinocytes. *J. Virol.* **88**: 4173-4179.

**Funding**

This work was supported by the Medical Research Council, Kidney Research UK and Yorkshire Kidney Research Fund.

**Collaborators**

***University of Leeds:*** N. Ranson (Faculty of Biological Sciences), S. Griffin (LIMM), R. Foster (School of Chemistry), A. Whitehouse (Faculty of Biological Sciences).
***External:*** S. Roberts (University of Birmingham, UK), N. Coleman (University of Cambridge, UK), S. Graham (University of Glasgow, UK), S. Arthur (University of Dundee, UK).

# Host cell ion channels as new anti-viral targets

Hessa Taqi, Zjofi Igloi, David Hughes, Adrian Whitehouse, Mark Harris, John Barr and Jamel Mankouri

## Introduction

Ion channels are pore-forming proteins that allow passage of selected ions across cell membranes. They perform a broad range of critical functions that control all aspects of cellular life, ranging from cell signaling, membrane potential regulation, ionic homeostasis and cell volume regulation. Work from our laboratories has shown that viruses actively subvert host cell ion channel function to modify the cell environment and favour their own life cycle at the detriment to the host. These discoveries have established ion channels as a viable class of anti-viral therapeutic targets.

## Results

We have identified a family of ion channels that are required during Hepatitis C virus (HCV) replication. Hepatocytes express an array of plasma membrane and intracellular ion channels but their role during the HCV lifecycle was largely undefined. We have shown that HCV increases intracellular hepatic chloride ($Cl^-$) influx that can be inhibited by selective $Cl^-$ channel blockers. Through pharmacological and siRNA mediated silencing we have demonstrated that $Cl^-$ channel inhibition is detrimental to HCV replication. This represents the first observation of the involvement of $Cl^-$ channels during the HCV lifecycle (Igloi *et al.*, 2015).

In collaboration with Dr John Barr, we have more recently investigated the effects of modulating cellular ion channel activity with ion channel modulating drugs during Bunyamwera virus (BUNV) infection. BUNV is a negative sense RNA virus that has characteristics similar to its more deadly cousins, yet poses fewer safety concerns. BUNV is therefore an excellent research tool to safely and rapidly accumulate information that can be applied to more lethal members of the negative sense RNA virus family. We performed BUNV infection assays and assessed virus production in the presence of broad acting inhibitors of the major $Cl^-$, $Ca^{2+}$, $Na^+$ and $K^+$ channel families. We could strongly inhibit virus infection with ion channel drugs targeting $K^+$ channels. Further pharmacological analysis of BUNV growth in response to a comprehensive panel of specific inhibitors identified a small and poorly characterized family of twin-pore $K^+$ channels required for BUNV infection. Interestingly, two members of this channel family are known to associate with BUNV proteins, as determined by proteomic analysis of cellular proteins co-precipitated with BUNV proteins during infection. Thus, clinically available $K^+$ channel inhibiting drugs have the potential as anti-viral agents for *Bunyaviridae* infections.

Using similar approaches we have identified specific ion channel modulators that impede the lifecycle of other zoonotic viruses including Schmallenberg virus and Rabies virus. Current approaches aim to characterise the virus dependent cellular processes impeded by these ion channel modulators and the ability of their viral proteins to manipulate cellular ion channel function.

## Funding

We gratefully thank the Royal Society for funding these studies.

**Collaborators**

***University of Leeds:*** A. Whitehouse, J. Barr, M. Harris, A. Macdonald, C. Peers and J. Lippiat.

***External:*** M. Reeves (UCL, UK), A. Kohl (University of Glasgow, UK), M. Dallas (University of (Reading, UK), C. Crump (University of Cambridge, UK). S.Finke (Friedrich-Loeffler-Institut), C.Mckimmie (University of Glasgow, UK), J.Daly (University of Nottingham, UK), E. Schnettler (University of Glasgow, UK).

# The first small-molecule inhibitors of members of the ribonuclease E family

Louise Kime, Stefanie Jourdan, Colin Fishwick and Kenneth McDowall

## Introduction

The *Escherichia coli* endoribonuclease RNase E is central to the processing and degradation of all types of RNA and as such is a pleotropic regulator of gene expression. It is essential for growth and was one of the first examples of an endonuclease that can recognise the 5'-monophosphorylated ends of RNA thereby increasing the efficiency of many cleavages. Homologues of RNase E can be found in many bacterial families including important pathogens, but no homologues have been identified in humans or animals.

## Results

RNase E represents a potential target for the development of new antibiotics to combat the growing number of bacteria that are resistant to antibiotics in use currently.

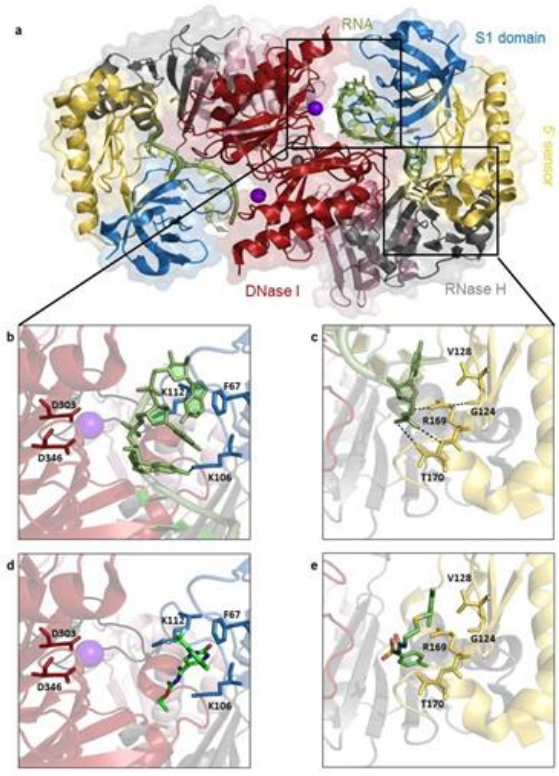


**Figure 1**: Structure of the RNase E catalytic domain and compound docking. (a) A top elevation of a principal dimer with bound RNA (green). Zinc and magnesium ions are shown as grey and magenta spheres, respectively. (b) The catalytic site. The DNase I domain presents a magnesium ion that is co-ordinated by the carboxylates of aspartic acid residues. The base of the nucleotide at the +2 position relative to the site of RNA cleavage is partitioned into a recess on the surface of the S1 domain. (c) The pocket for 5′- ends contacts both the monophosphate group and the base of the terminal nucleotide. (d) The site of catalysis, with predicted docking of compound M5. (e) The 5′-monophosphate binding pocket, with predicted docking of compound P11. The binding of compounds M5 and P11 sterically hinder binding of the RNA molecule.

Potent small molecule inhibitors that bind the active site of essential enzymes are proving to be a source of potential drug leads and tools to dissect function through chemical genetics. Here we

report the successful use of virtual high-throughput screening to obtain small molecules predicted to bind at sites in the N-terminal catalytic half of RNase E (Figure 1). We have shown that these compounds are able to bind with specificity and inhibit catalysis of *Escherichia coli* and *Mycobacterium tuberculosis* RNase E and also inhibit the activity of RNase G, a paralogue of RNase E. Two of the best compounds are predicted to sterically hinder binding of the RNA molecule.

**Publication**

Kime, L., Clarke, J., Romero, D., Grasby, J. & Mcdowall, K. (2014) Adjacent single-stranded regions mediate processing of tRNA precursors by RNase E direct entry. *Nucleic Acids Res.* **42**: 4577-4589.

**Funding**

This work was funded by the BBSRC and the EU through Marie Curie Actions (FP6)

**Collaborations**

***External:*** A. Callaghan (University of Portsmouth, UK)

# Direct entry by RNase E is a common pathway for the degradation and processing of RNA in *Escherichia coli*

Justin Clarke, Louise Kime, David Romero and Kenneth McDowall

## Introduction

*Escherichia coli* endoribonuclease E has a major influence on gene expression. It is essential for the maturation of ribosomal and transfer RNA as well as the rapid degradation of messenger RNA. The latter ensures that translation closely follows programming at the level of transcription. Last year we reported that one of the hallmarks of RNase E, *i.e.* its ability to bind via a 5′-monophosphorylated end, is unnecessary for the initial cleavage of at least some polycistronic tRNA precursors. The maturation of stable RNAs is one of the major activities of all forms of life.

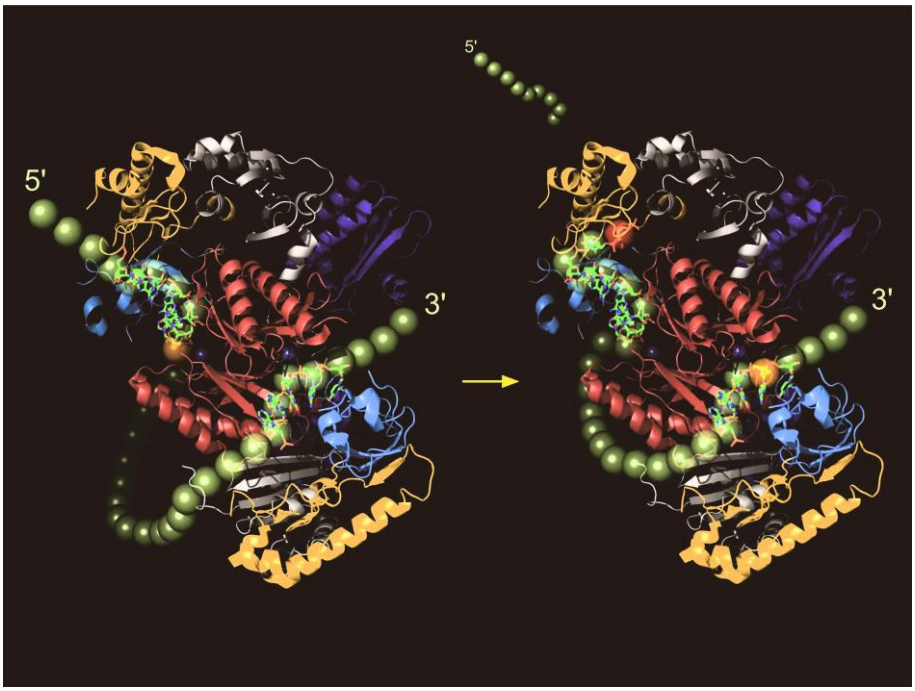


**Figure 1**: Pervasive endonucleolytic cleavage as mediated by simple cooperative interactions involving short unpaired stretches of RNA. The panel on the left shows an interpretive model of such an interaction, while the panel of the right shows how interaction with the 5'-monophosphorylated end of a downstream product of cleavage can facilitate another round of cleavage. The models are based on an X-ray crystal structure of the catalytic domain, which forms a homotetramer (2C0B). For simplicity only one of the principal dimers is shown. The cooperative interaction (left panel) is mediated by the binding of a substrate (chain of green spheres) using two identical but antiparallel RNA-binding channels that can accommodate only unpaired regions. Each channel is formed by an S1 domain (light blue) closed against a DNase I domain (red) that presents the catalytic magnesium (small purple sphere). Following cleavage (right panel), the 5'-monophosphorylated end of the downstream product (red sphere) is able to enter a pocket within the 5' sensor (yellow). This maintains the overall interaction such that cleavage can occur at a second site. The figures also show the positions of nucleotides downstream of bonds prior to their cleavage (orange spheres) and the RNase H (grey) and small domains (navy blue) of the catalytic domain. The small domain provides the surfaces for the dimerisation of the principal dimers. The role of the RNase H domain is not yet clear.

**Results**

This year we can report that 'direct entry' (5′-monophosphate-independent) cleavage is a major pathway for mRNA degradation as well as being required for normal tRNA processing, which is one of the major activities of the cell. Our work is considered a breakthrough as it dispels the notion that the only common mechanism by which RNase E cleaves RNA requires interaction with a 5'-monophosphorylated end. Moreover, we obtained further evidence that direct entry is facilitated by RNase E binding simultaneously to two or possibly more unpaired regions (Figure 1). These simple requirements may maximise the rate of degradation and processing by permitting multiple sites in a transcript to be surveyed directly without being constrained by 5′-end tethering. The specificity of RNase E is sufficiently flexible that it can cleave at some sites using different combinations of unpaired regions. Our work has been published and discusses the evolution of 5' sensing, which is one of the hallmarks of the RNase E family, the role of the RNA degradosome, and possible new roles for RNase E.

**Publication**

Clarke J.E., Kime L., Romero A., D. & McDowall, K. J. (2014). Direct entry by RNase E is a major pathway for the degradation and processing of RNA in *Escherichia coli*. *Nucleic Acids Res*. **42**:11733-11751.

**Funding**

This work was funded by the BBSRC.

# Understanding the mechanism and regulation of the Vacuolar ATPase

Sarah Harris, Michael Harrison John Trinick and Stephen Muench

## Introduction

The vacuolar ATPase (V-ATPase) is a large (1MDa) multi-subunit complex, which through a rotary mechanism transports protons across the membrane. It contains ~30 subunits of up to 14 different types separated into an ATP hydrolysing $V_1$ domain and proton translocating $V_o$ domain. Previous work by the group revealed the subunit organisation within the complex. The AB subunits in $V_1$ are responsible for ATP hydrolysis which drives the rotation of a central axle and c-ring relative to the *a* subunit, transporting protons over the membrane. Despite the progress which has been made with regards to understanding the structural arrangement of the V-ATPase and other members of the rotary ATPase family, we are only just starting to understand the mechanical properties which allow these complex rotary machines to work at close to 100% efficiency. Moreover, the V-ATPase plays a role in diseases such as cancer invasiveness, osteoporosis and kidney disease making it an important therapeutic target.

## Results

In 2014 our group has made significant steps forward in our structural and mechanical understanding of the V-ATPase. We have solved the highest reported rotary ATPase structure (9.4Å), providing new insights into the way in which the pumping ($V_o$) and motor domains ($V_1$) are connected. Moreover, our model is in a different conformational state from that previously reported, showing for the first time, any intact rotary ATPase trapped in two distinct catalytic states. We have also shown the presence of a conserved electrostatic bearing in the catalytic domain which contributes to the extraordinarily high efficiency of rotary ATPases (Figure 1A). To further understand V-ATPase mechanics the group reported the first use of Finite Fluctuating Element Analysis (FFEA), developed by Dr Harris in Leeds to carry out molecular dynamic simulations. This analysis revealed insights into the inherent flexibility within the rotary ATPase family and the role of an apparent stator connection to the central rotor axle (Figure 1B), which in conjuction with the electrostatic bearing plays an important role in the high efficiency of the V-ATPAse.

The role that the V-ATPase plays in disease states such as osteoporosis, cancer invasiveness and kidney disease has led to an interest in the design of targeted therapeutics. A novel V-ATPase inhibitor is Pea Albumin toxin 1 (PA1b) which has high selectivity for different species. We used biochemical analysis and a novel tagging system for electron microscopy to identify the binding site at the base of the complex (Figure 1C). Moreover, we have shown a novel mechanism of inhibition which will be used for future drug design efforts.

Other work in the laboratory has focused on the use of a new scaffold for membrane protein extraction which reduces the need for detergents and produces a more “native” lipidic environment.

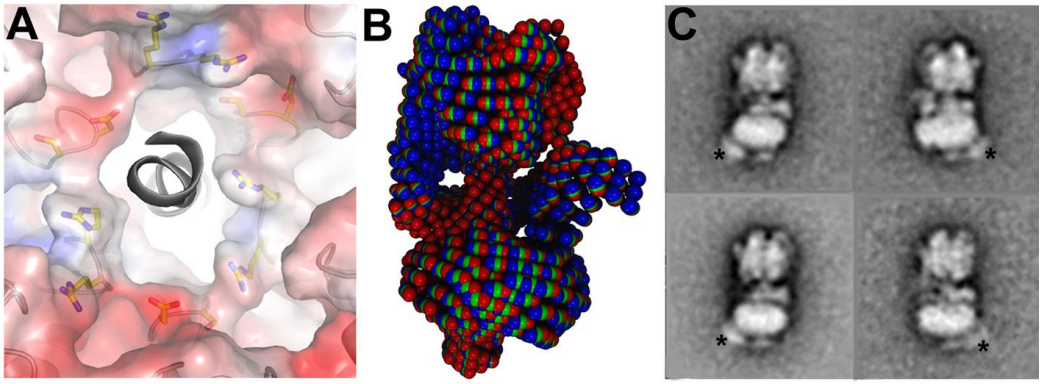


**Figure 1**: (A) Electrostatic surface at the bearing region of M. sexta V-ATPase which is implicated in the high efficiency. (B) The twist mode of the V-ATPase from FFEA calculations with the direction of motion going from red to blue. (C) Negative stain classes of *M. sexta* V-ATPase labeled with a PA1b-Strep-HRP construct, indicated by a star.

**Publications**

Richardson, R., Papachristos, K., Read, D., Harlen, O., Harrison, M., Paci, E., Muench, S. & Harris, S. (2014) Understanding the apparent stator-rotor connections in the rotary ATPase family using coarse-grained computer modeling. *Proteins* **82**: 3298-3311.

Muench, S., Rawson, S., Eyraud, V., Delmas, A., Da Silva, P., Phillips, C., Trinick, J., Harrison, M., Gressent, F. & Huss, M. (2014) PA1b inhibitor binding to subunits c and e of the vacuolar ATPase reveals its insecticidal mechanism. *J. Biol. Chem.* **289**: 16399-16408.

Caseley, E., Muench, S., Roger, S., Mao, H.-J., Baldwin, S. & Jiang, L.-H. (2014) Non-synonymous single nucleotide polymorphisms in the P2X receptor genes: Association with diseases, impact on receptor functions and potential use as diagnosis biomarkers. *Int. J. Mol. Sci.* **15**: 13344-13371.

Witola, W., Liu, S., Montpetit, A., Welti, R., Hypolite, M., Roth, M., Zhou, Y., Mui, E., Cesbron-Delauw, M.-F., Fournie, G., Cavailles, P., Bisanz, C., Boyer, K., Withers, S., Noble, A., Swisher, C., Heydemann, P., Rabiah, P., Muench, S. & Mcleod, R. (2014) ALOX12 in human toxoplasmosis. *Infect. Immun.* **82**: 2670-2679.

Wilkinson, C., Mcphillie, M., Zhou, Y., Woods, S., Afanador, G.A., Rawson, S., Khaliq, F., Prigge, S., Roberts, C., Rice, D., Mcleod, R., Fishwick, C. & Muench, S. (2014) The benzimidazole based drugs show good activity against *T. gondii* but poor activity against its proposed enoyl reductase enzyme target. *Bioorg. Med. Chem. Lett.* **24**: 911-916.

**Funding**

This work was supported by the MRC, Wellcome Trust and NIH

**Collaborators**

***External:*** H. Wieczorek (University of Osnabrueck, Germany), R. McLeod (University of Chicago, USA)

# Development of tools and approaches to facilitate the discovery of bioactive small molecules

George Burslem, Richard Doveston, Joachim Horn, Thomas James, George Karageorgis, Ho-Yin Li, Paul MacLellan, Stuart Warriner and Adam Nelson

## Introduction

Chemists have explored chemical space in an uneven and unsystematic manner. An analysis of the scaffolds of the 25 million known cyclic small molecules (in 2008) revealed that one sixth of the compounds are based on just 30 (out of the 2.5 million) known molecular scaffolds! To address this historic uneven exploration, we have developed a vibrant research programme focusing on the identification and development of synthetic methods that have potential to facilitate more systematic exploration of chemical space.

## Extension to lead-like chemical space

A strongly developed theme within the Nelson group has been to develop diversity-oriented synthetic approaches that map onto the requirements of drug discovery programmes. Established diversity-oriented approaches have tended to focus on small molecules that lie well outside drug-like space. It is now generally accepted that attrition rates in drug discovery are strongly linked to molecular properties such including molecular weight and lipophilicity. Optimisation almost always leads to increases in both molecular weight and lipophilicity, so it is important to control the properties of initial lead molecules. We are thus continuing to develop a robust and growing toolkit of synthetic reactions that address the challenges raised in the nascent field of lead-oriented synthesis. This research programme is now feeding into the €196M European Lead Factory in which Leeds is a partner.

## Realisation of activity-directed synthesis

We have described activity-directed synthesis (ADS), a novel discovery approach in which bioactive small molecules emerge in parallel with associated synthetic routes. Unlike conventional discovery approaches, ADS exploits promiscuous reactions with many alternative outcomes, and enables the exploration of diverse regions of chemical space. The approach is iterative, exploiting diverse reaction arrays whose design is informed by the activity of product mixtures formed in previous rounds. Ultimately, promising reactions are scaled up to reveal, after purification, the structures of the responsible bioactive molecules. ADS is thus a function-driven approach in which the discovery of bioactive molecules occurs in parallel with the emergence of an associated synthetic route.

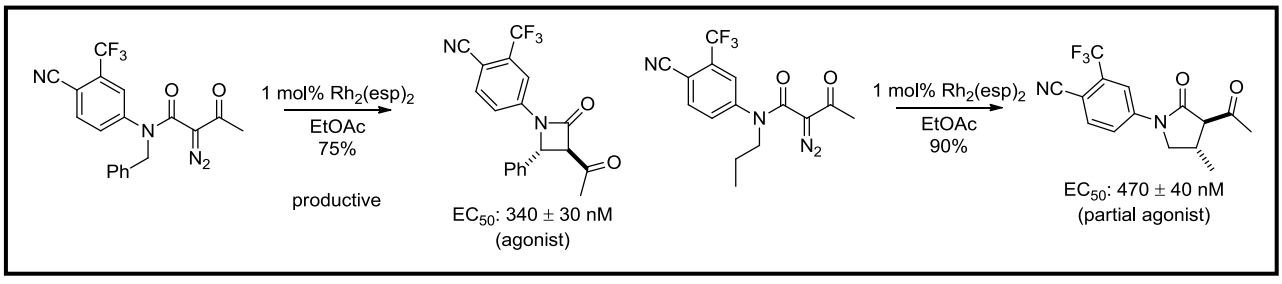


We have exemplified the ADS approach in the discovery of agonists of the androgen receptor. We harnessed the diverse reactivity of metal carbenoids to search chemical space, and to discover synthetic approaches to bioactive chemotypes. We demonstrated that the iterative activity-directed approach can result in either optimisation of the yield of a bioactive molecule; or in structural changes that improve biological activity. High-yielding syntheses of androgen receptor

modulators that emerged from our activity-directed approach are shown in the Scheme. Crucially, the chemotypes discovered did not have any previously annotated activity against the androgen receptor.

**Scheme:** Syntheses of androgen receptor modulators (with sub-micromolar activity) that emerged from our activity-directed approach. The chemotypes discovered did not have any previously annotated activity against the androgen receptor.

**Summary**

The development of general strategies that are able to deliver skeletally diverse compounds – but within the boundaries of lead-like chemical space – is demanding. Publications from this programme, and other programmes under active development in the group, are listed below. Further details of research within the Nelson group may be found at www.asn.leeds.ac.uk.

**Publications**

Doveston, R., Marsden, S. & Nelson, A. (2014) Towards the realisation of lead-oriented synthesis. *Drug Discov. Today* **19**: 813-819.

Fisher, M., Basak, R., Kalverda, A., Fishwick, C., Turnbull, W. & Nelson, A. (2014) Discovery of novel Fabf ligands inspired by platensimycin by integrating structure-based design with diversity-oriented synthetic accessibility. *Org. Biomol. Chem.* **12**: 486-494.

Daniels, A., Campeotto, I., Van Der Kamp, M., Bolt, A., Trinh, C., Phillips, S., Pearson, A., Nelson, A., Mulholland, A. & Berry, A. (2014) Reaction mechanism of n-acetylneuraminic acid lyase revealed by a combination of crystallography, QM/MM simulation, and mutagenesis. *ACS Chem. Biol.* **9**: 1025-1032.

Martin, H., Adams, M., Higgins, J., Bond, J., Morrison, E., Bell, S., Warriner, S., Nelson, A. & Tomlinson, D. (2014) High-content, high-throughput screening for the identification of cytotoxic compounds based on cell morphology and cell proliferation markers. *PLoS One* **9**: e88338.

Windle, C., Mueller, M., Nelson, A. & Berry, A. (2014) Engineering aldolases as biocatalysts. *Curr. Opin. Chem. Biol.* **19**: 25-33.

Burslem, G., Kyle, H., Breeze, A., Edwards, T., Nelson, A., Warriner, S. & Wilson, A. (2014) Small-molecule proteomimetic inhibitors of the HIF-1α-p300 protein-protein interaction. *Chembiochem* **15**: 1083-1087.

James, T., Maclellan, P., Burslem, G., Simpson, I., Grant, J., Warriner, S., Sridharan, V. & Nelson, A. (2014) A modular lead-oriented synthesis of diverse piperazine, 1,4-diazepane and 1,5-diazocane scaffolds. *Org. Biomol. Chem.* **12**: 2584-2591.

Li, H., Horn, J., Campbell, A., House, D., Nelson, A. & Marsden, S. (2014) A convergent rhodium-catalysed asymmetric synthesis of tetrahydroquinolines. *Chem. Commun.* **50**: 10222-10224.

Karageorgis, G., Warriner, S. & Nelson, A. (2014) Efficient discovery of bioactive scaffolds by activity-directed synthesis. *Nat. Chem.* **6**: 872-876.

This paper was featured on the front cover of the October 2014 edition of *Nature Chemistry*. It was featured in the editorial (*Nature Chem.* 2014, **6**, 841), an interview (*Nature Chem.* 2014, **6**, 845-6) and a *News & Views* article (Lowe; *Nature Chem.* 2014, **6**, 851-2).

**Funding**
We thank EPSRC, the Wellcome Trust, the EU, GSK and AstraZeneca for support.

**Collaborators**
***University of Leeds:*** S. Marsden (School of Chemistry) and S. Sridharan (School of Chemistry)
***External:*** I. Churcher (GSK,UK), D. House (GSK,UK), A. Campbell (GSK,UK), I. Simpson (AstraZeneca, UK) and A. Grant, (AstraZeneca, UK).
We also acknowledge other scientific collaborators from who have also contributed strongly to other aspects of our on-going research programme.

# Structural and mechanistic insights into the FusB family of fusidic acid resistance proteins

Jennifer Tomlinson, Gary Thompson, Arnout Kalverda, Anastasia Zhuravleva and Alex O'Neill

## Introduction

A major focus in the O'Neill laboratory is on understanding the mechanisms by which bacteria resist the effects of the antibiotics that are used to treat the infections they cause. The antibiotic fusidic acid inhibits bacterial protein synthesis in the bacterial pathogen *Staphylococcus aureus* by blocking release of the translocase, elongation factor G (EF-G), from the ribosome. Resistance to fusidic acid is most commonly mediated by proteins of the FusB family, which bind to elongation factor G and protect it from the inhibitory effect of fusidic acid. The mechanism by which the FusB-type proteins interact with EF-G to mediate resistance to fusidic acid is not fully understood, and recent efforts have therefore focused on gaining a detailed understanding of this protein-protein interaction (PPI).

## Determining a structural model of the FusB-EF-G complex by NMR

To understand the interaction between FusB-type proteins and EF-$G_{C3}$ (a fragment of EF-G composed of domains III-V that is sufficient for FusB binding), we used nuclear magnetic resonance (NMR) to produce a structural model of the complex and thereby facilitate a better understanding of this unusual antibiotic resistance mechanism. NMR residual dipolar couplings, intermolecular paramagnetic relaxation enhancement (PRE) distance restraints, solvent PREs and chemical shift perturbations were used to build a model of the complex structure based on the apo protein structures using the docking program HADDOCK. Our data have collectively established that FusB binds to EF-$G_{C3}$ via interaction between domain IV of EF-$G_{C3}$ and the C-terminal domain of FusB, with domain V of EF-$G_{C3}$ and the N-terminal domain of FusB forming a secondary interaction. To achieve this interaction, both EF-$G_{C3}$ and FusB undergo internal domain reorientation with domain V of EF-$G_{C3}$ moving by 21° relative to domain IV.

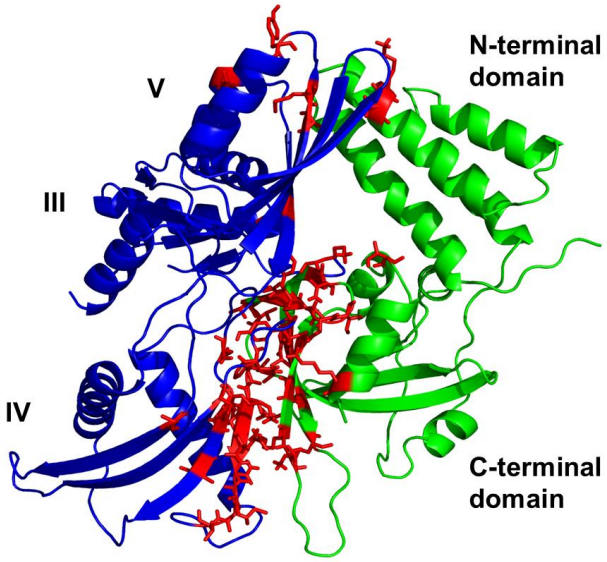


**Figure** 1: Structural model of the interaction between EF-G and FusB from NMR based docking of the crystal structures of the two proteins (PDB IDs 2XEX and 4ADN, respectively). Domains III-V of EF-G are shown in blue and FusB is shown in green. Residues forming the binding site are shown in red.

## FusB binding to EF-G prompts significant dynamic changes in domain III suggesting a possible mechanism of fusidic acid resistance

NMR signals from amides within EF-$G_{C3}$ domain III disappear from the spectrum upon FusB binding. This implies broadening of resonances, suggesting that FusB prompts conformational dynamics on the µs-ms timescale throughout this domain. Molecular dynamics simulations support the concept that domain III is more dynamic than domains IV and V, and suggest

movement consistent with the observed resonance broadening. Since domain III does not interact directly with FusB, this implies that FusB affects domain III allosterically. Domain III has an important role in transmitting conformational changes through EF-G, a role that is blocked by fusidic acid. Consequently, FusB appears to act as an allosteric effector that changes the conformational flexibility of domain III in order to rescue the stalled translocation complex, and

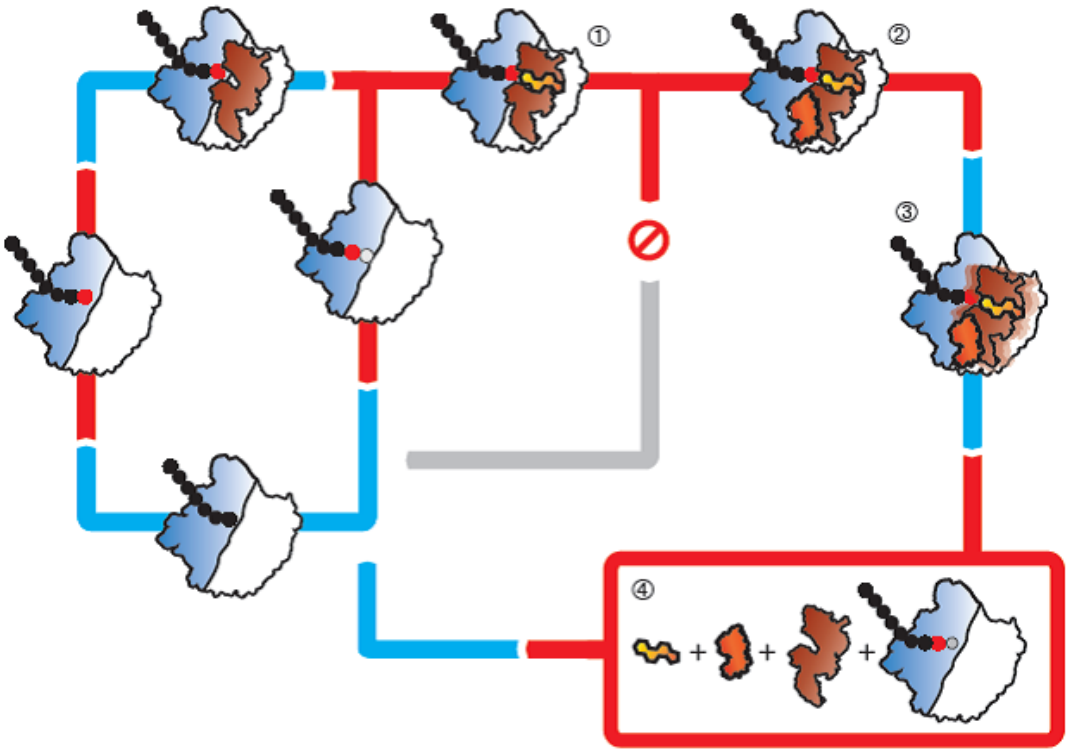


**Figure 2**: A suggested mechanism of FusB mediated fusidic acid resistance. 1. FA (yellow) binding to EF-G (brown) bound to the ribosome (blue and white) stalls protein synthesis by preventing EF-G release. Binding of FusB (orange) to EF-G in stalled complexes (2) induces a change in the dynamics of domain III of EF-G (3) facilitating conformational change in EF-G that promotes release from the ribosome, allowing protein synthesis to continue (4).

this mechanism therefore represents a new paradigm in antibiotic resistance.

**Funding**
This work is funded by the BBSRC.

# *In silico* studies of proteins: folding, mechanics, dynamics and self-assembly

Supreecha Rimratchada, Matthew Batchelor, James Ross, Sam Hickman, Kostas Papachristos, James Gowdy, Gael Radou and Emanuele Paci

## Introduction

Our group is interested in a broad range of research topics related to the behaviour of proteins. The tools we use are theoretical and computational, though most of our research involves experiments performed in collaboration with colleagues from the Astbury Centre and further afield.

## Results

One example of recent research involved the development of a theoretical protein-folding framework, and its application for the case of a model three-helix bundle (Rimratchada 2014). Proteins are polymeric molecules with many degrees of conformational freedom whose internal interactions are typically screened to small distances. Therefore, in the high-dimensional conformation space of a protein, the energy landscape is locally relatively flat, in contrast to low-dimensional representations, where, because of the induced entropic contribution to the full free energy, it appears funnel-like. Using a simple model that can be solved using pencil and paper, we proposed that proteins explore conformation space by searching these flat subspaces to find a narrow energetic alley that we call a hypergutter and then explore the next, lower-dimensional, subspace (Fig. 1). Such a framework provides an effective representation of the energy landscape and folding kinetics that does justice to the essential characteristic of high-dimensionality of the search-space and highlights the role of non-native interactions in defining folding pathways.

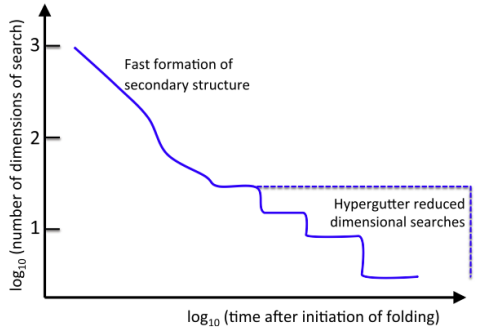


**Figure 1**: Schematic representation of protein folding using the hypergutter model. After most of the fine-grained degrees of freedom form into secondary structure, the remaining ~10 degrees of freedom may either suffer an extremely long simultaneous search ( dashed line), or fold exponentially faster via an energetically stabilised series of lower-dimensional subspaces (solid line), whose search times correlate with their dimension (Rimratchada 2014).

Much of our work involves molecular simulation of the dynamics and interactions within and between protein systems. Data generated from simulation are used to interpret and direct experimental measurements such as hydrogen-deuterium exchange probed by mass spectrometry of a hexameric helicase (Radou 2014), atomic force spectra of long alpha helices (Wolny 2014) and cryo-EM images of ATP-ases (Richardson 2014). In our group we also develop and implement methods to determine free energy projections along specific coordinates where sizeable free energy barriers prevent accurate sampling. One method uses a constant force applied to two atoms of a polypeptide (as in a force-clamp AFM experiment, Fig. 2) to enhance the sampling of "longer" conformations, thus allowing the sampling of all the possible values of the distance between the two atoms (Batchelor 2014). Another approach consists of splitting conformation space into "boxes", and sampling each box separately (Nogueira 2014).

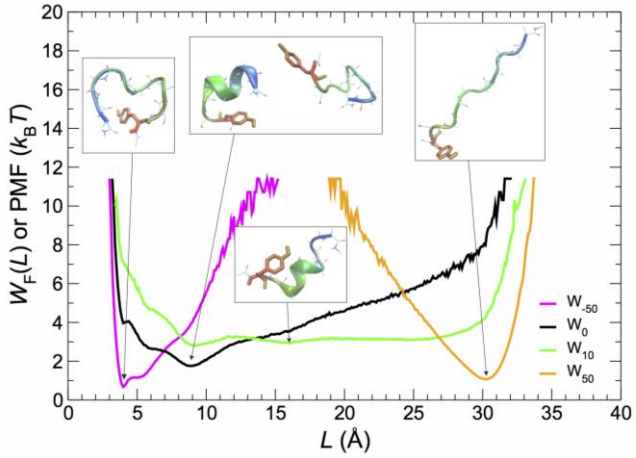


**Figure 2**: Potential of mean force (PMF) plots as a function of end-to-end distance ($L$) for $YSA_8$ under application of different external constant forces. The application of force combined with the weighted-histogram analysis method (WHAM) is used to enhance sampling of unlikely 'long' or 'short' conformations and obtain an improved PMF for all $L$, while also collecting dynamic properties of the chain under variable tension (Batchelor 2014).

**Publications**

Radou, G., Dreyer, F., Tuma, R. & Paci, E. (2014) Functional dynamics of hexameric helicase probed by hydrogen exchange and simulation. *Biophys. J.* **107**: 983-990.

Richardson, R., Papachristos, K., Read, D., Harlen, O., Harrison, M., Paci, E., Muench, S. & Harris, S. (2014) Understanding the apparent stator-rotor connections in the rotary ATPase family using coarse-grained computer modeling. *Proteins* **82**: 3298-3311.

Rimratchada, S., Mcleish, T., Radford, S. & Paci, E. (2014) The role of high-dimensional diffusive search, stabilization, and frustration in protein folding. *Biophys. J.***106**: 1729-1740.

Wolny, M., Batchelor, M., Knight, P., Paci, E., Dougan, L. & Peckham, M. (2014) Stable single alpha-helices are constant force springs in proteins. *J. Biol. Chem.* **289**: 27825-27835.

**Funding**

This work was partly funded by the BBSRC and Wellcome Trust.

**Collaborators**

***University of Leeds:*** M. Peckham, P. Knight, L. Dougan, R. Tuma, S. Muench, D. Shalashilin
***External:*** S. Vazquez, T. McLeish

# Cytoskeletal motors, muscle and single alpha helical domains, intriguing structural elements in proteins

Kasia Makowska, Ruth Hughes, Marcin Wolny, Matthew Batchelor, Francine Parker, Brendan Rogers, Glen Carrington, Adriana Klyszejko, Anna Lopata, Romina Bennewitz and Michelle Peckham

## Introduction

Our research is targeted at understanding how myosin contributes to contraction in muscle (Colegrave & Peckham, 2014) how muscle proteins are assembled into highly ordered structures, how myosin molecules in non-muscle cells contribute to their behaviour, how kinesin molecules traffic cargo (Soppina et al., 2014) and how an intriguing structural element found in myosin molecules and many other proteins, the single alpha helical (SAH) domain contributes to protein function (Wolny et al., 2014, Batchelor et al., 2015). We have developed many techniques for investigating these questions, and we are currently building super-resolution microscopes to perform photo-activated light microscopy (PALM) and stochastic optical reconstruction microscopy (STORM), providing us with resolutions of up to 20nm, as well as a novel type of structured illumination microscopy called iSIM, which provides roughly double the resolution of a normal light microscope.

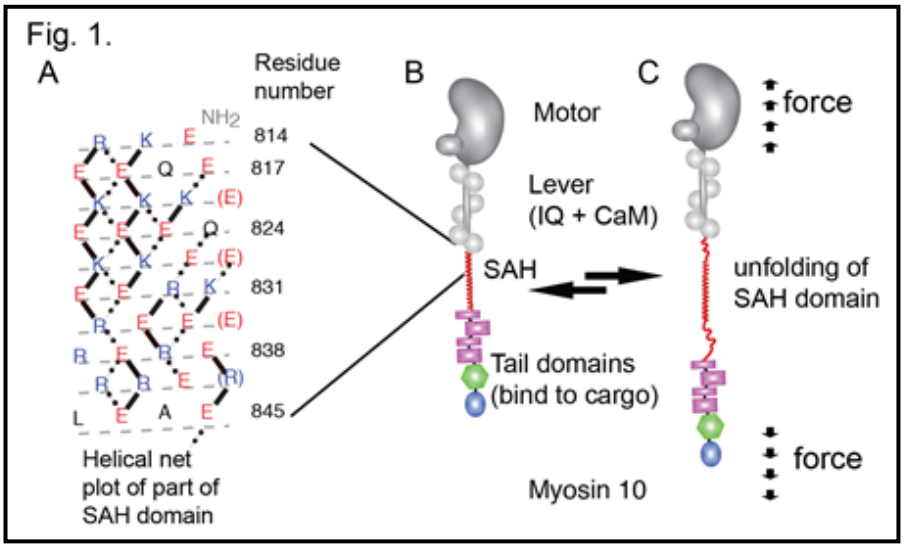


SAH domains are particularly interesting, as unusually for α-helices, they are completely stable in isolation, not requiring any interaction with any other protein, or part of the same protein to maintain stability. They are rich in charged residues (R, K and E), and ionic interactions between these charged residues help to stabilise the helix (Fig. 1A). We have already shown that these domains are rigid, and can be used to replace the lever in myosins (Baboolal et al., PNAS, 2009), and probably extend the effective length of the lever in those myosins in which they occur (e.g. Myosin 10, Fig. 1B). We have now tested how these domains unfold when subjected to axial forces using atomic force microscopy (AFM) and by using in silico modelling of this domain.

## Results

We have discovered that SAH domains unfold under low forces (lower than ~30pN) and that this unfolding is reversible (Wolny et al., 2014). Moreover, when the SAH domain is extended, force initially rises but then remains constant while the SAH domain continues to lengthen. This unusual behaviour is different to that observed for a 'Hookean' spring, where force would continue to increase during lengthening. Instead, the SAH domain behaves as a constant force spring.

The consequence of this behaviour is likely to mean that unfolding of the SAH domain in the cell will contribute to the function of the protein. For example, when myosin moves along an actin track, with its tail domains bound to cargo, hit a roadblock or obstacle, the SAH domain is able to

extend at these low forces, and prevent the motor detaching from the track, until the obstacle is removed (Fig. 1C). Extending this to the wide array of other proteins that contain SAH domains, a SAH domain inserted between two or more protein domains would be able to unfold under low forces, protecting the surrounding domains from detaching from their interacting proteins, providing stability to protein complexes that experience force.

**Super-resolution Microscopy.**
Our 3D-PALM/STORM and iSIM systems are built, and we are starting to capture images using these systems.

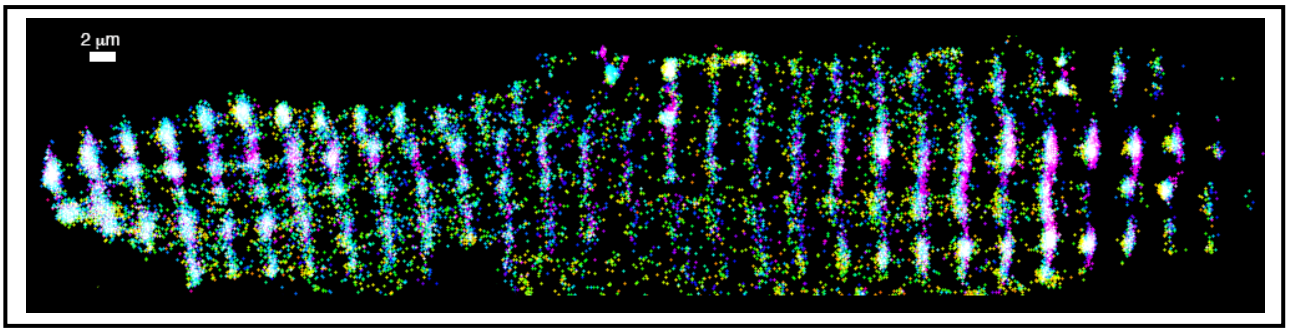


As an example, this is a projection image of α-actinin fused to mEos2 in an adult cardiomyocyte, obtained using 3D-PALM. The image has been colour coded for depth. The stripy appearance is due to the predominant localisation of α-actinin in the Z-discs (~100nm wide) in this muscle cell. The precision with which we can localise individual molecules is ~20nm. Our collaborators on this project are Hari Shroff, Hari Takagi, Robert Adelstein and Andrew York (at NIH, Bethesda, USA).

**Publications**
Wolny, M., Batchelor, M., Knight, P., Paci, E., Dougan, L. & Peckham, M. (2014) Stable single alpha-helices are constant force springs in proteins. *J. Biol. Chem.* **289**: 27825-27835.

Soppina, V., Norris, S., Dizaji, A., Kortus, M., Veatch, S., Peckham, M. & Verhey, K. (2014) Dimerization of mammalian kinesin-3 motors results in superprocessive motion. *Proc. Natl Acad. Sci USA* **111**: 5562-5567.

Colegrave, M. & Peckham, M. (2014) Structural implications of beta-cardiac myosin heavy chain mutations in human disease. *Anat. Rec.* **297**: 1670-1680.

**Funding**
This work was funded by CRUK, BBSRC, the Wellcome Trust and MRC.

**Collaborators**
***University of Leeds:*** L. Dougan, E. Paci, P. Knight, S. Harris, O. Harlen, D. Read
***External:*** H. Shroff, H. Takagi, R. Adelstein, A. York, J. Sellers (NIH, Bethesda, USA), K. Verhey (University of Michigan, USA), J. Molloy (NIMR, UK)

# Targeting transient and lowly-populated species during amyloid assembly

Theodoros Karamanos, Claire Sarell, Simon White, Amy Baker, Gary Thompson, Arnout Kalverda, Peter Stockley and Sheena Radford

## Introduction

Protein misfolding that leads to the accumulation of proteinaceous filamentous aggregates, known as amyloid fibrils, has been associated with numerous human diseases such as Alzheimer's and Parkinson's disease. Despite the large scientific interest, amyloid assembly remains ill-defined mainly due to the transient and heterogeneous nature of the species involved. Here we aim to characterize the early events during amyloid assembly of human $\beta_2$-miroglobulin (h$\beta_2$m) using its amyloidogenic variant ΔN6 and the non-aggregation prone murine version of the protein (m$\beta_2$m). Utilizing cutting edge NMR spectroscopy and RNA aptamer selection in combination with a wealth of biophysical tools we were able to visualize and target species that are <5% populated in solution.

## Visualization of transient protein-protein interactions that promote or inhibit amyloid assembly

Despite the high sequence and structural similarity between the three $\beta_2$m variants (h$\beta_2$m m$\beta_2$m, ΔN6) interaction between ΔN6-m$\beta_2$m inhibits assembly while binding of ΔN6 to h$\beta_2$m promotes assembly of the later (Figure 1A), offering an ideal system to study protein-protein interaction in the early stages of assembly. Using paramagnetic NMR (Figures 1B, 1C), chemical shift analysis and computational approaches we showed that inhibition and promotion of assembly both involve head-to-head interactions. Although the interactions surfaces are similar for the promotion and inhibition of amyloid formation, assembly is governed by the precise chemical details of the interface. Specifically, inhibition occurs via rigid body docking of monomers in a head-to-head orientation to form kinetically trapped dimers. By contrast, the promotion of fibrillation involves relatively weak protein association in a similar orientation, which results in conformational changes in the initially non-fibrillogenic partner (h$\beta_2$m). These studies provide the first molecular insights in phenomena such as prion infectivity and species barriers.

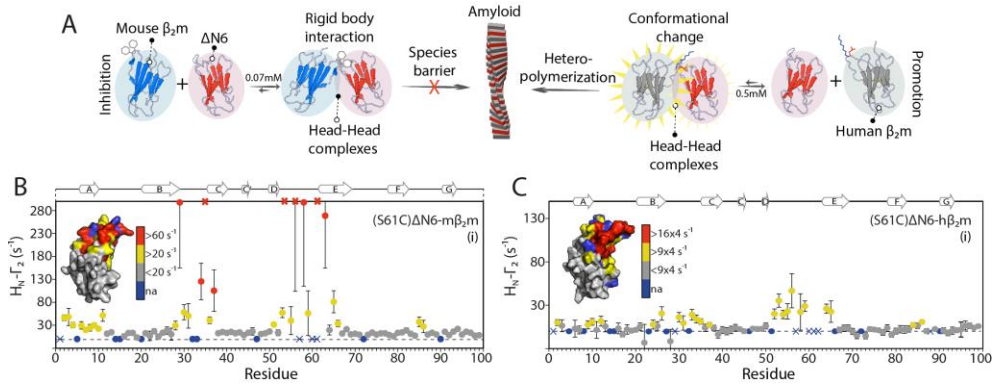


**Figure 1**: (A) Schematic showing the inhibition and promotion of amyloid assembly. Interaction of ΔN6 with mβ2m results in kinetically trapped head-head dimers (Kd=70μM), while the weaker (Kd=500μM) ΔN6-hβ2m association although involving similar surfaces, results in conformational changes that prime the molecules for further aggregation. (B) Example PRE profiles for the ΔN6-mβ2m interaction. Increased PRE rates in the BC and DE loop (locating on the top of the protein) highlight the head-head interaction. The structure of mβ2m coloured by the PRE rates is shown as inset. (C) As in (B) but for the ΔN6-hβ2m interaction.

**Targeting amyloid precursors with an RNA aptamer**

Native hβ$_2$m is not amyloidogenic at neutral pH. At physiological conditions, amyloid formation is initiated by the formation of a structured intermediate ($I_T$) that is transiently populated. The truncated variant ΔN6, although very similar in backbone structure to native hβ$_2$m, has been shown to be a good mimic of $I_T$. Hβ$_2$m can co-polymerize with ΔN6 *in vitro* to form hetero-polymeric fibrils with different structures and stabilities compared with their homo-polymeric counterparts. Discrimination between the different assembly precursors; for example by binding of a biomolecule to one species in a mixture of conformers, offers an opportunity to alter the course of co-assembly and the properties of the fibrils formed. Using *in vitro* RNA selection we were able to identify an RNA aptamer that binds tightly to hβ$_2$m but has no affinity for ΔN6 (Figure 2). The binding interaction was characterized by SPR, fluorescence and NMR to show that the aptamer binds to one side of the protein, consisting of the A,B,E,D β-strands. The same part of the molecule shows altered physicochemical properties between the two β$_2$m variants explaining the preferential binding. Importantly, binding of the aptamer to hβ$_2$m alters the kinetics of co-polymerisation of the two proteins showing that RNA aptamers can be used to derive mechanistic details of amyloid assembly.

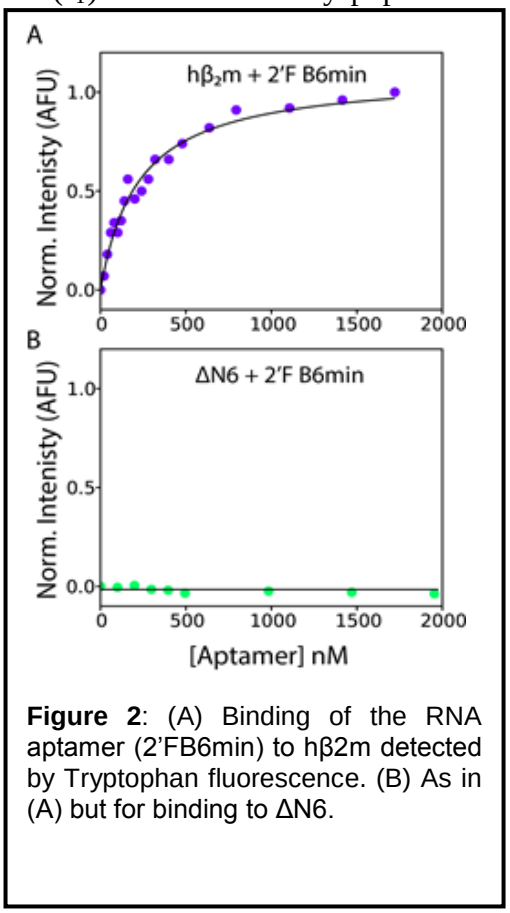


**Figure 2**: (A) Binding of the RNA aptamer (2'FB6min) to hβ2m detected by Tryptophan fluorescence. (B) As in (A) but for binding to ΔN6.

**Publications**

Karamanos, T., Kalverda, A., Thompson, G. & Radford, S. (2014) Visualization of transient protein-protein interactions that promote or inhibit amyloid assembly. *Mol. Cell* **55**: 214-226.

Sarell, C., Karamanos, T., White, S., Bunka, D., Kalverda, A., Thompson, G., Barker, A., Stockley, P. & Radford, S. (2014) Distinguishing closely related amyloid precursors using an RNA aptamer. *J. Biol. Chem.* **289**: 26859-26871.

Su, Y., Sarell, C., Eddy, M., Debelouchina, G., Andreas, L., Pashley, C., Radford, S. & Griffin, R. (2014) Secondary structure in the core of amyloid fibrils formed from human β$_2$m and its truncated variant ΔN6. *J. Am. Chem. Soc.* **136**: 6313-6325.

**Funding**

This work was supported by The Wellcome Trust, BBSRC, the MRC and the ERC.

**Collaborators**

***External:*** R. Griffin (Massachusetts Institute of Technology, USA) and D. Bunka (Aptamer Solutions and Aptamer Diagnostics Ltd., UK)

## Novel methods for screening and classifying small molecule inhibitors of protein aggregation

Janet Saunders, Lydia Young, Rachel Mahood, Charlotte Revill, Richard Foster, David Brockwell, Alison Ashcroft and Sheena Radford

## Introduction

Preventing protein aggregation is of paramount importance in the mission to alleviate some of the most prevalent diseases in the developed world, from the neurodegenerative disorders of Alzheimer's and Parkinson's disease, to systemic diseases such as type II diabetes mellitus. The key pathological hallmark of these amyloid diseases is the accumulation of aggregated proteins into large fibrillated structures known as amyloid plaques. However, low molecular weight soluble oligomers, and high molecular weight prefibrillar intermediates *en route* to amyloid fibrils, are also key to amyloid toxicity. One approach to prevent protein oligomerisation is the use of small molecules to bind specifically to the protein of interest, and inhibit the initial stages of misfolding or aggregation. However, for aggregation-prone proteins that lack defined structure, discovery of small molecule inhibitors of aggregation is limited to screening using relatively low resolution approaches, such as dye binding assays. Our work aims to develop novel, cost-effective and sensitive techniques for measuring protein aggregation and its inhibition.

## Screening and classifying small molecule inhibitors of amyloid formation using ion mobility spectrometry-mass spectrometry

Most biophysical techniques lack the sensitivity and resolution to detect and individually characterise oligomers during aggregation and, therefore, cannot identify the unique protein subspecies with which the small molecule inhibitor interacts.

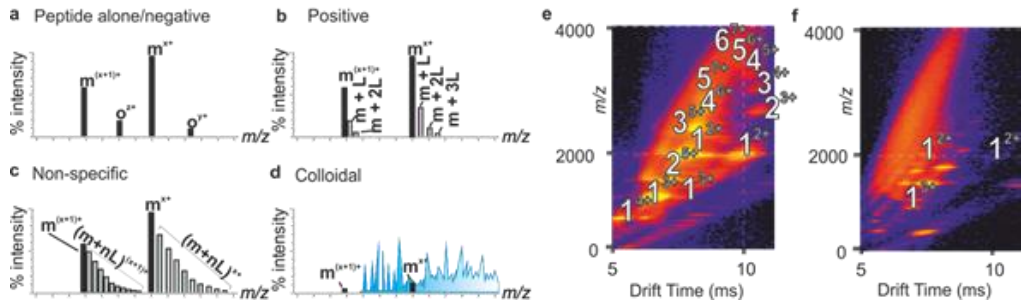


**Figure 1**: ESI-IMS-MS demonstrates the mode or lack of inhibition of protein aggregation by small molecules. (a-d) Schematic of ESI-MS spectra for the various small molecule binding modes. Peptide monomer peaks are denoted 'm', oligomer peaks 'o' and bound ligand 'm+xL'. Charge states are in superscript. (a) A non-interacting small molecule will produce a spectrum the same as the peptide alone. (b) A small molecule that specifically interacts with the peptide will produce a binomial distribution of bound peaks (purple). (c) A non-specific ligand will bind, but result in a Poisson distribution of bound peaks (green). (d) A colloidal inhibitor will produce overlapping peaks due to self-association of the small molecule (blue). (e-f) ESI-IMS-MS Driftscope plot of hIAPP alone and in the presence of a 1:10 molar ratio of the specific inhibitor of hIAPP aggregation, Fast green FCF.

Electrospray ionization-ion mobility spectrometry-mass spectrometry (ESI-IMS-MS) circumvents these disadvantages, allowing the rapid identification of inhibitors and the identification of the individual species

to which the small molecule binds. ESI-IMS-MS is rapid (<1 minute/sample), consumes low amounts of sample (~1000 molecules screened per mg protein), does not require sample labelling or immobilisation, and provides stoichiometric and conformer-specific information. We demonstrated the ability of ESI-IMS-MS to differentiate and classify compounds that do not bind, and those that bind specifically, non-specifically or colloidally, to proteins of interest based solely on the ESI mass spectra (**Figure 1 a-d**). Furthermore, ESI-IMS-MS Driftscope plots can be used to identify the oligomeric distribution in the sample in the absence (**Figure 1e**), or the presence, (**Figure 1f**) of small molecule inhibitors. This work has now been published in *Nature Chemistry* ((2015),**7**: 73-81).

**An *in vivo* platform for studying protein aggregation**

A pre-requisite to studying protein aggregation *in vitro* is the challenging purification of the protein of interest. To bypass this issue, we have developed an *in vivo* system that directly links the aggregation-propensity of a test protein to a simple phenotypic readout: antibiotic resistance. Aggregation-prone sequences, and inhibitors that prevent protein aggregation, can be identified *in vivo* via a β-lactamase-tripartite fusion system (**Figure 2a**), where the minimal inhibitory concentration of antibiotic (MIC), conferred by the β-lactamase enzyme, is used to evaluate the level of test protein aggregation. The aggregation propensity of the two disease-related proteins hIAPP and Aβ40 was found to be significantly higher than non-aggregating controls (**Figure 2b**). Furthermore, growing bacteria expressing the β-lactamase-test protein in the presence of known inhibitors of protein aggregation resulted in growth rescue, in a quantitative manner (**Figure 2c**). This novel and experimentally simple *in vivo* system provides rapid and accurate analysis of protein aggregation and its inhibition, without requiring any prior knowledge of the protein's structure or function. In principle, the assay can be performed where the primary sequence of the protein of interest is the only available information.

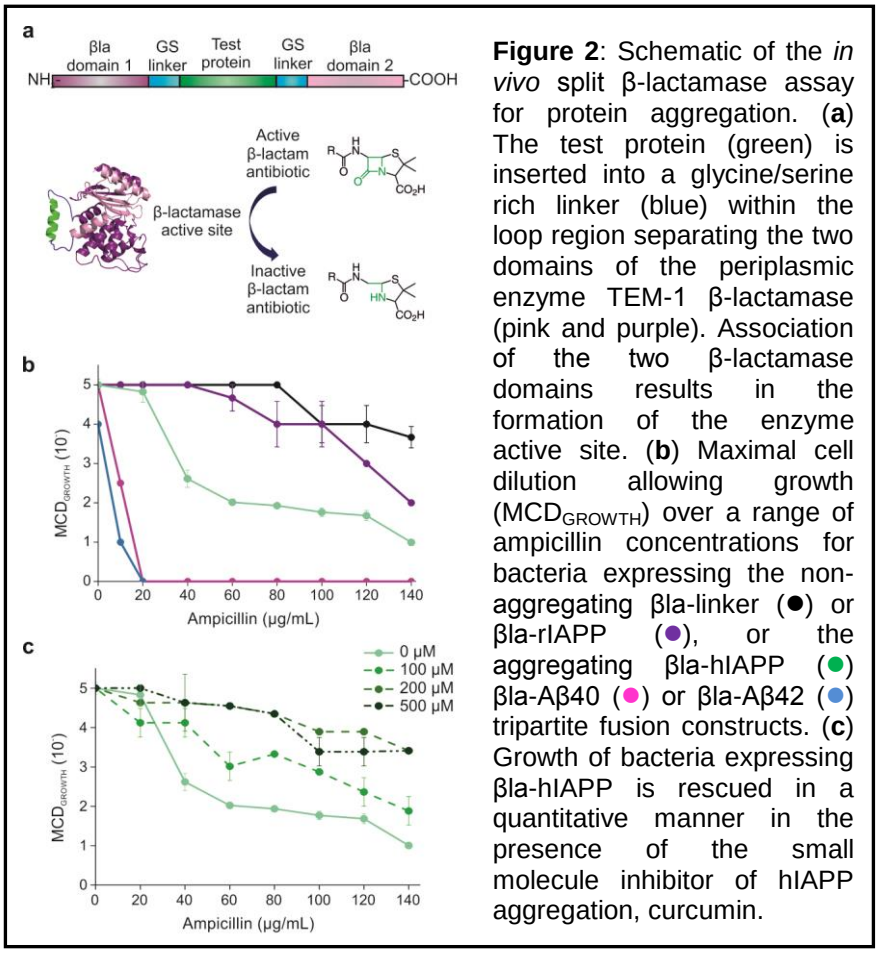


**Figure 2**: Schematic of the *in vivo* split β-lactamase assay for protein aggregation. (**a**) The test protein (green) is inserted into a glycine/serine rich linker (blue) within the loop region separating the two domains of the periplasmic enzyme TEM-1 β-lactamase (pink and purple). Association of the two β-lactamase domains results in the formation of the enzyme active site. (**b**) Maximal cell dilution allowing growth ($MCD_{GROWTH}$) over a range of ampicillin concentrations for bacteria expressing the non-aggregating βla-linker (●) or βla-rIAPP (●), or the aggregating βla-hIAPP (●) βla-Aβ40 (●) or βla-Aβ42 (●) tripartite fusion constructs. (**c**) Growth of bacteria expressing βla-hIAPP is rescued in a quantitative manner in the presence of the small molecule inhibitor of hIAPP aggregation, curcumin.

**Publications**

Young, L., Cao, P., Raleigh, D., Ashcroft, A. & Radford, S. (2014) Ion mobility spectrometry-mass spectrometry defines the oligomeric intermediates in amylin amyloid formation and the mode of action of inhibitors. *J. Am. Chem. Soc.* **136**: 660-670.

**Funding**
BBSRC, ERC, Micromass UK Ltd/Waters Corpn, and Avacta Analytical PLC.

**Collaborators**
External: D. Raleigh (Stony Brook, NY, USA) and A. Smith (Avacta Analyticl PLC, UK).

## Heterologous production of kitamycin by *Escherichia coli*

Ryan Seipke

**Introduction**

More than two-thirds of all therapeutic small molecules used in medicine are derived from or inspired by complex natural products produced by filamentous actinobacteria, most notably *Streptomyces* spp. Antimycin-type depsipeptides are a large family of natural products produced by actinomycetes. Key members of the family include antimycin (9-membered ring), JBIR-09 (12-membered ring), neoantimycin (15-membered ring) and respirantin (18-membred ring). These compounds have diverse targets and tremendous therapeutic potential for the treatment of chronic human illnesses including cancer and neurodegenerative conditions including Alzheimer's and Parkinson's diseases. Antimycin-type depsipeptides show clear evidence of a shared evolutionary history and it is remarkable to observe how nature has used combinatorial biosynthesis (a technique synthetic biologists and bioengineers have yet to master) to engineer ring expansion within this family of natural products as well as a high degree of promiscuity in the selection of building block monomers. These features make them ideal for rational drug design. Our work aims to expand the chemical space of antimycin-type depsipeptides to produce new therapeutics to treat cancer and neurodegenerative disorders. Here, we engineered *E. coli* to be an expression chassis for antimycins and used this robust system to reveal the timing of *N*-forymylation of 3-aminosalicylate.

**Results**

*E. coli* was engineered to heterologously produce the antimycin compound, kitamycin using a modular approach. Rather than cloning and introducing the kitamycin biosynthetic machinery (~25 kb) into *E. coli* on one mobile genetic element, the machinery was modularised and cloned into three compatible protein expression vectors. Expression of the core biosynthetic genes (*antCDEFGHIJKLMNO*) by *E. coli* during fed batch fermentation resulted in the production of kitamycin at 2 mg/L. Engineering the heterologous production of *Streptomyces*
natural products by *E. coli* is notoriously difficult. This work is a major step forwards because of the wealth of synthetic biology tools available for pathway engineering in *E. coli* and the relative ease which they can be used to generate new antimycin analogues.

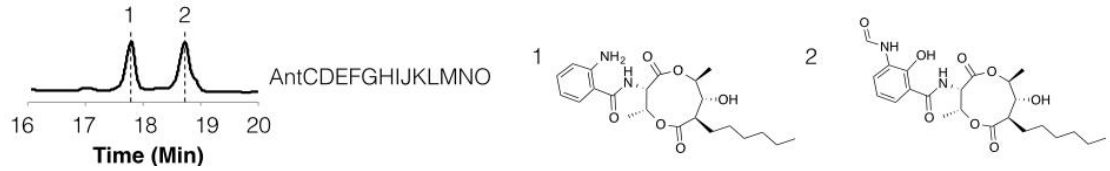


**Figure 1**: *E. coli* production of kitamycin A2. HPLC analysis of chemical extracts prepared from *E. coli* expressing *antCDEFGHIJKLMNO.* produces both compound 1 and compound 2, kitamycin A2.

High resolution LC-ESI-MS of chemical extracts prepared from a series of kitamycin-producing *E. coli* mutants and mutant strains of the native *Streptomyces* producer, revealed that AntO is an *N*-formyltransferase that transforms 3-aminosalicylate into 3-formamidosalicylate whilst it is bound to the peptidyltransferase, AntG before it is presented as a starter unit for the non-ribosomal peptide synthetase, AntC.

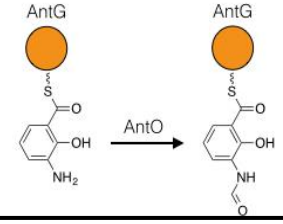


**Figure 2**: AntO is a 3-aminosalicylate *N*-forymltransferase. AntO formylates 3-aminosalicylate to produce the 3-formamidosalicylate starter unit utilised by AntC in the first step of antimycin-type depsipeptide biosynthesis.

Currently, work is in progress utilising this system to produce new antimycin analogues test their therapeutic potential. Work is also in progress exploiting this system to expand the chemical space of other antimycin-type depsipeptides and elucidate and interrogate their mode of action.

**Publications**

Liu, J., Zhu, X., Seipke, R. & Zhang, W. (2014) Biosynthesis of antimycins with a reconstituted 3-formamidosalicylate pharmacophore in *Escherichia coli*. *ACS Synth Biol* doi:10.1021/sb5003136

**Funding**

This work was funded by the University of Leeds New Lecturer Startup Fund and the British Society for Antimicrobial Chemotherapy

**Collaborators**

***External:*** W. Zhang (Department of Chemical and Biomolecular Engineering, University of California at Berkeley).

# Cryo-electron tomography of isolated muscle Z-discs

Mara Rusu, Luigi Fiaschi, Charlotte Scarff, Patrick Harrison and John Trinick

## Introduction

Molecular architecture in muscle sarcomeres has been extensively studied for more than 60 years, mostly by electron microscopy; however, despite extensive efforts none of the four major sarcomere elements (thick and thin filaments, M- and Z-lines) is solved to molecular resolution. In addition to the actin and myosin that sarcomeres are principally composed of, there are as many as 100 other sarcomere proteons. Without knowledge of their layout in the sarcomere it is hard to pose focussed hypotheses to understand the mechanisms and functions of these other components. It also limits understanding of the many muscle diseases that result from mutation of sarcomere proteins.

Failure to describe sarcomere architecture stems mainly from the problems of electron microscopy applied to bulk biological tissue generally. Resolution attained is generally worse than 5 nm, whereas at least 2 nm is needed to recognise protein shapes and accurately dock crystal structures. EM normally requires specimen thickness <200 nm. Thick cells or bulk tissues such as muscle therefore require to be sectioned, which generally first involves chemical fixation, dehydration and embedding in epoxy resin. X-ray fibre diffraction of embedded muscle blocks can show better than 1.2 nm resolution. However, sections cut from the same blocks show worse than 5 nm resolution, indicating that cutting causes most fine detail loss.

EM of sarcomere Z-discs need not necessitate sectioning. The Z-disc alone is inherently thin and it was demonstrated more than 60 years ago that separated Z-discs can be prepared. Isolated Z-discs therefore circumvent of the necessity of sectioning and the damage it causes, offering the prospect of molecular resolution using modern EM techniques such as cryo-EM tomography and image processing. A further advantage of isolated Z-dics is they can be purified and their composition easily monitored.

Z-disc functions were long thought to be purely mechanical. However, roles are now known to be much more complex and Z-discs have been shown to be the location of some 40 proteins. Some of these other components are known to be stress sensors that feed into signalling pathways affecting muscle muscle growth, wasting and breakdown. The goal of our work was to use state-of-the-art cryo-tomography to get 3D models of isolated Z-discs into which crystal structures can be docked accurately; also to sudy Z-disc composition.

## Results

Negative stain and cryo-EM images of isolated honey bee flight muscle Z-discs were obtained on electron microscopes in Leeds and using the FEI Krios 300 kV microscope with Falcon direct electron detector at the MRC Laboratory of Molecular Biology (LMB), Cambridge. Composition of the Z-discs was monitored by SDS-PAGE with excised bands sequenced by mass spectrometry.

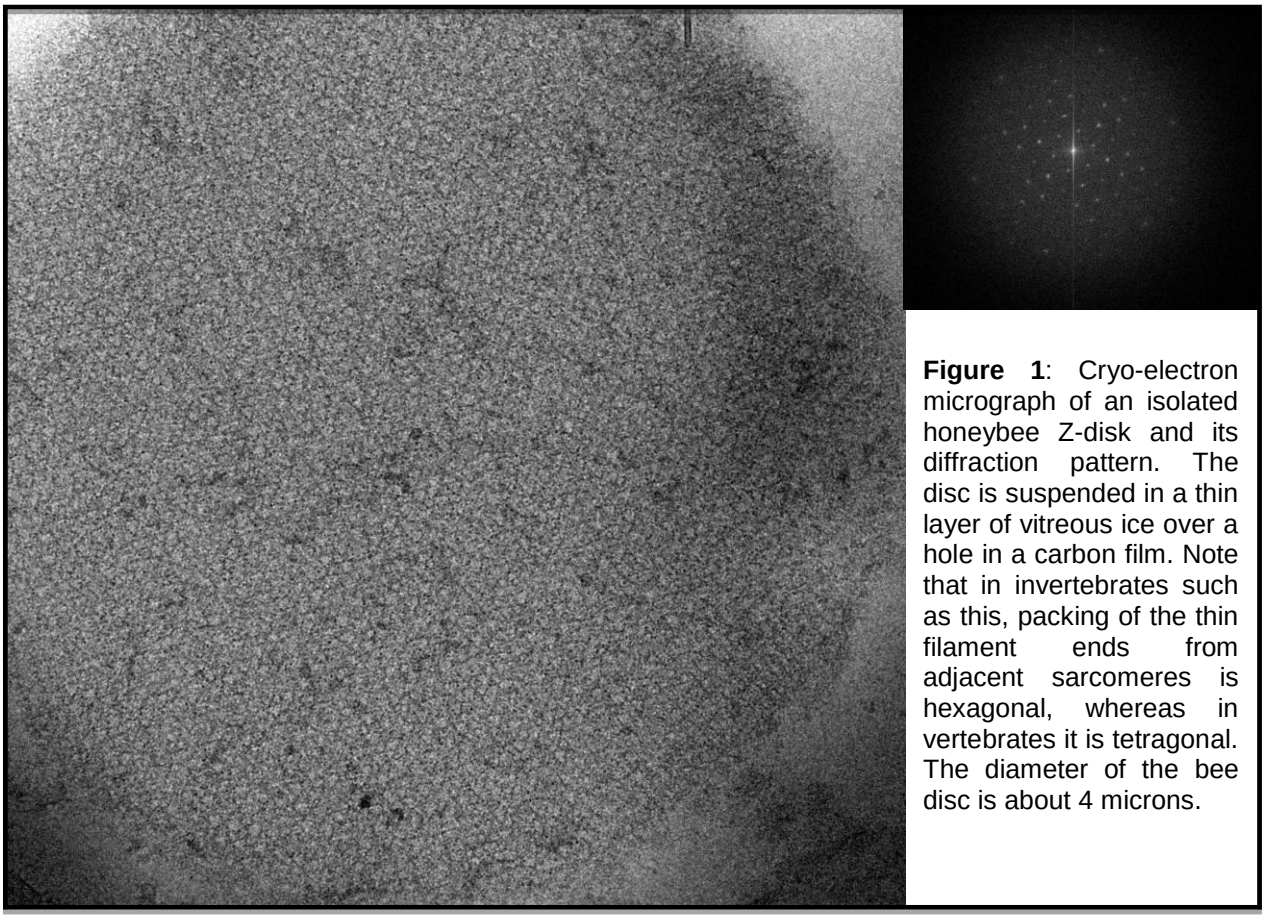

**Figure 1**: Cryo-electron micrograph of an isolated honeybee Z-disk and its diffraction pattern. The disc is suspended in a thin layer of vitreous ice over a hole in a carbon film. Note that in invertebrates such as this, packing of the thin filament ends from adjacent sarcomeres is hexagonal, whereas in vertebrates it is tetragonal. The diameter of the bee disc is about 4 microns.

**Publications**

Rusu M., Taylor, K. A. & Trinick J. (2014) Cryo-EM of Z-Discs isolated from Honeybee flight muscle. *Biophys. J.* **106**: 454.

Muench, S., Rawson, S., Eyraud, V., Delmas, A., Da Silva, P., Phillips, C., Trinick, J., Harrison, M., Gressent, F. & Huss, M. (2014) PA1b inhibitor binding to subunits c and e of the vacuolar ATPase reveals its insecticidal mechanism. *J. Biol. Chem.* **289**: 16399-16408.

Jiao, Y., Walker, M., Trinick, J., Pernier, J., Montaville, P. & Carlier, M.-F. (2014) Mutagenetic and electron microscopy analysis of actin filament severing by Cordon-Bleu, a WH2 domain protein. *Cytoskeleton* **71**: 170-183.

**Funding**

Funded by the EU Muzic Consortium and British Heart Foundation.

**Collaborators**

***University of Leeds:*** S. Muench

***External:*** K. Taylor (Florida State University, USA), H. White (Eastern Virginia Medical School, USA)

# Domain movements of the enhancer-dependent sigma factor drive DNA delivery into the RNA polymerase active site

Amit Sharma, Robert Leach, Christopher Gell, Alastair Smith, Peter Stockley and Roman Tuma

## Introduction

Gene transcription is a tightly regulated cellular process. The basic features of the transcription machinery are conserved through all kingdoms of life, with the multi-subunit RNA polymerase (RNAP) playing a central role. Bacteria use a sequence-specific DNA-binding protein, the sigma (σ) factor, which together with five core subunits ($\alpha_2\beta\beta'\omega$) forms the RNAP holoenzyme that performs promoter recognition and DNA opening during transcription initiation. Two principal classes of σ factors are known, the $\sigma^{70}$ and $\sigma^{54}$. The former mediates transcription of house-keeping genes while the latter activates gene expression in response to environmental cues. The $\sigma^{54}$-dependent transcription system encounters a kinetic barrier to open, transcriptionally active complex (RPo) formation and required Bacterial Enhancer Binding Proteins (bEBPs) for activation. These proteins, such as PspF (Phage Shock Protein F), belong to the ATPases Associated with various cellular Activities (AAA+) family, bind to upstream enhancer binding sequences and couple the energy associated with ATP hydrolysis to remodel the inactive closed complex (RPc) into RPo.

A large scale domain reorganization of $\sigma^{54}$ occurs when the holoenzyme interacts with PspF in the presence of ADP.AlFx, suggesting that ATP hydrolysis is key to removal of the 'roadblock' but little is known about these well-orchestrated but largely unmapped intermediate steps. In order to map these steps we have employed complementary single molecule fluorescence (SMF) techniques, Alternating Laser Excitation (ALEX), Total Internal Reflection Fluorescence Microscopy (TIRFM) and Fluorescence Correlation Spectroscopy (FCS) to probe the domain movements in $\sigma^{54}$ upon holoenzyme formation, in the closed promoter complex, upon binding to a pre-melted *nifH* promoter mimicking the open complex, upon PspF-mediated transition state of ATP hydrolysis and RPo formation, and finally upon RNA primed initiation and subsequent transcript elongation.

## Results

Here, we complement the proposed multi-step kinetic model by assigning the kinetic steps to defined structural rearrangements of Regions I and III with respect to each other, and to the promoter. The irreversible, ATP hydrolysis-driven step is preceded by two reversible steps. No domain separation occurs during the first step (step II to III, Figure 1), modelled here by $E\sigma^{54}$ binding to the early-melted promoter. However, the second step, which is modelled by $E\sigma^{54}$-late-melted promoter complex formation, leads to significant separation between Regions I and III (step III to IV, Figure 1) but without DNA repositioning. Since this domain movement only happens on the partially melted promoter it is most likely driven by ssDNA recognition, as in the case of $\sigma^{70}$ where sequence-specific ssDNA binding is coupled to promoter unwinding. The domain separation is further stabilized by interaction with the activator PspF even in the absence of ATP (Figure 1, IV to V). In the presence of the transition state analogue ADP:$AlF_x$ $\sigma^{54}$ domains become further separated and Region I moves towards the leading edge of the promoter (Figure 1, V to VI). However, only ATP hydrolysis makes the protein rearrangement irreversible (Figure 1, VI to VII), the domain separation decreasing to the one seen in the nucleotide-free state (V in Figure 1) but with both regions closer to the leading edge. This most likely reflects loading of the template DNA strand into the active site, resulting in bending of the promoter and polymerase ββ' clamp closure. DNA footprints of the $E\sigma^{54}$ RPc and RPo show little difference at the upstream trailing edge, whereas in RPo the downstream footprint is extended, the interaction with the downstream fork junction is changed and the start site DNA is well within RNAP. Thus,

changes in trailing edge FRET with the Region III label may reflect increased upstream wrapping of DNA in RPo, and changes in $\sigma^{54}$ Region I to III separations between RPo and RPc are dominated by a movement of Region I relative to a more static Region III.

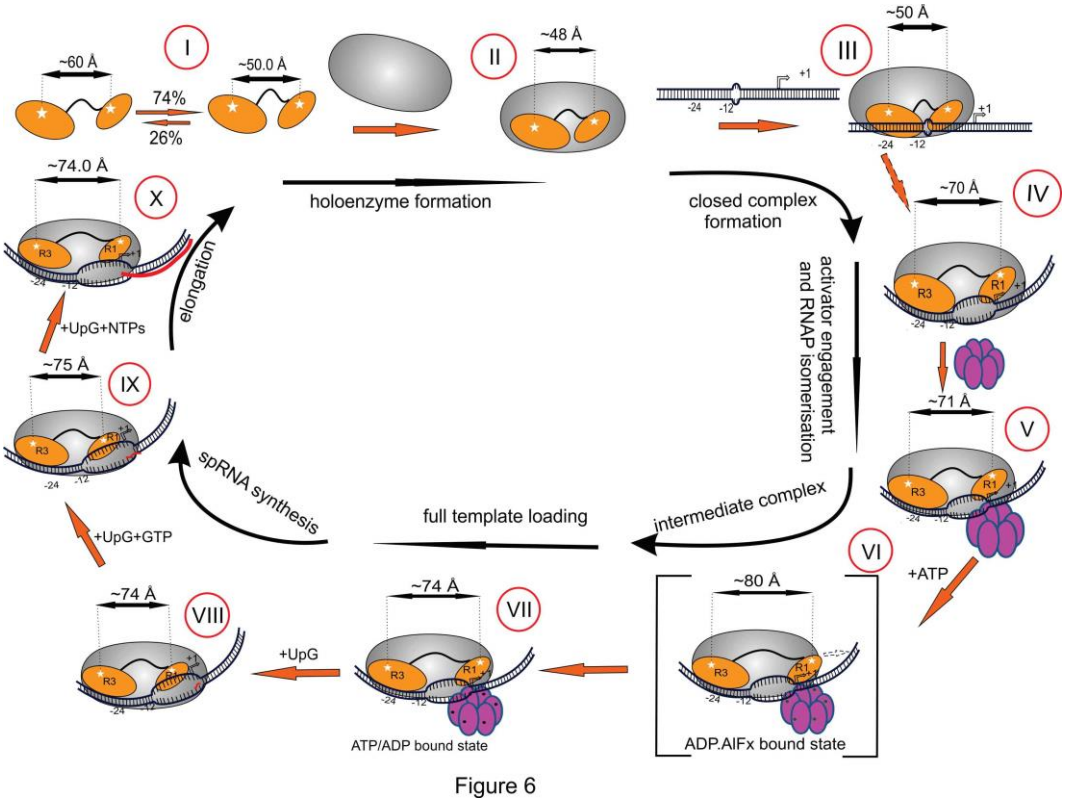


Figure 6

**Figure 1**: Tracking conformation dynamics of $\sigma^{54}$ during the transcription cycle. Model shows the domain disposition adopted by the Region I and III of $\sigma^{54}$ with respect to each other and also in the context of the *nifH* promoter DNA beginning from free $\sigma^{54}$ in solution (stage I), holoenzyme formation (stage II), closed promoter complex (RPc,stage III), activator engagement and RNAP isomerisation (stage IV-V), intermediate complex (RPi) formation (stage VI), full template loading (stage VII),initial transcript formation (stage VIII-IX), elongation complex (stage X).

Our results demonstrate that there are fundamental differences between the initiation at $\sigma^{70}$ and $\sigma^{54}$ promoters. Whereas for $\sigma^{70}$ proteins where the Region1.1 is repositioned from the RNAP DNA-binding channel to allow RPo formation, $\sigma^{54}$ Region I is actively relocated by the ATPase during hydrolysis. In contrast, for $\sigma^{70}$ RPo formation signals from DNA may induce opening and closing of the RNAP clamp, causing Region 1.1 to move away from the RNAP main channel. Hence for $\sigma^{54}$ RPo formation is coupled to its cognate enzymatic ATPase, for $\sigma^{70}$ to promoter DNA motions.

**Publications**

Sharma, A., Leach, R., Gell, C., Zhang, N., Burrows, P., Shepherd, D., Wigneshweraraj, S., Smith, D., Zhang, X., Buck, M., Stockley, P. & Tuma, R. (2014) Domain movements of the enhancer-dependent sigma factor drive DNA delivery into the RNA polymerase active site: insights from single molecule studies. *Nucleic Acids Res.* **42**: 5177-5190.

**Funding**
This work was funded by the BBSRC.

**Collaborators**
***External:*** N. Zhang, P. Burrows, S. Wigneshweraraj, X. Zhang and M. Buck (Imperial College London, UK)

# An engineered glycoprotein inhibitor of cholera toxin

Thomas Branson, Martin Fascione, Tom M$^{c}$Allister, James Ross, Stuart Warriner and Bruce Turnbull

## Introduction

Protein-carbohydrate interactions at cell surfaces mediate many important processes in biology from fertilisation to adhesion of viruses, bacteria and their toxins. Individually, protein-sugar interactions are usually very weak, but both affinity and binding selectivity can be enhanced through a phenomenon called multivalency: multiple binding sites on the protein interact simultaneously with multiple copies of the sugar ligand to achieve a high avidity and enhance binding selectivity. A good example of this class of proteins is the cholera toxin which binds to five copies of a specific glycolipid ligand on the surface of cells that line the intestine. Binding to the cell surface leads to internalisation of the toxin, therefore, inhibitors of the protein-sugar interaction have the potential to be used as anti-toxin drugs.

We have developed methods to make chemically defined glycoprotein inhibitors that are matched in size and valency to the target toxin. The cholera toxin B-subunit was first converted to a non-binding mutant, to which the carbohydrate ligands were appended selectively at the N-termini of the pentameric protein by an oxime ligation reaction. The glycoprotein inhibitor was around 14,000 times more potent as an inhibitor than the monovalent carbohydrate. A combination of dynamic light scattering and analytical ultracentrifugation demonstrated that the inhibitor formed 1:1 complexes with the target toxin. The methods developed in this project have the potential to provide a general strategy for making inhibitors against multimeric proteins.

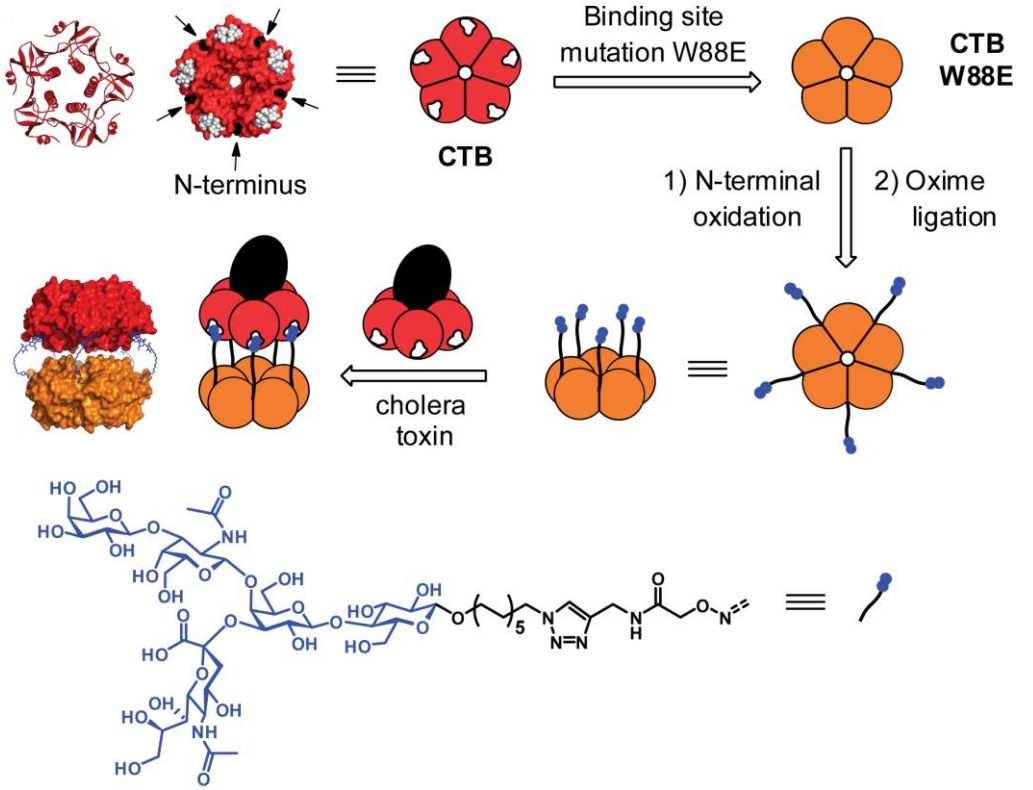


**Figure 1**: Re-engineering the cholera toxin B-subunit by site-directed mutagenesis and N-terminal oxidation and oxime ligation. Part of the figure is reproduced with permission from Branson et al., (2014) *Angew. Chem. Int. Ed*. **53**, 8323-8327.

**Publications**

Branson, T., Mcallister, T., Garcia-Hartjes, J., Fascione, M., Ross, J., Warriner, S., Wennekes, T., Zuilhof, H. & Turnbull, W. (2014) A protein-based pentavalent inhibitor of the cholera toxin B-subunit. *Angew. Chem. Int. Ed. Engl.* **53**: 8323-8327.

**Funding**

This work was funded by the Royal Society, EPSRC, the Wellcome Trust, COST Action CM1102 and the University of Leeds.

**Collaborators**

***External:*** J. Garcia-Hartjes, T. Wennekes, H. Zuilhof (Wageningen University, the Netherlands.)

# Transcellular stress signalling: How proteotoxic stress is communicated between different tissues in *C.elegans*

Patricija van Oosten-Hawle

## Introduction

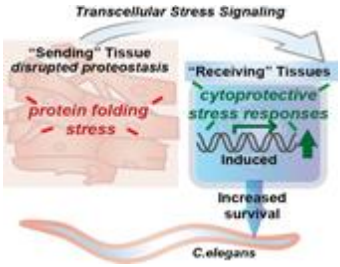


**Figure 1**: Model explaining Transcellular Stress Signalling in C. elegans.

In all biological systems, cells throughout their lifetime are exposed to different physiological and environmental stress conditions that lead to protein damage and cellular dysfunction – and ultimately disease. Cumulative protein misfolding and aggregation is one of the hallmarks implicated in the pathologies of misfolding diseases associated with neurodegeneration, including Alzheimer's disease, amyotrophic lateral sclerosis, Huntington's disease and Parkinson's disease, as well as cancer, diabetes and several myopathies. Maintaining a healthy cellular proteome is crucial to cellular viability. This is achieved by the proteostasis network, which integrates protein biogenesis, protein folding by molecular chaperones, as well as clearance mechanisms and stress response pathways. However, in an entire organism, cellular damage associated with misfolded proteins are rarely confined to a single tissue, but often involve peripheral tissues in ways we are only beginning to understand. Because the regulation of stress response mechanisms that maintain cellular proteostasis have been historically investigated in isolated tissue culture cells and unicellular organisms, regulation of proteostasis is understood in a strict cell-autonomous manner, regardless of the health state of neighbouring cells. Recent evidence in different multicellular model systems, such as fruit fly *D. melanogaster* and nematode *C. elegans* as well as mammalian tissue culture now show that cellular stress responses are organized coordinately between and across tissues by transcellular stress signalling in metazoans. For example an imbalance of proteostasis within one tissue is sensed and signalled to other tissues within the organism to adjust chaperone levels, minimize the risk of proteotoxic damage and increase survival (Figure 1).

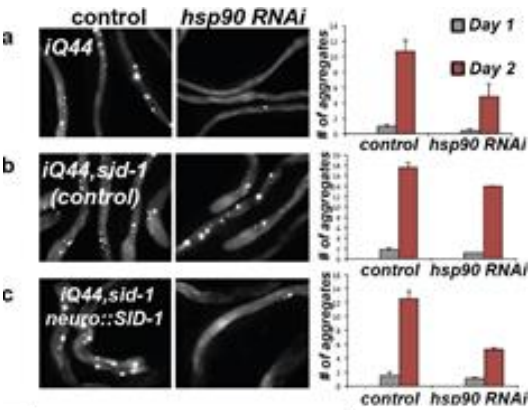


**Figure** 2:Transcellular stress delays polyQ aggregation of an intestinal iQ44::YFP disease model. (a) Systemic RNAi-mediated knockdown of hsp90 reduces age-dependent Q44 aggregation. (b) iQ44::YFP animals in the background of the RNAi-insensitive sid-1 mutant are unaffected by RNAi. (c) Neuron-specific hsp90 RNAi reduces intestinal iQ44::YFP aggregation by almost 50%, when compared to RNAi insensitive iQ44,sid-1 control animals in (b).

**Results**

This project aims to determine how the transcellular stress signalling response between tissues can be utilized to enhance cytoprotective stress responses to restore the health of tissues affected by protein folding disease. To address these questions, we use *C. elegans*, a well-established metazoan model organism for protein misfolding diseases and proteostasis. First results using a *C. elegans* Huntington's (PolyQ) disease model, where Q44 fused to YFP is expressed the intestine shows that transcellular stress signalling may indeed alleviate age-dependent aggregation. For example, by tissue-specific genetic manipulation of *hsp90* levels in neurons, which induces the heat shock response and cytoprotective chaperones in multiple tissues, aggregation of intestinal polyQ (*iQ44::YFP*) is reduced by almost 50% (Figure 2). Current studies are aimed at identifying transcellular signalling molecules mediating this response and extending to other *C. elegans* neurodegenerative disease models.

**Publications**

Van Oosten-Hawle, P. & Morimoto, R. (2014) Transcellular chaperone signaling: An organismal strategy for integrated cell stress responses. *J. Exp. Biol.* **217**:129-136.

**Funding**

We thank the University of Leeds for start-up funding.

# Modulation of biologically relevant processes using small molecules

George Burslem, Anna Barnard, Jennifer Miles, Valeria Azzarito, Hannah Kyle, Kerya Long, Panchami Prabhakaran, George Preston, David Yeo, Alison Ashcroft, Alex Breeze, Thomas Edwards, Adam Nelson, Sheena Radford, Stuart Warriner and Andrew Wilson

## Introduction

This report summarises our group's efforts to develop inhibitors of protein-protein interactions (PPIs) using oligobenzamide helix mimetics, as well as a comparative study of photoinduced cross-linking (PIC) reagents as chemical tools.

## Proteomimetics as inhibitors of the HIF-1α/p300 PPI

Around 30% of all PPIs are mediated by α-helices and thus represent targets for generic inhibitor design. We introduced oligobenzamide proteomimetics as inhibitors of helix mediated PPIs; these scaffolds project functional groups that match the spatial orientation of key side chains of native α-helices. We have identified a series of 3-*O*-alkylated oligobenzamides as the first biophysically characterised inhibitors of the interaction between the transcription factor HIF-1α and its co-activator protein p300 (Figure 1a) – an important target in tumour metabolism. Potent compounds were identified (9.2 μM *vs.* 0.2 μM for the 42 residue p300 binding sequence of HIF-1α) with a selective binding profile (100-fold selectivity over the eIF4E/eIF4G interaction).

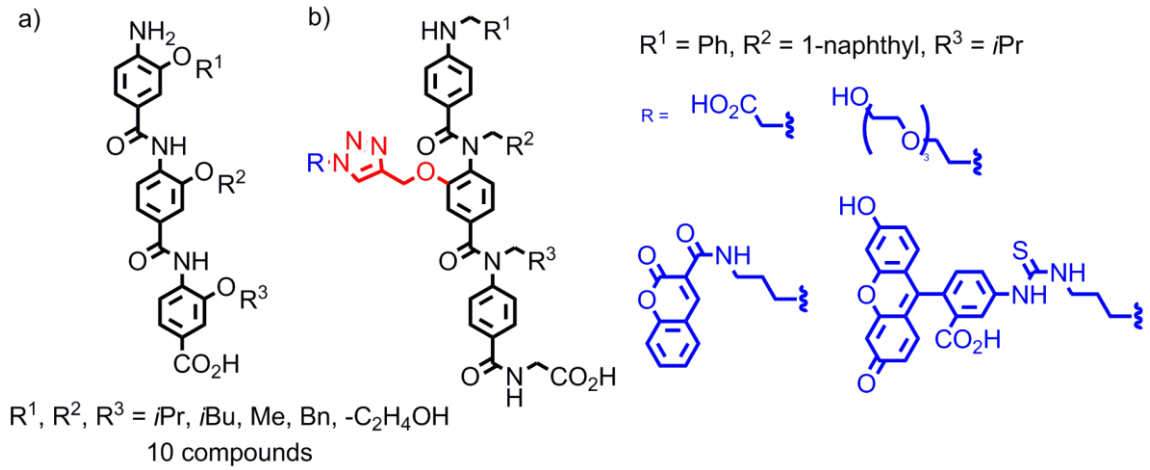


**Figure 1**: a) Chemical structure of 3-*O*-alkylated oligobenzamide helix mimetics used as inhibitiors of the HIF-1□/p300 PPI and b) structures of orthogonally functionalised *N*-alkylated oligobenzamides (triazole linker shown in *red*; side chain functionalities in *blue*).

## Orthogonal functionalisation of oligobenzamide helix mimetics

In order to endow our oligobenzamide helix mimetics with additional tailor-made features (*e.g.* enhanced solubility, cellular uptake), we investigated orthogonal functionalisation on the non-protein binding face of *N*-alkylated aromatic oligoamides (Figure 1b). We were able to show that installation of an alkyne group on the central building block was possible and that the target compounds were amenable to automated solid phase synthesis. Functionalisation of these oligoamides by 'click chemistry' on resin and final cleavage yielded compounds with diverse functional groups. A simple acidic group and an oligoethylene moiety were intended to improve solubility properties, while a coumarin derivative and a fluorescein label were installed for use in direct binding fluorescence anisotropy experiments. Our functionalised compounds were tested for their efficiency to inhibit PPIs and were shown to act as low micromolar (~ 20-40 μM) inhibitors of the p53/*h*DM2 interaction, showing some degree of binding selectivity when tested

for other related PPIs (Mcl-1/NOXA-B and Bcl-$x_L$/BAK). Although the new series shows slightly reduced inhibitory activity compared to the unfunctionalised anaolgues (~ 10 μM), the fact that such proteomimetics can be structurally modified on the non-binding side, while still retaining activity and their selectivity profile will permit their use in further studies.

**Investigations of photoinduced cross-linking probes**

Photoinduced cross-linking (PIC) is a powerful tool for the identification and analysis of interactions between biomacromolecules and their ligands. In a comparative study, we investigated the PIC properties of three commonly used reagents, *i.e.* phenyl trifluoromethyldiaziridine (TFMD), phenylazide (PA) and benzophenone (BP). Amyloid-like nanostructures of A$\beta_{16\text{-}22}$ (amyloid beta; residues 16-22) assembled from TFMD variants were chosen as a model system for our cross-linking studies (Figure 2). Analysis of the cross-linked aggregates by different MS techniques revealed TFMD to be superior over PA and BP in terms of higher cross-linking efficiency and simpler product distribution. TFMD generated only intermolecular cross-links (in the presence of nanostructure), an important feature for gathering structural information.

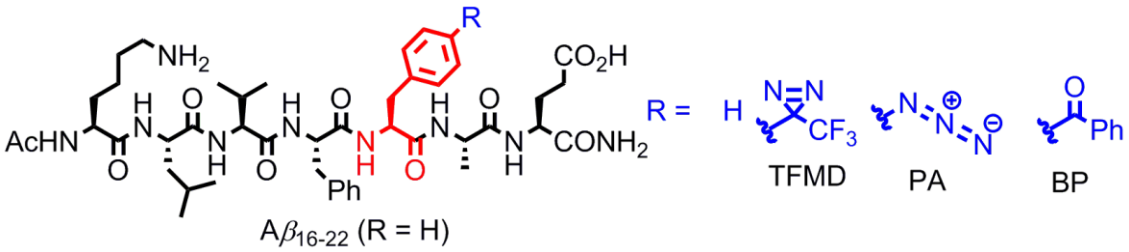


**Figure 2**: Chemical structure of A□16-22 (R = H) and derivatives with incorporated PIC reagents (blue; 4-substituted phenylalanine residue used for introduction of the photoreactive groups is highlighted in red; TFMD = phenyl trifluoromethyldiaziridine, PA = phenylazide, BP = benzophenone).

**Publications**


Burslem, G., Kyle, H., Breeze, A., Edwards, T., Nelson, A., Warriner, S. & Wilson, A. (2014) Small-molecule proteomimetic inhibitors of the HIF-1α-p300 protein-protein interaction. *Chembiochem* **15**: 1083-1087.

Burslem, G. & Wilson, A. (2014) Synthesis of oligobenzamide alpha-helix mimetics. *Synlett* **25**: 324-335.

Barnard, A., Long, K., Yeo, D., Miles, J., Azzarito, V., Burslem, G., Prabhakaran, P., Edwards, T. & Wilson, A. (2014) Orthogonal functionalisation of alpha-helix mimetics. *Org. Biomol. Chem.* **12**: 6794-6799.

Preston, G., Radford, S., Ashcroft, A. & Wilson, A. (2014) Analysis of amyloid nanostructures using photo-cross-linking: *in situ* comparison of three widely used photo-cross-linkers. *ACS Chem. Biol.* **9**: 761-768.


**Funding**


We gratefully acknowledge The University of Leeds, EPSRC, ERC, EU-COST, AstraZeneca and The Leverhulme Trust for financial support of this research.

# Crystal structures of heterodimeric POZ domains

Mark Stead and Stephanie Wright

## Introduction

The POZ domain is a protein-protein interaction domain found at the N-terminus of approximately forty mammalian transcription factors. Several POZ-domain transcription factors are overexpressed in specific human malignancies, and targeting their interaction interfaces is a potential therapeutic strategy. POZ domains form well-characterised dimers and they also mediate the recruitment of transcriptional co-regulators. The transcriptional properties of many POZ-domain transcription factors are critically altered by their heteromeric associations with each other; however, the stoichiometry of heteromeric POZ-POZ interactions is not known, and structures of heteromeric POZ domains have not been reported. Miz1 is a POZ-domain transcription factor that regulates cell-cycle arrest and DNA-damage responses, and whose activities are altered by its interaction with the POZ-domain transcriptional repressors BCL6 and NAC1; these interactions have been implicated in B-cell lymphomas and in ovarian serous carcinomas that overexpress BCL6 and NAC1 respectively. We developed a strategy for the purification of tethered POZ domains that form forced heterodimers, and solved the crystal structures of the heterodimeric POZ domains of Miz1/BCL6 and Miz1/NAC1.

## Results

In order to produce heterodimeric POZ domains in bacteria, we expressed chimeric proteins that contained the Miz1 POZ domain joined to either the BCL6- or NAC1 POZ domain by a Gly+Ser-rich linker that was predicted to form a flexible hydrophilic tether. The tethered Miz1/BCL6 and Miz1/NAC1 POZ domains eluted at the same volume as classic POZ-domain homodimers when purified by size-exclusion chromatography. The tethered POZ domains were crystallised and X-ray structures were determined by molecular replacement using the constituent POZ-domain monomers are search models. Structures of Miz1/BCL6 and Miz1/NAC1 were determined to 2.2Å and 2.3Å resolution respectively. The overall structures of the heterodimeric POZ domains resemble the structures of reported POZ-domain homodimers, and contain a central hydrophobic interface of alpha helices together with a beta-sheet interface that contains one strand contributed from each constituent monomer (Figure 1).

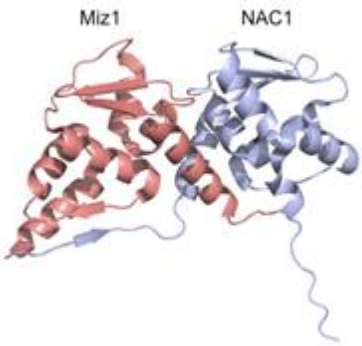


**Figure 1**: Ribbon representation of the heterodimeric Miz1/NAC1 POZ domain

We showed that several of the residues involved in interactions at the interface of the Miz1 POZ domain homodimer are also involved in similar interactions in both the Miz1/BCL6 and Miz1/NAC1 heterodimers. The production of heterodimeric POZ domains is now enabling a direct experimental analysis of their co-repressor interactions, and the structures will inform the design of therapeutic inhibitors. In addition, the network of heteromeric interactions between POZ-domain transcription factors has not been extensively studied, and structures of further forced POZ-domain heterodimers will most likely reveal features that determine the specificity of these associations.

**Publications**

Stead, M. & Wright, S. (2014) Nac1 interacts with the POZ-domain transcription factor, miz1. *Biosci. Rep.* **34**: 227-235.

Stead, M. & Wright, S. (2014) Structures of heterodimeric POZ domains of miz1/BCL6 and miz1/NAC1. *Acta Crystallogr. F* **70**: 1591-1596.

**Funding**

This work was funded by Yorkshire Cancer Research.

# Molecular-level regulation of molecular chaperones

Saeid Shahidi, Philip Rowell, Hugh Smith and Anastasia Zhuravleva

## Introduction

### Molecular mechanisms of regulation of BIP, a Hsp70 chaperone in the ER

The endoplasmic reticulum (ER) is an essential organelle in eukaryotic cells responsible for folding and maturation of the majority of secreted and membrane proteins. A central player of the ER protein folding machinery is the chaperone immunoglobulin heavy-chain binding protein (BIP; also known as GRP78 and HSP5A). As the only Hsp70 chaperone in the ER, BIP binds to the majority of unfolded and misfolded proteins in this organelle to promote their folding and prevent aggregation. Failure of BIP function results in an imbalance of ER protein homeostasis. Mounting evidence suggests that BIP activity is linked to neurodegenerative diseases, diabetes, cardiovascular diseases, cancer progression and anticancer drug resistance. Several unique features associated with BIP regulation distinguish BIP from other Hsp70s, suggesting that the regulation of BIP activity is potential rational target for disease research and drug development. We are using the latest methodological advantages in NMR, combined with other biophysical methods and computational tools, to elucidate the critical molecular features of BIP activity and its regulation.

To elucidate structural, thermodynamic and functional features of the BIP chaperone cycle and characterize its conformational landscape, we have produced several key BIP constructs, including full-length BIP, its isolated domains, SBD and βSBD (to dissect an αLid role), several NBD (to dissect an interdomain linker role). We have established robust protocols for the production of NMR samples for all these constructs using *E. coli* expression in $D_2O$ media and His-tagged purification of NMR labeled BIP. To obtain backbone and methyl chemical shift assignments, we are using several approaches, including divide-and-conquer approach, selective isotopic unlabeling and cell-free protein production and specific labelling. As a complementary technique to site-specific information provided by NMR, we use ITC to characterize global thermodynamic features of the BIP functional cycle (Fig. 1). We hope to answer several fundamental questions regarding the molecular basis of BIP function and regulation and well as better understand allosteric signal transduction in large multidomain and multicomponent biological machines.

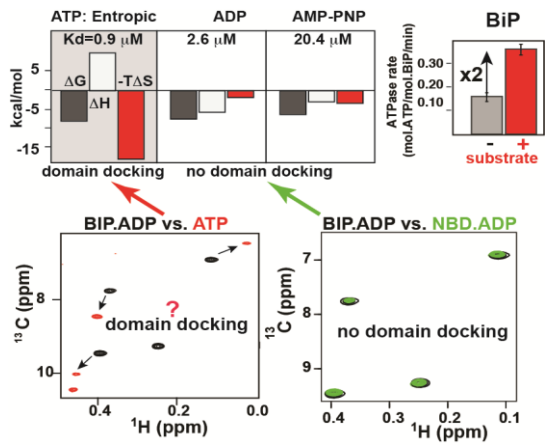


**Figure 1**: Experimental approaches for the characterization of the BIP conformational landscape:
**ITC**: The change in enthalpy (ΔH; shown in light grey) and the change in entropy (ΔS) multiplied by the absolute temperature (T=298K) (shown in red), the change in free energy (ΔG; shown in dark gray), and the dissociation constant $K_d$ (annotated) upon nucleotide binding (ATP, ADP, and a non-hydrolysable ATP analogue, AMP-PNP) to ATPase-deficient BIP-T229G.
**Functional assay**: ATPase activity in the presence and the absence of its model substrate (HTFPAVL)
**Methyl NMR**: Blow-ups of representative regions of methyl-TROSY spectra of the ADP-/peptide-bound BIP (black) overlaid with the spectra of ATP-bound BIP (red) and ADP-bound NBD (green).

**Linking inter- and intradomain allostery in Hsp70 chaperones**

Through a study of the *E. coli* Hsp70 (DnaK) using computational methods and NMR, we investigated allosteric signalling in its substrate-binding domain (SBD). We identified two subdomains of the β-sandwich portion of the SBD (the βSBD) that rock around a hinge region to mediate interconversion between states with higher and lower affinity for substrate, and greater or lesser tendency to dock onto the NBD. ATP-mediated NBD conformational changes trigger conversion of the SBD from a high to low substrate affinity state by favouring formation of contacts with lynchpin sites on the βSBD. Steric constraints on these βSBD sites force disengagement of SBD strand β8 from strand β7, re-packing of a βSBD hydrophobic cluster, disruption of the hydrophobic arch over the substrate-binding cleft, and increased dynamics throughout the entire βSBD. Our work reveals that changes in both conformation and dynamics within the βSBD play a central role in interdomain allosteric communication in the Hsp70, DnaK.

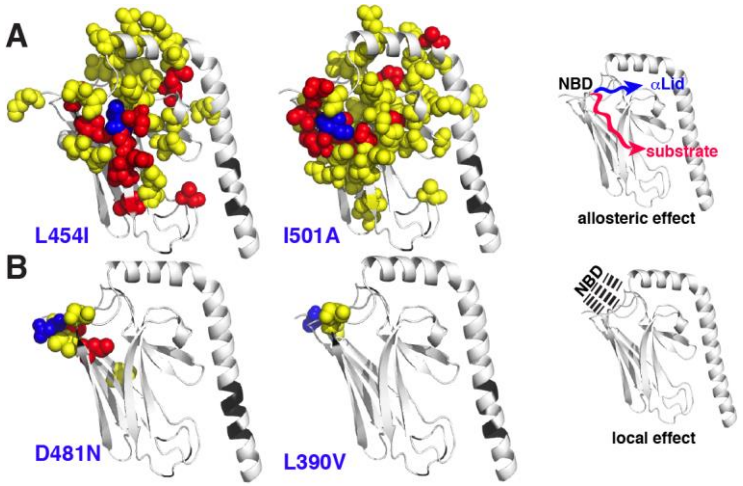


**Figure 2**: Allosteric networks in the βSBD as indicated by NMR chemical shift perturbations **(**CSPs) between DnaK and its variants (A) L454I and I501A and (B) D481N and L390V. CSPs for individual residues were calculated using differences in chemical shifts for backbone amide $^{1}H$ ($\Delta\omega_H$) and $^{15}N$ ($\Delta\omega_N$) using the following equation: $CSP=\sqrt{[\Delta\omega_H^2 + (0.154\ \Delta\omega_N^2]}$. CSPs are mapped onto the domain-undocked structure of the SBD. CSPs are shown in yellow when $\Delta\omega_H > 0.03$ ppm or/and $\Delta\omega_N > 0.3$ ppm and red if CSPs larger than 0.1; the mutation sites are shown in blue; residues without experimental data are shown in black. Cartoons on the left schematically illustrate that perturbations on the interdomain interface (i.e., NBD binding) may result in: allosteric (long-range) changes in the βSBD (as reported by CSPs in A) or only direct (local) effects around βSBD that interact with the NBD (as reported by CSPs in B).

**Publications**

Zhuravleva A. & Radford S. (2014) How TriC Folds Tricky Proteins. *Cell* **159:**1251-1252.

**Funding**

FBS start-up grant & Royal Society research grant.

**Collaborators**

***External:*** L. M. Gierasch (University of Massachusetts at Amherst, USA), D. Ron (University of Cambridge, UK), L. Hendershot (St. Jude Children's Research Hospital, USA)

## ASTBURY SEMINARS 2014

**16th January**
Prof Mark Bradley, University of Edinburgh
*"Two Adventures in Chemical Biology - Palladium Mediated Cellular Chemistry and in vivo Imaging"*

**6th March**
Prof Laura Machesky, Beatson Institute for Cancer Research, Glasgow
*"Signalling to the actin cytoskeleton in migration and invasion of cancer cells"*

**20th March**
Prof Peter Rich, Dept. Structural and Molecular Biology, University College London
*"Yeast cytochrome c oxidase: A link between the structures and mechanisms of bacterial and mammalian enzymes"*

**30th May**
Dr Esko Oksanen, European Spallation Source & Lund University
*"Neutron crystallography - insights to enzyme mechanisms and prospects at the European Spallation Source"*

**5th June**
Prof David Case, Rutgers University
*"Bridging the divide: all atom molecular dynamics simulations of biomolecular crystals"*

**3rd July**
**Astbury Annual Lecture**
Prof Andrew Hamilton, FRS, University of Oxford
*"Targeting Protein Surfaces using Designed Proteomimetics"*

**4th September**
Dr Ilme Schlichting , Max Plank Institute, Heidelberg
*"X-ray free-electron lasers, emerging opportunities for structural biology"*

**24th September**
Dr Shaun Lott, University of Auckland
*"The structure of ABC toxins"*

**2nd October**
Prof Joost Schymkowitz, VIB, Belgium
*"Rational engineering of protein aggregation in biotech applications"*

**6th November**
Dr James Baker, UCL
*"Homogeneous antibody conjugation by disulfide bridging"*

**4th December**
Dr Uli Schwarz-Linek , University of St Andrews
*"Covalent host binding by Gram-positive bacteria"*

# PUBLICATIONS BY ASTBURY CENTRE MEMBERS 2014


Abdul-Sada, H., Knight, L., Griffiths, D., Whitehouse, A. & Macdonald, A. (2014) Merkel cell polyomavirus - the new kid on the tumour virus block. *Int. J. Mol. Med.* **34**: S107-S107.

Abou-Saleh, R., Swain, M., Evans, S. & Thomson, N. (2014) Poly(ethylene glycol) lipid-shelled microbubbles: abundance, stability, and mechanical properties. *Langmuir* **30**: 5557-5563.

Adams, M., Cookson, V., Higgins, J., Martin, H., Tomlinson, D., Bond, J., Morrison, E. & Bell, S. (2014) A high-throughput assay to identify modifiers of premature chromosome condensation. *J. Biomol. Screen.* **19**: 176-183.

Akhbari, P., Whitehouse, A. & Boyne, J. (2014) Long non-coding RNAs drive metastatic progression in melanoma (review). *Int. J. Oncol.* **45**: 2181-2186.

Aramini, J., Hamilton, K., Ma, L.-C., Swapna, G., Leonard, P., Ladbury, J., Krug, R. & Montelione, G. (2014) $F^{19}$ NMR reveals multiple conformations at the dimer interface of the nonstructural protein 1 effector domain from influenza A virus. *Structure* **22**: 515-525.

Atkins, E., Tatineni, R., Li, H., Gretch, D., Harris, M. & Griffin, S. (2014) The stability of secreted, acid-labile H77/JFH-1 hepatitis C virus (HCV) particles is altered by patient isolate genotype 1a p7 sequences. *Virology* **448**: 117-124.

Ayton, S., Zhang, M., Roberts, B., Lam, L., Lind, M., Mclean, C., Bush, A., Frugier, T., Crack, P. & Duce, J. (2014) Ceruloplasmin and beta-amyloid precursor protein confer neuroprotection in traumatic brain injury and lower neuronal iron. *Free Radic. Biol. Med.* **69**: 331-337.

Bakker, S., Groppelli, E., Pearson, A., Stockley, P., Rowlands, D. & Ranson, N. (2014) Limits of structural plasticity in a picornavirus capsid revealed by a massively expanded equine rhinitis A virus particle. *J Virol.* **88**: 6093-6099.

Barnard, A., Long, K., Yeo, D., Miles, J., Azzarito, V., Burslem, G., Prabhakaran, P., Edwards, T. & Wilson, A. (2014) Orthogonal functionalisation of alpha-helix mimetics. *Org. Biomol. Chem.* **12**: 6794-6799.

Beales, P. & Vanderlick, T. (2014) Application of nucleic acid-lipid conjugates for the programmable organisation of liposomal modules. *Adv. Colloid Interface Sci.* **207**: 290-305.

Belyaeva, T., Nicol, C., Cesur, O., Trave, G., Blair, G. & Stonehouse, N. (2014) An RNA aptamer targets the PDZ-binding motif of the HPV16 E6 oncoprotein. *Cancers* **6**: 1553-1569.

Bentham, M., Marraiki, N., Mccormick, C., Rowlands, D. & Griffin, S. (2014) Ns2 is dispensable for efficient assembly of hepatitis C virus-like particles in a bipartite trans-encapsidation system. *J. Gen. Virol.* **95**: 2427-2441.

Billingsley, D., Lee, A., Johansson, N., Walton, A., Stanger, L., Crampton, N., Bonass, W. & Thomson, N. (2014) Patchiness of ion-exchanged mica revealed by DNA binding dynamics at short length scales. *Nanotechnology* **25**: 025704.

Billington, N., Revill, D., Burgess, S., Chantler, P. & Knight, P. (2014) Flexibility within the heads of muscle myosin-2 molecules. *J. Mol. Biol.* **426**: 894-907.

Bolze, C., Helbling, R., Owen, R., Pearson, A., Pompidor, G., Dworkowski, F., Fuchs, M., Furrer, J., Golczak, M., Palczewski, K., Cascella, M. & Stocker, A. (2014) Human cellular retinaldehyde-binding protein has secondary thermal 9-cis-retinal isomerase activity. *J. Am. Chem. Soc.* **136**: 137-146.

Branson, T., Mcallister, T., Garcia-Hartjes, J., Fascione, M., Ross, J., Warriner, S., Wennekes, T., Zuilhof, H. & Turnbull, W. (2014) A protein-based pentavalent inhibitor of the cholera toxin B-subunit. *Angew. Chem. Int. Ed. Engl.* **53**: 8323-8327.

Burslem, G., Kyle, H., Breeze, A., Edwards, T., Nelson, A., Warriner, S. & Wilson, A. (2014) Small-molecule proteomimetic inhibitors of the HIF-1α-p300 protein-protein interaction. *Chembiochem* **15**: 1083-1087.

Burslem, G. & Wilson, A. (2014) Synthesis of oligobenzamide alpha-helix mimetics. *Synlett* **25**: 324-335.

Cain, R., Narramore, S., Mcphillie, M., Simmons, K. & Fishwick, C. (2014) Applications of structure-based design to antibacterial drug discovery. *Bioorg. Chem.* **55**: 69-76.

Care, M., Cocco, M., Laye, J., Barnes, N., Huang, Y., Wang, M., Barrans, S., Du, M., Jack, A., Westhead, D., Doody, G. & Tooze, R. (2014) SPIB and BATF provide alternate determinants of IRF4 occupancy in diffuse large B-cell lymphoma linked to disease heterogeneity. *Nucleic Acids Res.* **42**: 7588-7610.

Caseley, E., Muench, S., Roger, S., Mao, H.-J., Baldwin, S. & Jiang, L.-H. (2014) Non-synonymous single nucleotide polymorphisms in the P2X receptor genes: Association with diseases, impact on receptor functions and potential use as diagnosis biomarkers. *Int. J. Mol. Sci.* **15**: 13344-13371.

Ceasar, S., Hodge, A., Baker, A. & Baldwin, S. (2014) Phosphate concentration and arbuscular mycorrhizal colonisation influence the growth, yield and expression of twelve PHT1 family phosphate transporters in foxtail millet (*Setaria italica*). *PLoS One* **9**: e108459.

Cherukuri, A., Rothstein, D., Clark, B., Carter, C., Davison, A., Hernandez-Fuentes, M., Hewitt, E., Salama, A. & Baker, R. (2014) Immunologic human renal allograft injury associates with an altered IL-10/TNF-α expression ratio in regulatory B cells. *J. Am. Soc. Nephrol.* **25**: 1575-1585.

Colegrave, M. & Peckham, M. (2014) Structural implications of beta-cardiac myosin heavy chain mutations in human disease. *Anat. Rec.* **297**: 1670-1680.

Cookson, N., Henkelis, J., Ansell, R., Fishwick, C., Hardie, M. & Fisher, J. (2014) Encapsulation of sodium alkyl sulfates by the cyclotriveratrylene-based, [$Pd_6L_8^{12+}$] stella octangula cage. *Dalton Trans.* **43**: 5657-5661.

Cunningham, F., Mcphillie, M., Johnson, A. & Fishwick, C. (2014) An *in silico* structure- based approach to anti- infective drug discovery. *Parasitology* **141**: 17-27.

Czajlik, A., Thompson, G., Khan, G., Kalverda, A., Homans, S. & Trinick, J. (2014) $H^1$, $N^{15}$ and $C^{13}$ backbone chemical shift assignment of titin domains A59-A60 and A60 alone. *Biomol. NMR Assign.* **8**: 429-433.

Daniels, A., Campeotto, I., Van Der Kamp, M., Bolt, A., Trinh, C., Phillips, S., Pearson, A., Nelson, A., Mulholland, A. & Berry, A. (2014) Reaction mechanism of n-acetylneuraminic acid lyase revealed by a combination of crystallography, QM/MM simulation, and mutagenesis. *ACS Chem. Biol.* **9**: 1025-1032.

D'annessa, I., Coletta, A., Sutthibutpong, T., Mitchell, J., Chillemi, G., Harris, S. & Desideri, A. (2014) Simulations of DNA topoisomerase 1b bound to supercoiled DNA reveal changes in the flexibility pattern of the enzyme and a secondary protein-DNA binding site. *Nucleic Acids Res.* **42**: 9304-9312.

De Colibus, L., Wang, X., Spyrou, J., Kelly, J., Ren, J., Grimes, J., Puerstinger, G., Stonehouse, N., Walter, T., Hu, Z., Wang, J., Li, X., Peng, W., Rowlands, D., Fry, E., Rao, Z. & Stuart, D. (2014) More-powerful virus inhibitors from structure-based analysis of HEV71 capsid-binding molecules. *Nat. Struct. Mol. Biol.* **21**: 282-288.

Doble, R., Mcdermott, M., Cesur, O., Stonehouse, N. & Wittmann, M. (2014) IL-17A RNA aptamer: Possible therapeutic potential in some cells, more than we bargained for in others? *J. Invest. Dermatol.* **134**: 852-855.

Doveston, R., Marsden, S. & Nelson, A. (2014) Towards the realisation of lead-oriented synthesis. *Drug Discov. Today* **19**: 813-819.

Dowall, S., Matthews, D., Garcia-Dorival, I., Taylor, I., Kenny, J., Hertz-Fowler, C., Hall, N., Corbin-Lickfett, K., Empig, C., Schlunegger, K., Barr, J., Carroll, M., Hewson, R. & Hiscox, J. (2014) Elucidating variations in the nucleotide sequence of Ebola virus associated with increasing pathogenicity. *Genome Biol.* **15**: 540.

Drake, M., Furuta, T., Suen, K., Gonzalez, G., Liu, B., Kalia, A., Ladbury, J., Fire, A., Skeath, J. & Arur, S. (2014) A requirement for ERK-dependent dicer phosphorylation in coordinating oocyte-to-embryo transition in *C. elegans*. *Dev. Cell* **31**: 614-628.

Dudutiene, V., Matuliene, J., Smirnov, A., Timm, D., Zubriene, A., Baranauskiene, L., Morkunaite, V., Smirnoviene, J., Michailoviene, V., Juozapaitiene, V., Mickeviciute, A., Kazokaite, J., Baksyte, S., Kasiliauskaite, A., Jachno, J., Revuckiene, J., Kisonaite, M., Pilipuityte, V., Ivanauskaite, E., Milinaviciute, G., Smirnovas, V., Petrikaite, V., Kairys, V., Petrauskas, V., Norvaisas, P., Linge, D., Gibieza, P., Capkauskaite, E., Zaksauskas, A., Kazlauskas, E., Manakova, E., Grazulis, S., Ladbury, J. & Matulis, D. (2014) Discovery and characterization of novel selective inhibitors of carbonic anhydrase IX. *J. Med. Chem.* **57**: 9435-9446.

Duval, C., Allan, P., Connell, S., Ridger, V., Philippou, H. & Ariens, R. (2014) Roles of fibrin alpha- and gamma-chain specific cross-linking by FXIIIa in fibrin structure and function. *Thromb. Haemost.* **111**: 842-850.

Dykeman, E., Stockley, P. & Twarock, R. (2014) Solving a Levinthal's paradox for virus assembly identifies a unique antiviral strategy. *Proc. Natl Acad. Sci USA* **111**: 5361-5366.

Elsheshiny, A., Ashcroft, A. & Harris, S. (2014) A comparison of the electromechanical properties of structurally diverse proteins by molecular dynamics simulation. *J. Biomol. Struct. Dyn.* **32**: 1734-1741.

Eves-Van Den Akker, S., Lilley, C., Ault, J., Ashcroft, A., Jones, J. & Urwin, P. (2014) The feeding tube of cyst nematodes: Characterisation of protein exclusion. *PLoS One* **9**: e87289.

Fearnley, G., Smith, G., Odell, A., Latham, A., Wheatcroft, S., Harrison, M., Tomlinson, D. & Ponnambalam, S. (2014). Vascular endothelial growth factor a-stimulated signaling from endosomes in primary endothelial cells. *Methods Enzymol.* **535**: 265-292.

Fisher, M., Basak, R., Kalverda, A., Fishwick, C., Turnbull, W. & Nelson, A. (2014) Discovery of novel Fabf ligands inspired by platensimycin by integrating structure-based design with diversity-oriented synthetic accessibility. *Org. Biomol. Chem.* **12**: 486-494.

Forrest, S., Lear, Z., Herod, M., Ryan, M., Rowlands, D. & Stonehouse, N. (2014) Inhibition of the foot-and-mouth disease virus subgenomic replicon by RNA aptamers. *J. Gen. Virol.* **95**: 2649-2657.

Foster, T., Thompson, G., Kalverda, A., Kankanala, J., Bentham, M., Wetherill, L., Thompson, J., Barker, A., Clarke, D., Noerenberg, M., Pearson, A., Rowlands, D., Homans, S., Harris, M., Foster, R. & Griffin,

S. (2014) Structure-guided design affirms inhibitors of hepatitis C virus p7 as a viable class of antivirals targeting virion release. *Hepatology* **59**: 408-422.

Fu, B., Sahakyan, A., Camilloni, C., Gaetano Tartaglia, G., Paci, E., Caflisch, A., Vendruscolo, M. & Cavalli, A. (2014) ALMOST: An all atom molecular simulation toolkit for protein structure determination. *J. Comput. Chem.* **35**: 1101-1105.

Gad, S., Regan, S., Wu, C., Smith, K., Yao, S., Ng, A., Karpinski, E., Baldwin, S., Baldwin, J., Postis, V., Cass, C. & Young, J. (2014) Identification and functional characterization of the primary sodium binding site of human concentrative nucleoside transporter 3, hCNT3 (SLC28A3). *Biochem. Cell Biol.* **92**: 584-585.

Gao, H., Grueschow, S., Barke, J., Seipke, R., Hill, L., Orivel, J., Yu, D., Hutchings, M. & Goss, R. (2014) Filipins: The first antifungal "weed killers" identified from bacteria isolated from the trap-ant. *RSC Adv.* **4**: 57267-57270.

Garcia-Dorival, I., Wu, W., Dowall, S., Armstrong, S., Touzelet, O., Wastling, J., Barr, J., Matthews, D., Carroll, M., Hewson, R. & Hiscox, J. (2014) Elucidation of the Ebola virus VP24 cellular interactome and disruption of virus biology through targeted inhibition of host-cell protein function. *J Proteome Res.* **13**: 5120-5135.

Gershenson, A., Gierasch, L., Pastore, A. & Radford, S. (2014) Energy landscapes of functional proteins are inherently risky. *Nat. Chem. Biol.* **10**: 884-891.

Gilmour, J., Assi, S., Jaegle, U., Kulu, D., Van De Werken, H., Clarke, D., Westhead, D., Philipsen, S. & Bonifer, C. (2014) A crucial role for the ubiquitously expressed transcription factor Sp1 at early stages of hematopoietic specification. *Development* **141**: 2391-2401.

Giusti, F., Rieger, J., Catoire, L., Qian, S., Calabrese, A., Watkinson, T., Casiraghi, M., Radford, S., Ashcroft, A. & Popot, J.-L. (2014) Synthesis, characterization and applications of a perdeuterated amphipol. *J. Membr. Biol.* **247**: 909-924.

Goodchild, S., Sheynis, T., Thompson, R., Tipping, K., Xue, W.-F., Ranson, N., Beales, P., Hewitt, E. & Radford, S. (2014) $\beta_2$-microglobulin amyloid fibril-induced membrane disruption is enhanced by endosomal lipids and acidic pH. *PLoS One* **9**: e104492.

Griffin, S. (2014) 'Too little, too late?' Will inhibitors of the hepatitis C virus p7 ion channel ever be used in the clinic? *Future Med. Chem.* **6**: 1893-1907.

Hamed, M., Brown, R.J., Zothner, C., Urbanowicz, R., Mason, C., Krarup, A., Mcclure, C., Irving, W., Ball, J., Harris, M., Hickling, T. & Tarr, A. (2014) Recombinant human L-ficolin directly neutralizes hepatitis C virus entry. *J. Innate Immun.* **6**: 676-684.

Heath, G., Abou-Saleh, R., Peyman, S., Johnson, B., Connell, S. & Evans, S. (2014) Self-assembly of actin scaffolds on lipid microbubbles. *Soft Matter* **10**: 694-700.

Heath, G., Roth, J., Connell, S. & Evans, S. (2014) Diffusion in low-dimensional lipid membranes. *Nano Lett.* **14**: 5984-5988.

Hellewell, A., Foresti, O., Gover, N., Porter, M. & Hewitt, E. (2014) Analysis of familial hemophagocytic lymphohistiocytosis type 4 (FHL-4) mutant proteins reveals that S-acylation is required for the function of syntaxin 11 in natural killer cells. *PLoS One* **9**: e98900.

Henkelis, J., Fisher, J., Warriner, S. & Hardie, M. (2014) Solvent-dependent self-assembly behaviour and speciation control of $Pd_6L_8$ metallo-supramolecular cages. *Chem. Eur. J.* **20**: 4117-4125.

Hiruma-Shimizu, K., Kalverda, A., Henderson, P., Homans, S. & Patching, S. (2014) Synthesis of uniformly deuterated n-dodecyl-β-D-maltoside ($d_{39}$-ddm) for solubilization of membrane proteins in TROSY NMR experiments. *J. Labelled Comp. Radiopharm.* **57**: 737-743.

Hrast, M., Anderluh, M., Knez, D., Randall, C., Barreteau, H., O'Neill, A., Blanot, D. & Gobec, S. (2014) Design, synthesis and evaluation of second generation MurF inhibitors based on a cyanothiophene scaffold. *Eur. J. Med. Chem.* **73**: 83-96.

Jackson, B., Noerenberg, M. & Whitehouse, A. (2014) A novel mechanism inducing genome instability in kaposi's sarcoma-associated herpesvirus infected cells. *PLoS Pathog.* **10**: e1004098.

Jakhria, T., Hellewell, A., Porter, M., Jackson, M., Tipping, K., Xue, W.-F., Radford, S. & Hewitt, E. (2014) $\beta_2$-microglobulin amyloid fibrils are nanoparticles that disrupt lysosomal membrane protein trafficking and inhibit protein degradation by lysosomes. *J. Biol. Chem.* **289**: 35781-35794.

James, T., Maclellan, P., Burslem, G., Simpson, I., Grant, J., Warriner, S., Sridharan, V. & Nelson, A. (2014) A modular lead-oriented synthesis of diverse piperazine, 1,4-diazepane and 1,5-diazocane scaffolds. *Org. Biomol. Chem.* **12**: 2584-2591.

Jiao, Y., Walker, M., Trinick, J., Pernier, J., Montaville, P. & Carlier, M.-F. (2014) Mutagenetic and electron microscopy analysis of actin filament severing by Cordon-Bleu, a WH2 domain protein. *Cytoskeleton* **71**: 170-183.

Jose Nogueira, J., Wang, Y., Martin, F., Acami, M., Glowacki, D., Shalashilin, D., Paci, E., Fernandez-Ramos, A., Hase, W.L., Martinez-Nunez, E. & Vazquez, S. (2014) Unraveling the factors that control soft landing of small silyl ions on fluorinated self-assembled monolayers. *J. Phys. Chem. C* **118**: 10159-10169.

Kalverda, A., Gowdy, J., Thompson, G., Homans, S., Henderson, P. & Patching, S. (2014) TROSY NMR with a 52 kDa sugar transport protein and the binding of a small-molecule inhibitor. *Mol. Membr. Biol.* **31**: 131-140.

Karageorgis, G., Warriner, S. & Nelson, A. (2014) Efficient discovery of bioactive scaffolds by activity-directed synthesis. *Nat. Chem.* **6**: 872-876.

Karamanos, T., Kalverda, A., Thompson, G. & Radford, S. (2014) Visualization of transient protein-protein interactions that promote or inhibit amyloid assembly. *Mol. Cell* **55**: 214-226.

Kato, Y., Yagi, T., Harris, S., Ohki, S.-Y., Yura, K., Shimizu, Y., Honda, S., Kamiya, R., Burgess, S. & Tanokura, M. (2014) Structure of the microtubule-binding domain of flagellar dynein. *Structure* **22**: 1628-1638.

Kime, L., Clarke, J., Romero, D., Grasby, J. & Mcdowall, K. (2014) Adjacent single-stranded regions mediate processing of tRNA precursors by RNase E direct entry. *Nucleic Acids Res.* **42**: 4577-4589.

King, R., Tiede, C., John, V., Trehan, A., Tomlinson, D. & Ajjan, R. (2014) Inhibiting complement C3 and fibrinogen interaction: a potential novel therapeutic target to reduce cardiovascular disease in diabetes. *Diabet. Med.* **31**: 57-58.

Klein, T., Tucker, J., Holdgate, G., Norman, R. & Breeze, A. (2014) FGFR1 kinase inhibitors: close regioisomers adopt divergent binding modes and display distinct biophysical signatures. *ACS Med. Chem. Lett.* **5**: 166-171.

Kraatz, I., Booth, M., Whitaker, B., Nix, M. & Critchley, K. (2014) Sub-bandgap emission and intraband defect-related excited-state dynamics in colloidal $CuInS_2$/ZnS quantum dots revealed by femtosecond pump-dump-probe spectroscopy. *J. Phys. Chem. C* **118**: 24102-24109.

Krivov, S., Fenton, H., Goldsmith, P., Prasad, R., Fisher, J. & Paci, E. (2014) Optimal reaction coordinate as a biomarker for the dynamics of recovery from kidney transplant. *PLoS Comput. Biol.* **10**: e1003685.

Lanyon-Hogg, T., Hooper, J., Gunn, S., Warriner, S. & Baker, A. (2014) PEX14 binding to arabidopsis PEX5 has differential effects on PTS1 and PTS2 cargo occupancy of the receptor. *FEBS Lett.* **588**: 2223-2229.

Latham, A., Kankanala, J., Fearnley, G., Gage, M., Kearney, M., Homer-Vanniasinkam, S., Wheatcroft, S., Fishwick, C. & Ponnambalam, S. (2014) *In silico* design and biological evaluation of a dual specificity kinase inhibitor targeting cell cycle progression and angiogenesis. *PLoS One* **9**: e110997.

Leney, A., Pashley, C., Scarff, C., Radford, S. & Ashcroft, A. (2014) Insights into the role of the β2-microglobulin D-strand in amyloid propensity revealed by mass spectrometry. *Mol. Biosyst.* **10**: 412-420.

Levesley, A., Paxton, S., Collins, R., Baker, A. & Knight, C. (2014) Engaging students with plant science: The plant science tree. *New Phytol.* **203**: 1041-1048.

Li, H., Horn, J., Campbell, A., House, D., Nelson, A. & Marsden, S. (2014) A convergent rhodium-catalysed asymmetric synthesis of tetrahydroquinolines. *Chem. Commun.* **50**: 10222-10224.

Liebens, V., Gerits, E., Knapen, W., Swings, T., Beullens, S., Steenackers, H., Robijns, S., Lippell, A., O'Neill, A., Veber, M., Froehlich, M., Krona, A., Loevenklev, M., Corbau, R., Marchand, A., Chaltin, P., De Brucker, K., Thevissen, K., Cammue, B., Fauvart, M., Verstraeten, N. & Michiels, J. (2014) Identification and characterization of an anti-pseudomonal dichlorocarbazol derivative displaying anti-biofilm activity. *Bioorg. Med. Chem. Lett.* **24**: 5404-5408.

Lolicato, M., Bucchi, A., Arrigoni, C., Zucca, S., Nardini, M., Schroeder, I., Simmons, K., Aquila, M., Difrancesco, D., Bolognesi, M., Schwede, F., Kashin, D., Fishwick, C., Johnson, A., Thiel, G. & Moroni, A. (2014) Cyclic dinucleotides bind the C-linker of HCN4 to control channel cAMP responsiveness. *Nat. Chem. Biol.* **10**: 457-462.

Ma, J., Mcleod, S., Maccormack, K., Sriram, S., Gao, N., Breeze, A. & Hu, J. (2014) Real-time monitoring of New Delhi metallo-β-lactamase activity in living bacterial cells by $H^1$ NMR spectroscopy. *Angew. Chem. Int. Ed. Engl.* **53**: 2130-2133.

MacDonald, S., Martin, J., Chance, R., Warriner, S., Saiz-Lopez, A., Carpenter, L. & Plane, J. (2014) A laboratory characterisation of inorganic iodine emissions from the sea surface: Dependence on oceanic variables and parameterisation for global modelling. *Atmos. Chem. Phys.* **14**: 5841-5852.

Martin, H., Adams, M., Higgins, J., Bond, J., Morrison, E., Bell, S., Warriner, S., Nelson, A. & Tomlinson, D. (2014) High-content, high-throughput screening for the identification of cytotoxic compounds based on cell morphology and cell proliferation markers. *PLoS One* **9**: e88338.

Martin, H., Smith, L. & Tomlinson, D. (2014) Multidrug-resistant breast cancer: Current perspectives. *Breast cancer* **6**: 1-13.

McAllister, T., Horner, K. & Webb, M. (2014) Evaluation of the interaction between phosphohistidine analogues and phosphotyrosine binding domains. *ChemBioChem* **15**: 1088-1091.

McMorran, L., Brockwell, D. & Radford, S. (2014) Mechanistic studies of the biogenesis and folding of outer membrane proteins *in vitro* and *in vivo*: what have we learned to date? *Arch. Biochem. Biophys.* **564**: 265-280.

Mu, Q., David, C.A., Galceran, J., Rey-Castro, C., Krzeminski, L., Wallace, R., Bamiduro, F., Milne, S., Hondow, N., Brydson, R., Vizcay-Barrena, G., Routledge, M., Jeuken, L. & Brown, A. (2014) Systematic investigation of the physicochemical factors that contribute to the toxicity of ZnO nanoparticles. *Chem. Res. Toxicol.* **27**: 558-567.

Muench, S., Rawson, S., Eyraud, V., Delmas, A., Da Silva, P., Phillips, C., Trinick, J., Harrison, M., Gressent, F. & Huss, M. (2014) PA1b inhibitor binding to subunits c and e of the vacuolar ATPase reveals its insecticidal mechanism. *J. Biol. Chem.* **289**: 16399-16408.

Muench, S., Scheres, S., Huss, M., Phillips, C., Vitavska, O., Wieczorek, H., Trinick, J. & Harrison, M. (2014) Subunit positioning and stator filament stiffness in regulation and power transmission in the V1 motor of the *Manduca sexta* V-ATPase. *J. Mol. Biol.* **426**: 286-300.

Munoz, W., Lee, M., Miller, R., Ahmed, Z., Ji, H., Link, T., Lee, G., Kloc, M., Ladbury, J. & Mccrea, P. (2014) Plakophilin-3 catenin associates with the ETV1/ER81 transcription factor to positively modulate gene activity. *PLoS One* **9**: e86784.

Murray, J., Nowak, D., Pukenas, L., Azhar, R., Guillorit, M., Waelti, C., Critchley, K., Johnson, S. & Bon, R. (2014) Solid phase synthesis of functionalised SAM-forming alkanethiol-oligoethyleneglycols. *J. Mater. Chem. B* **2**: 3741-3744.

O'Sullivan, D., Murray, B., Malkin, T., Whale, T., Umo, N., Atkinson, J., Price, H., Baustian, K., Browse, J. & Webb, M. (2014) Ice nucleation by fertile soil dusts: Relative importance of mineral and biogenic components. *Atmos. Chem. Phys.* **14**: 1853-1867.

Panjwani, A., Strauss, M., Gold, S., Wenham, H., Jackson, T., Chou, J., Rowlands, D., Stonehouse, N., Hogle, J. & Tuthill, T. (2014) Capsid protein vp4 of human rhinovirus induces membrane permeability by the formation of a size-selective multimeric pore. *PLoS Pathog.* **10**: e1004294.

Paudyal, R., Jamaluddin, A., Warren, J., Doyle, S., Robert, S., Warriner, S. & Baker, A. (2014) Trafficking modulator tenin1 inhibits endocytosis, causes endomembrane protein accumulation at the pre-vacuolar compartment and impairs gravitropic response in *Arabidopsis thaliana*. *Biochem. J.* **460**: 177-185.

Pecci, A., Klersy, C., Gresele, P., Lee, K., De Rocco, D., Bozzi, V., Russo, G., Heller, P., Loffredo, G., Ballmaier, M., Fabris, F., Beggiato, E., Kahr, W., Pujol-Moix, N., Platokouki, H., Van Geet, C., Noris, P., Yerram, P., Hermans, C., Gerber, B., Economou, M., De Groot, M., Zieger, B., De Candia, E., Fraticelli, V., Kersseboom, R., Piccoli, G., Zimmermann, S., Fierro, T., Glembotsky, A., Vianello, F., Zaninetti, C., Nicchia, E., Guethner, C., Baronci, C., Seri, M., Knight, P., Balduini, C. & Savoia, A. (2014) Myh9-related disease: A novel prognostic model to predict the clinical evolution of the disease based on genotype-phenotype correlations. *Hum. Mutat.* **35**: 236-247.

Preston, G., Radford, S., Ashcroft, A. & Wilson, A. (2014) Analysis of amyloid nanostructures using photo-cross-linking: *in situ* comparison of three widely used photo-cross-linkers. *ACS Chem. Biol.* **9**: 761-768.

Pritchard, C., Groves, K., Biesenbruch, S., O'Connor, G., Ashcroft, A., Arsene, C., Schulze, D. & Quaglia, M. (2014) Quantification of human growth hormone in serum with a labeled protein as an internal standard: Essential considerations. *Anal. Chem.* **86**: 6525-6532.

Prompinit, P., Achalkumar, A., Walton, A., Bushby, R., Waelti, C. & Evans, S. (2014) Reversible metallisation of soft UV patterned substrates. *J. Mater. Chem. C* **2**: 5916-5923.

Ptasinska, A., Assi, S., Martinez-Soria, N., Imperato, M., Piper, J., Cauchy, P., Pickin, A., James, S., Hoogenkamp, M., Williamson, D., Wu, M., Tenen, D., Ott, S., Westhead, D., Cockerill, P., Heidenreich, O. & Bonifer, C. (2014) Identification of a dynamic core transcriptional network in t(8;21) AML that regulates differentiation block and self-renewal. *Cell Rep.* **8**: 1974-1988.

Radou, G., Dreyer, F., Tuma, R. & Paci, E. (2014) Functional dynamics of hexameric helicase probed by hydrogen exchange and simulation. *Biophys. J.* **107**: 983-990.

Radu, V., Frielingsdorf, S., Evans, S., Lenz, O. & Jeuken, L. (2014) Enhanced oxygen-tolerance of the full heterotrimeric membrane-bound [NiFe] -hydrogenase of *Ralstonia eutropha*. *J. Am. Chem. Soc.* **136**: 8512-8515.

Ravichandran, S., Singh, N., Donnelly, D., Migliore, M., Johnson, P., Fishwick, C., Luke, B., Martin, B., Maudsley, S., Fugmann, S. & Moaddel, R. (2014) Pharmacophore model of the quercetin binding site of the SIRT6 protein. *J. Mol. Graph. Model.* **49**: 38-46.

Richards, K., Doble, R., Wasson, C., Haider, M., Blair, G., Wittmann, M. & Macdonald, A. (2014) Human papillomavirus e7 oncoprotein increases production of the anti-inflammatory interleukin-18 binding protein in keratinocytes. *J. Virol.* **88**: 4173-4179.

Richardson, R., Papachristos, K., Read, D., Harlen, O., Harrison, M., Paci, E., Muench, S. & Harris, S. (2014) Understanding the apparent stator-rotor connections in the rotary ATPase family using coarse-grained computer modeling. *Proteins* **82**: 3298-3311.

Rimratchada, S., Mcleish, T., Radford, S. & Paci, E. (2014) The role of high-dimensional diffusive search, stabilization, and frustration in protein folding. *Biophys. J.***106**: 1729-1740.

Roberts, B., Lim, N., Mcallum, E., Donnelly, P., Hare, D., Doble, P., Turner, B., Price, K., Lim, S., Paterson, B., Hickey, J., Rhoads, T., Williams, J., Kanninen, K., Hung, L., Liddell, J., Grubman, A., Monty, J.-F., Llanos, R., Kramer, D., Mercer, J., Bush, A., Masters, C., Duce, J., Li, Q.-X., Beckman, J., Barnham, K., White, A. & Crouch, P. (2014) Oral treatment with $Cu^{ii}$(atsm) increases mutant SOD1 *in vivo* but protects motor neurons and improves the phenotype of a transgenic mouse model of amyotrophic lateral sclerosis. *J. Neurosci.* **34**: 8021-8031.

Romero, D., Hasan, A., Lin, Y.-F., Kime, L., Ruiz-Larrabeiti, O., Urem, M., Bucca, G., Mamanova, L., Laing, E., Van Wezel, G., Smith, C., Kaberdin, V. & Mcdowall, K. (2014) A comparison of key aspects of gene regulation in *Streptomyces coelicolor* and *Escherichia coli* using nucleotide-resolution transcription maps produced in parallel by global and differential RNA sequencing. *Mol. Microbiol.* **94**: 963-987.

Ross-Thriepland, D. & Harris, M. (2014) Insights into the complexity and functionality of hepatitis C virus NS5A phosphorylation. *J. Virol.* **88**: 1421-1432.

Sarell, C., Karamanos, T., White, S., Bunka, D., Kalverda, A., Thompson, G., Barker, A., Stockley, P. & Radford, S. (2014) Distinguishing closely related amyloid precursors using an RNA aptamer. *J. Biol. Chem.* **289**: 26859-26871.

Scott, J., Kupinski, A., Kirkham, C., Tuma, R. & Boyes, J. (2014) Tale proteins bind to both active and inactive chromatin. *Biochem. J.* **458**: 153-158.

Seipke, R., Patrick, E. & Hutchings, M. (2014) Regulation of antimycin biosynthesis by the orphan ECF RNA polymerase σ factor $sigma^{AntA}$. *PeerJ* **2**: e253.

Sharma, A., Leach, R., Gell, C., Zhang, N., Burrows, P., Shepherd, D., Wigneshweraraj, S., Smith, D., Zhang, X., Buck, M., Stockley, P. & Tuma, R. (2014) Domain movements of the enhancer-dependent sigma factor drive DNA delivery into the RNA polymerase active site: insights from single molecule studies. *Nucleic Acids Res.* **42**: 5177-5190.

Shepherd, D., Ariza, A., Edwards, T., Barr, J., Stonehouse, N. & Ashcroft, A. (2014) Probing bunyavirus N protein oligomerisation using mass spectrometry. *Rapid Commun. Mass Spectrom.* **28**: 793-800.

Shoura, M., Ranatunga, R., Harris, S., Nielsen, S. & Levene, S. (2014) Contribution of fluorophore dynamics and solvation to resonant energy transfer in protein-DNA complexes: a molecular-dynamics study. *Biophys. J.* **107**: 700-710.

Simmons, K., Jackson, S., Brueckner, F., Patching, S., Beckstein, O., Ivanova, E., Geng, T., Weyand, S., Drew, D., Lanigan, J., Sharples, D.J, Sansom, M., Iwata, S., Fishwick, C., Johnson, A., Cameron, A. & Henderson, P. (2014) Molecular mechanism of ligand recognition by membrane transport protein, MHP1. *EMBO J.* **33**: 1831-1844.

Soppina, V., Norris, S., Dizaji, A., Kortus, M., Veatch, S., Peckham, M. & Verhey, K. (2014) Dimerization of mammalian kinesin-3 motors results in superprocessive motion. *Proc. Natl Acad. Sci USA* **111**: 5562-5567.

Stadler, L., Tomlinson, D., Lee, T., Knowles, M. & Ferrigno, P. (2014) The use of a neutral peptide aptamer scaffold to anchor BH3 peptides constitutes a viable approach to studying their function. *Cell Death Dis***. 5**: e1037.

Stakaityte, G., Wood, J., Knight, L., Abdul-Sada, H., Adzahar, N., Nwogu, N., Macdonald, A. & Whitehouse, A. (2014) Merkel cell polyomavirus: molecular insights into the most recently discovered human tumour virus. *Cancers* **6**: 1267-1297.

Stead, M. & Wright, S. (2014) Nac1 interacts with the POZ-domain transcription factor, miz1. *Biosci. Rep.* **34**: 227-235.

Stead, M. & Wright, S. (2014) Structures of heterodimeric POZ domains of miz1/BCL6 and miz1/NAC1. *Acta Crystallogr. F* **70**: 1591-1596.

Su, Y., Sarell, C., Eddy, M., Debelouchina, G., Andreas, L., Pashley, C., Radford, S. & Griffin, R. (2014) Secondary structure in the core of amyloid fibrils formed from human $\beta_2$m and its truncated variant $\Delta$N6. *J. Am. Chem. Soc.* **136**: 6313-6325.

Tang, T.-C., Amadei, C., Thomson, N. & Chiesa, M. (2014) Ion exchange and DNA molecular dip sticks: Studying the nanoscale surface wetting of muscovite mica. *J. Phys. Chem. C* **118**: 4695-4701.

Tanner, S., Ariza, A., Richard, C.-A., Kyle, H., Dods, R., Blondot, M.-L., Wu, W., Trincao, J., Trinh, C., Hiscox, J., Carroll, M., Silman, N., Eleouet, J.-F., Edwards, T. & Barr, J. (2014) Crystal structure of the essential transcription antiterminator M2-1 protein of human respiratory syncytial virus and implications of its phosphorylation. *Proc. Natl Acad. Sci USA* **111**: 1580-1585.

Tate, D., Abdelbasit, M., Kilner, C., Shepherd, H., Warriner, S. & Bushby, R. (2014) A simple route to derivatives of benzo[*j*]fluoranthene. *Tetrahedron* **70**: 67-74.

Taylor, R., Benz, F., Sigle, D., Bowman, R., Bao, P., Roth, J., Heath, G., Evans, S. & Baumberg, J. (2014) Watching individual molecules flex within lipid membranes using SERS. *Sci. Rep.* **4**: 5940.

.

Thomson, N., Santos, S., Mitchenall, L., Stuchinskaya, T., Taylor, J. & Maxwell, A. (2014) DNA G-segment bending is not the sole determinant of topology simplification by type II DNA topoisomerases. *Sci. Rep.* **4**: 6158.

Tian, P., Jonsson, S., Ferkinghoff-Borg, J., Krivov, S., Lindorff-Larsen, K., Irback, A. & Boomsma, W. (2014) Robust estimation of diffusion-optimized ensembles for enhanced sampling. *J. Chem. Theory Comput.* **10**: 543-553.

Tiede, C., Tang, A., Deacon, S., Mandal, U., Nettleship, J., Owen, R., George, S., Harrison, D., Owens, R., Tomlinson, D. & Mcpherson, M. (2014) Adhiron: a stable and versatile peptide display scaffold for molecular recognition applications. *Protein Eng. Des. Sel.* **27**: 145-155.

Timmer, C., Michmerhuizen, N., Witte, A., Van Winkle, M., Zhou, D. & Sinniah, K. (2014) An isothermal titration and differential scanning calorimetry study of the G-quadruplex DNA-insulin interaction. *J. Phys. Chem. B* **118**: 1784-1790.

Timsah, Z., Ahmed, Z., Lin, C.-C., Melo, F., Stagg, L., Leonard, P., Jeyabal, P., Berrout, J., O'Neil, R., Bogdanov, M. & Ladbury, J. (2014) Competition between Grb2 and Plcγ1 for FGFR2 regulates basal phospholipase activity and invasion. *Nat. Struct. Mol. Biol.* **21**: 180- 188.

Toroz, D., Hammond, R., Roberts, K., Harris, S. & Ridley, T. (2014) Molecular dynamics simulations of organic crystal dissolution: The lifetime and stability of the polymorphic forms of para-amino benzoic acid in aqueous environment. *J. Cryst. Growth* **401**: 38-43.

Tsai, J.-Y., Kellosalo, J., Sun, Y.-J. & Goldman, A. (2014) Proton/sodium pumping pyrophosphatases: The last of the primary ion pumps. *Curr. Opin. Struct. Biol.* **27**: 38-47.

Tucker, J., Klein, T., Breed, J., Breeze, A., Overman, R., Phillips, C. & Norman, R. (2014) Structural insights into FGFR kinase isoform selectivity: diverse binding modes of AZD4547 and Ponatinib in complex with FGFR1 and FGFR4. *Structure* **22**: 1764-1774.

Tulloch, F., Pathania, U., Luke, G., Nicholson, J., Stonehouse, N., Rowlands, D., Jackson, T., Tuthill, T., Haas, J., Lamond, A. & Ryan, M. (2014) FMDV replicons encoding green fluorescent protein are replication competent. *J. Virol. Methods* **209**: 35-40.

Tych, K., Wood, C., Burnett, A., Pearson, A., Davies, A., Linfield, E. & Cunningham, J. (2014) Probing temperature- and solvent-dependent protein dynamics using terahertz time-domain spectroscopy. *J. Appl. Crystallogr.* **47**: 146-153.

Vajpai, N., Schott, A.-K., Vogtherr, M. & Breeze, A. (2014) NMR backbone assignments of the tyrosine kinase domain of human fibroblast growth factor receptor 1. *Biomol. NMR Assign.* **8**: 85-88.

Vakurov, A., Galluzzi, M., Podesta, A., Gamper, N., Nelson, A. & Connell, S. (2014) Direct characterization of fluid lipid assemblies on mercury in electric fields. *ACS Nano* **8**: 3242-3250.

Van Oosten-Hawle, P. & Morimoto, R. (2014) Organismal proteostasis: Role of cell-nonautonomous regulation and transcellular chaperone signaling. *Genes Dev.* **28**: 1533-1543.

Van Oosten-Hawle, P. & Morimoto, R. (2014) Transcellular chaperone signaling: An organismal strategy for integrated cell stress responses. *J. Exp. Biol.* **217**: 129-136.

Voeroes, J., Urbanek, A., Rautureau, G., O'connor, M., Fisher, H., Ashcroft, A. & Ferguson, N. (2014) Large-scale production and structural and biophysical characterizations of the human hepatitis B virus polymerase. *J. Virol.* **88**: 2584-2599.

Wang, F., Shen, Y., Zhang, W., Li, M., Wang, Y., Zhou, D. & Guo, S. (2014) Efficient, dual-stimuli responsive cytosolic gene delivery using a rgd modified disulfide-linked polyethylenimine functionalized gold nanorod. *J. Control. Release* **196**: 37-51.

Wang, Y., Wang, F., Guo, Y., Chen, R., Shen, Y., Guo, A., Liu, J., Zhang, X., Zhou, D. & Guo, S. (2014) Controlled synthesis of monodisperse gold nanorods with different aspect ratios in the presence of aromatic additives. *J. Nanopart. Res.* **16**: 2806.

Wasson, C., Muller, M., Prescott, E., Roberts, S. & Macdonald, A. (2014) Insights into the elusive human papillomavirus e5 oncogene. *Int. J. Mol. Med.* **34**: S107-S107.

Webb, M., Yorke, B., Kershaw, T., Lovelock, S., Lobley, C., Kilkenny, M., Smith, A., Blundell, T., Pearson, A. & Abell, C. (2014) Threonine 57 is required for the post-translational activation of *Escherichia coli* aspartate α-decarboxylase. *Acta Crystallogr. D* **70**: 1166-1172.

Wilkinson, C., Mcphillie, M., Zhou, Y., Woods, S., Afanador, G.A., Rawson, S., Khaliq, F., Prigge, S., Roberts, C., Rice, D., Mcleod, R., Fishwick, C. & Muench, S. (2014) The benzimidazole based drugs show good activity against *T. gondii* but poor activity against its proposed enoyl reductase enzyme target. *Bioorg. Med. Chem. Lett.* **24**: 911-916.

Williamson, D., Webb, M. & Turnbull, W. (2014) Depsipeptide substrates for sortase-mediated N-terminal protein ligation. *Nat. Protoc.* **9**: 253-262.

Windle, C., Mueller, M., Nelson, A. & Berry, A. (2014) Engineering aldolases as biocatalysts. *Curr. Opin. Chem. Biol.* **19**: 25-33.

Witola, W., Liu, S., Montpetit, A., Welti, R., Hypolite, M., Roth, M., Zhou, Y., Mui, E., Cesbron-Delauw, M.-F., Fournie, G., Cavailles, P., Bisanz, C., Boyer, K., Withers, S., Noble, A., Swisher, C., Heydemann, P., Rabiah, P., Muench, S. & Mcleod, R. (2014) ALOX12 in human toxoplasmosis. *Infect. Immun.* **82**: 2670-2679.

Wolny, M., Batchelor, M., Knight, P., Paci, E., Dougan, L. & Peckham, M. (2014) Stable single alpha-helices are constant force springs in proteins. *J. Biol. Chem.* **289**: 27825-27835.

Wong, B., Ayton, S., Lam, L., Lei, P., Adlard, P., Bush, A. & Duce, J. (2014) A comparison of ceruloplasmin to biological polyanions in promoting the oxidation of $Fe^{2+}$ under physiologically relevant conditions. *Biochim. Biophys. Acta* **1840**: 3299-3310.

Wong, B. & Duce, J. (2014) The iron regulatory capability of the major protein participants in prevalent neurodegenerative disorders. *Front. Pharmacol.* **5**: 81.

Wong, B., Hung, Y., Bush, A. & Duce, J. (2014) Metals and cholesterol: two sides of the same coin in Alzheimer's disease pathology. *Front. Aging Neurosci.* **6**: 91.

Wong, B., Tsatsanis, A., Lim, L., Adlard, P., Bush, A. & Duce, J. (2014) β-amyloid precursor protein does not possess ferroxidase activity but does stabilize the cell surface ferrous iron exporter ferroportin. *PLoS One* **9**: e114174.

Yamashita, M., Shepherd, M., Booth, W., Xie, H., Postis, V., Nyathi, Y., Tzokov, S., Poole, R., Baldwin, S. & Bullough, P. (2014) Structure and function of the bacterial heterodimeric ABC transporter CydDC stimulation of ATPase activity by thiol and heme compounds. *J. Biol. Chem.* **289**: 23177-23188.

Yan, R., Hallam, A., Stockley, P. & Boyes, J. (2014) Oncogene dependency and the potential of targeted RNAi-based anti-cancer therapy. *Biochem. J.* **461**: 1-13.

Yang, S., Barbu-Tudoran, L., Orzechowsk, M., Craig, R., Trinick, J., White, H. & Lehman, W. (2014) Three-dimensional organization of troponin on cardiac muscle thin filaments in the relaxed state. *Biophys. J.* **106**: 855-864.

Yorke, B., Beddard, G., Owen, R. & Pearson, A. (2014) Time-resolved crystallography using the hadamard transform. *Nat. Methods* **11**: 1131-1134.

Young, L., Cao, P., Raleigh, D., Ashcroft, A. & Radford, S. (2014) Ion mobility spectrometry-mass spectrometry defines the oligomeric intermediates in amylin amyloid formation and the mode of action of inhibitors. *J. Am. Chem. Soc.* **136**: 660-670.

Yule, I., Czaplewski, L., Pommier, S., Davies, D., Narramore, S. & Fishwick, C. (2014) Pyridine-3-carboxamide-6-yl-ureas as novel inhibitors of bacterial DNA gyrase: Structure based design, synthesis, SAR and antimicrobial activity. *Eur. J. Med. Chem.* **86**: 31-38.

Zhang, S., Chen, R., Malhotra, G., Critchley, K., Vakurov, A. & Nelson, A. (2014) Electrochemical modelling of qd-phospholipid interactions. *J. Colloid Interface Sci.* **420**: 9-14.

Zhou, Y., Fomovska, A., Muench, S., Lai, B.-S., Mui, E. & Mcleod, R. (2014) Spiroindolone that inhibits PfATPase4 is a potent, cidal inhibitor of *Toxoplasma gondii* tachyzoites *in vitro* and *in vivo*. *Antimicrob. Agents Chemother*. **58**: 1789-1792.

Zhuravleva, A. & Radford, S. (2014) How TriC folds tricky proteins. *Cell* **159**: 1251-1252.